ROLE OF CARBON DIOXIDE IN GAS EXPANDED LIQUIDS FOR REMOVAL OF PHOTORESIST AND ETCH RESIDUE

A Thesis
Presented to
The Academic Faculty

by

Ingu Song

In Partial Fulfillment
of the Requirements for the Degree
PhD in the
School of Chemical and Biomolecular Engineering

Georgia Institute of Technology
December 2007

ROLE OF CARBON DIOXIDE IN GAS EXPANDED LIQUIDS FOR REMOVAL OF PHOTORESIST AND ETCH RESIDUE

Approved by:

Dr. Dennis Hess, Advisor
School of Chemical and Biomolecular Engineering
Georgia Institute of Technology

Dr. Clifford L. Henderson
School of Chemical and Biomolecular Engineering
Georgia Institute of Technology

Dr. Charles A. Eckert
School of Chemical and Biomolecular Engineering
Georgia Institute of Technology

Dr. Charles L. Liotta
School of Chemistry and Biochemistry
Georgia Institute of Technology

Dr. Albert B. Frazier
School of Electrical and Computer Engineering
Georgia Institute of Technology

Date Approved: 9/24/2007

ACKNOWLEDGEMENTS

This PhD thesis is not my individual work alone but a collaboration of many people's work, time, and commitment. My advisor Dr. Hess provided direction and guidance with a sense of humor and warmth that reflected his desire to not only produce another PhD student but a well rounded person. Besides Dr. Hess, the other members of our research group provided both technical and non-technical support. As a first year, I shared our office with Dr. Satya Myneni who influenced me with his amazing work ethic. After his departure Shantanu C. Pathak joined me in our office. He provided the much needed non-research oriented conversation that made my research successes and failures more enjoyable. Research scientist Dr. Galit Levitin worked with me on the details and brainstorming of my projects. Her constructive criticisms were always thoughtful. Much is indebted to past members of the group Dr. Matthew Spuller, Dr. Jie Diao, Dr. Chris Timmons, Dr. Sudeep Vaswani, Dr. Qian Luo, Dr. Prabhakar Tamirisa, and Dr. Ashwini Sinha. In addition current members Lingbo Zhu, Yonghao Xiu, Balamurali Balu, Ashish Pande, and Fangyu Wu have been a source of encouragement.

Each of the committee members Dr. Eckert, Dr. Frazier, Dr. Henderson, and Dr. Liotta added a unique perspective to my research. They provided broad big picture views while their graduate students and research scientists in particular Jackson Ford and Dr. Julie Lu from Dr. Eckert and Dr. Liotta's group; Yueming Hua, Cheng-Tsung Lee, and Richard Lawson from Dr. Henderson's group; and Youngdo Jung from Dr. Frazier's group worked with me on the specifics.

Gloria Beale was very helpful processing all my orders in a timely manner. Kevin Guger and Tommie Taylor were always available to ensure my computer was optimally running. Brad Parker and Jeff Andrews in the machine shop helped design and build my experimental setups. All the Korean graduate students in CHBE and Dr. Jay Lee created a sense of Korean culture and family. In particular my past roommate Jeongwoo Lee introduced me to what it means to be really Korean and we kept each other motivated as we endured our first year of grad school together. I thank my Bible study group including Jang Choe, Bill Hallsworth, Barnabas Kane, Alex Lee, Mike Promhan, Hannah Snyder, Wei-lin Sun, Pahk Thepchatri, David Tran, and Mark Yang who kept me spiritually accountable. I also like to thank my roommates from the bitter cold Cornell days, Mashfique Hassan and Gene Park.

I would like to thank my girlfriend Woomi Lee for encouraging me through my final year of graduate school. Many times I was searching for a particular journal paper or equation when in fact all I needed was Woomi's shoulder to lean on. When everything seemed hopeless she provided hope. I thank my brother Moses Song and my parents Chulkun and Jaehyun Song for loving me unconditionally. Finally, I give thanks to God who makes all things possible according to his will.

TABLE OF CONTENTS

LIST OF TABLES

Page

LIST OF FIGURES

Page

LIST OF SYMBOLS AND ABBREVIATIONS

A	area of electrode (m^2)
c	capacitance (F)
C_m	mass sensitivity constant $\left(\frac{Hz^2}{g/cm^2 s}\right)$
d	film thickness (nm)
D	diffusivity (cm^2/s)
E_B	binding energy (eV)
E_K	kinetic energy (eV)
ΔF_m	frequency change due to mass (Hz)
ΔF_p	frequency change due to pressure (Hz)
ΔF_n	frequency change due to viscosity (Hz)
F	current frequency (Hz)
F_o	original frequency (Hz)
h	Planck's contant (6.626068 × 10-34 m^2 kg/s)
I_t	transmitted light intensity
I_o	original light intensity
k	extinction coefficient
M	molecular weight (g/mole)
n	refractive index
n_o, n_1, n_2	fitted Cauchy parameters

$\widetilde{N}$	complex refractive index
r	Fresnel reflection coefficient
R	total reflection coefficient
T_w	fraction of light transmitted
W	work function (eV)
x	mole fraction of liquid in GXL

Greek

α	pressure correction factor
β	phase angle (^{o})
ε	permittivity in a vacuum (8.854×10^{-12} F/m)
ϕ	incident angle (^{o})
ϕ	solvent association factor
γ_{lv}	surface tension between liquid and vapor interface (dynes/cm)
γ_{sv}	surface tension between solid and vapor interface (dynes/cm)
γ_{sl}	surface tension between solid and liquid interface (dynes/cm)
η_f	viscosity of fluid (g/cm-s)
κ	dielectric constant
λ	wavelength (nm)
μ	viscosity (g/cm-s)
μ_q	shear modulus of crystal (g/cm-s^2)
ν	frequency (Hz)

θ_Y	contact angle (^{o})
ρ_f	density of fluid (g/cm^3)
ρ_q	density of crystal (g/cm^3)

SUMMARY

Progress in the microelectronics industry is driven by smaller and faster transistors. As feature sizes in integrated circuits become smaller and liquid chemical waste becomes an even greater environmental concern, gas expanded liquids (GXLs) may provide a possible solution to future device fabrication limitations relative to the use of liquids. The properties of GXLs such as surface tension can be tuned by the inclusion of high pressure gases; thereby, the reduced surface tension will allow penetration of cleaning solutions into small features on the nanometer scale. In addition, the inclusion of the gas decreases the amount of liquid necessary for the photoresist and etch residue removal processes. This thesis explores the role of CO_2-based GXLs for photoresist and etch residue removal. The gas used for expansion is CO_2 while the liquid used is methanol. The cosolvent serving as the removal agent is tetramethyl ammonium hydroxide (TMAH) which upon reacting with CO_2 becomes predominantly tetramethyl ammonium bicarbonate (TMAB).

First this study determines the feasibility of GXLs for photoresist and etch residue removal by applying GXLs to commercially patterned semiconductor wafers. At 90^{o}C and pressures >1000psi, photoresist and etch residue are removed by a CO_2 expanded TMAB solution diluted with methanol. The mechanism of GXL film and residue removal appears to be swelling of the photoresist and subsequent penetration of the photoresist by cosolvent, followed by an etch of the underlying SiO_2 by hydroxide ions in equilibrium with the bicarbonate. The etch process releases the photoresist and etch residue from the surface by lift-off.

Besides feasibility of photoresist and etch residue removal by GXLs, this work confirms the compatibility of GXLs with low k materials such as methylsilsesquioxane (MSQ) which is present on state-of-the-art ICs. Low k materials are currently incorporated in industry as an insulation layer between metal layers that form the interconnects between transistors. The dielectric constant of these materials must remain low (~2.7) to serve as effective insulation between metal layers. Due to the absorption of tetramethyl ammonium, bicarbonate, and hydroxide ions into the MSQ film, the dielectric constant increases. However, a 2200psi CO_2/CH_3OH is able to solubilize and remove these ions to recover the low k dielectric constant value. These experiments demonstrate that GXLs can be used to remove photoresist and etch residues while remaining compatible with low k materials which makes GXLs a possible choice for these cleaning processes for future IC fabrication.

In certain GXLs, the CO_2 gas is replaced with C_2H_6 in order to compare the quadrupolar nature of CO_2 to that of the nonpolar C_2H_6. However, C_2H_6 does not react with TMAH and therefore the concentration of the hydroxide ion removal agent is different as well. Although direct comparisons cannot be made, C_2H_6 is able to remove the photoresist and etch residue films at a lower temperature of 50^{o}C relative to CO_2 due to the increased hydroxide ion concentration. However, this higher hydroxide ion concentration etches the low k dielectric films.

The expansion gases CO_2 and C_2H_6 are directly compared via their absorption into polyhydroxystyrene (PHOST) and polystyrene (PS), since PS lacks the hydroxyl group of PHOST. A quartz crystal microbalance was used to measure mass uptake of the gases. PHOST absorbed a higher ratio of CO_2/C_2H_6 compared to PS suggesting an

interaction of the quadrupole moment of CO_2 with the hydroxyl group in PHOST via a Lewis acid-base interaction.

CHAPTER 1

INTRODUCTION

Motivation

The purpose of all corporations is to generate revenue, but the cost to society may have a high price tag. Often, the cost incurred is the environment and technical innovation. These are the two main topics that will be addressed in the form of application of gas expanded liquids (GXLs) for photoresist and etch residue removal. Current photoresist and etch residue removal processes use large quantities of water and hazardous chemicals. GXLs provide a more environmentally friendly alternative through the use of CO_2 as a solvent to reduce liquid solvent usage. In addition, as feature sizes in current integrated circuits decrease, liquids with higher viscosities and surface tensions than GXLs may be unable to penetrate into the smaller features to remove contaminants.

Introduction to the Microelectronics Industry

Competition to gain consumer market share through better products and services drives all industries. However, an additional challenge motivates the microelectronics industry, namely Moore's Law, which originally stated that the number of transistors doubles every two years[1]. Transistors are the tiny switches that are at the heart of microprocessors. Although an ambitious prediction, the microelectronics industry has achieved or even exceeded this claim for the past 40 years through various innovations. Current production technology according to Intel, is based on the 65nm node, half the pitch distance between two adjacent gates. But production on the 45nm generation will

begin at the first half of 2008 to meet Moore's Law prediction[2]. Figure 1.1 shows a cross section of a 65nm node transistor where the gate length is a mere 35nm.

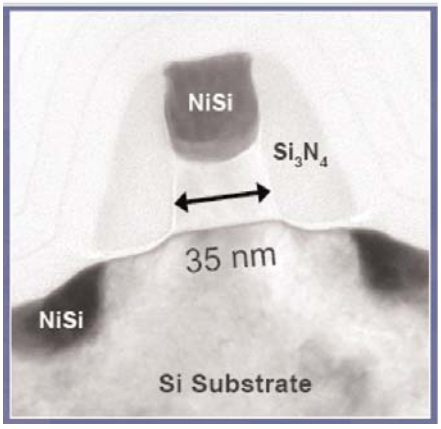

Figure 1.1: Cross-section of a 35nm gate using 65nm technology[3].

In order to achieve the predicted trend, several new technologies have been implemented over the past decade, such as strained silicon, low-k dielectric materials such as carbon doped oxide, and 300mm silicon wafers[4]. For the 45nm node, other new innovations will include high k dielectrics for the transistor gate dielectric and metals for the transistor gate electrode[2].

In order to increase the data processing speed of transistors, many approaches are being considered such as reducing gate length, lowering the dielectric constant of the material serving as insulation between interconnect layers, increasing the dielectric constant of the gate material, using interconnect material with higher conductivity, or even using a completely different material instead of silicon. In general, the feature sizes of integrated circuits are ever-shrinking. Effective creation of these smaller features in more complex devices requires a combined effort from photolithography, deposition, etching, and removal of photoresist and etch residue. The specific step in microelectronic

fabrication that will be investigated in this thesis is the photoresist and etch residue removal step.

Photoresists and Etch Residue

A total of 33 photoresist removal steps are involved in the creation of a state-of-the-art microprocessor unit (MPU)[5]. Photoresists and etch residues must be removed in order to ensure clean surfaces for subsequent deposition steps. Incomplete removal can cause high resistivity metal contacts, increased dielectric constant for interlayer dielectrics, and can change feature dimensions. Photoresists are the radiation (light) sensitive films used to create patterns on silicon wafers. The etch residue forms on top of the photoresist and along the sidewalls of the etched via or trench due to plasma-based etching. A typical process for creating patterns is shown in Figure 1.2

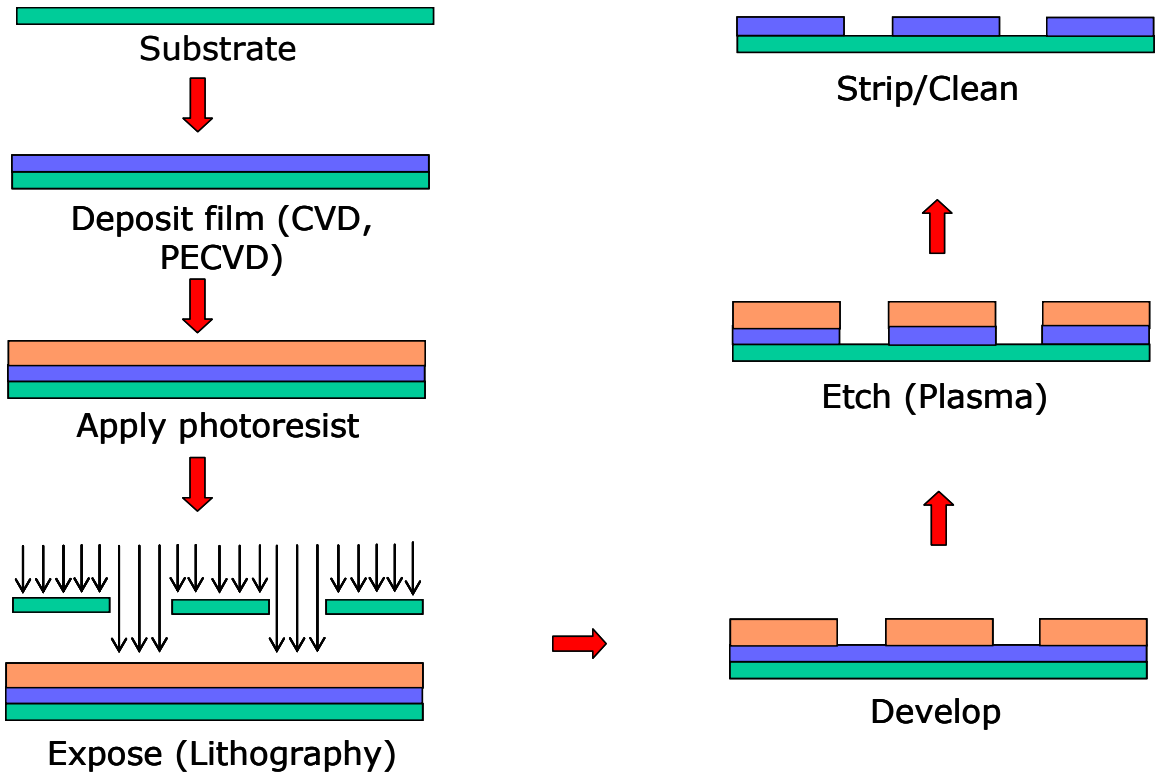

Figure 1.2: Processes in IC fabrication.

In Figure 1.2 the photoresist is a positive photoresist which means that when it is exposed to UV, chemical and/or physical changes occur to render the exposed material more soluble in a developer solution. During the development step, the photoresist that was exposed to UV radiation dissolves in a developer liquid solution and is removed. The structure remaining is exposed to a plasma etch process where the film not protected by the photoresist (i.e., the film exposed directly to the plasma) is etched. In addition, the photoresist is also etched, but due to etch rate differences (selectivity) the film is etched at a higher rate compared to the photoresist. After the etching step, the photoresist is no longer necessary and must be removed.

The two main types of photoresists currently employed are (1) those that upon UV exposure directly change their solubility in developer solution and (2) those that are chemically amplified where a post exposure bake causes a chemical reaction that changes the solubility of the resist[6]. Novolak resin, diazonaphthoquinone (DNQ) photoactive compound (PAC), and propylene glycol methyl ether acetate (PGMEA) solvent serve effectively as a resist system wherein the resist material changes solubility upon UV exposure due to UV-initiated chemical reaction and molecular rearrangement. Polyhydroxystyrene (PHOST) resin with a t-butoxycarbonyl (t-BOC) group, triphenylsulfonium aniomate photoacid generator (PAG), and PGMEA solvent is a type of chemically amplified resist[7]. Both of the photoresist materials cited here are positive photoresists, which means that upon UV exposure, the photoresist becomes more soluble in a developer solution relative to the unexposed material[8].

Novolak resin as shown in Figure 1.3 was used in the integrated circuit (IC) industry from the late 1970s to the mid 1990s.

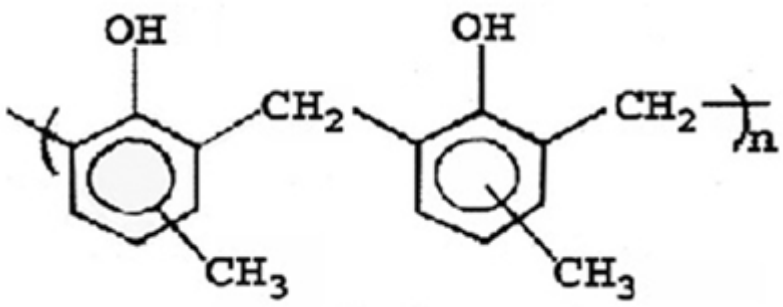

Figure 1.3: Novolak resin.

The novolak/DNQ photoresist system uses g-line (436nm) and i-line (365nm) wavelength light exposure from an Hg arc lamp. Upon exposure to UV light, the dissolution inhibitor DNQ shown in Figure 1.4 undergoes a chemical reaction and molecular rearrangement.

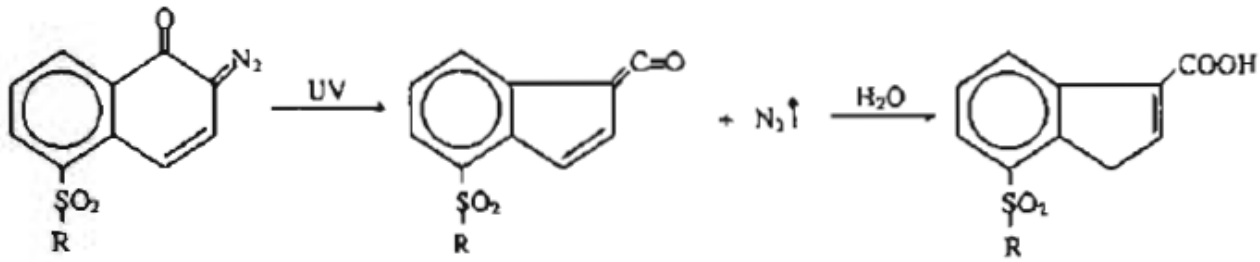

Figure 1.4: Chemical reaction of DNQ upon UV exposure.

Due to the formation of the carboxylic acid, the resulting product is soluble in an alkali solution such as tetramethyl ammonium hydroxide (TMAH).

Chemically amplified photoresists are more complicated due to a specific two step procedure for image formation. Whereas the novolac/DNQ photoresist is exposed to UV light and then becomes more soluble in basic solution, PHOST-tBOC requires exposure and bake steps[9]. In the first step, the PAG triphenylsulfonium salt is exposed to deep ultraviolet light (DUV) at 248nm using a KrF excimer laser which results in the creation of trifluoroacetic acid that catalyzes the next step in the reaction sequence, as described in Figures 1.5 and 1.6.

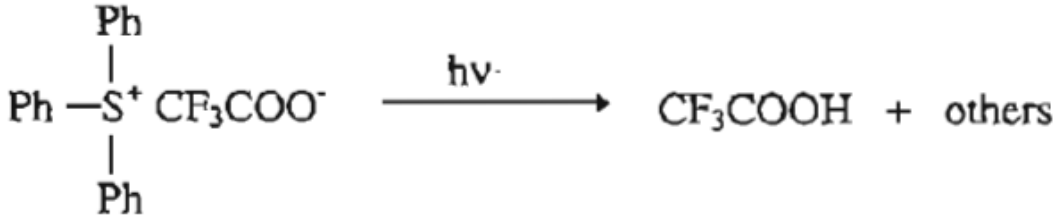

Figure 1.5: Creation of trifluoroacetic acid from a triphenylsulfonium salt.

The PHOST-tBOC/PAG system is then baked at 110°C and the acid catalyzes the detachment of the tBOC group from PHOST as shown in Figure 1.6[10].

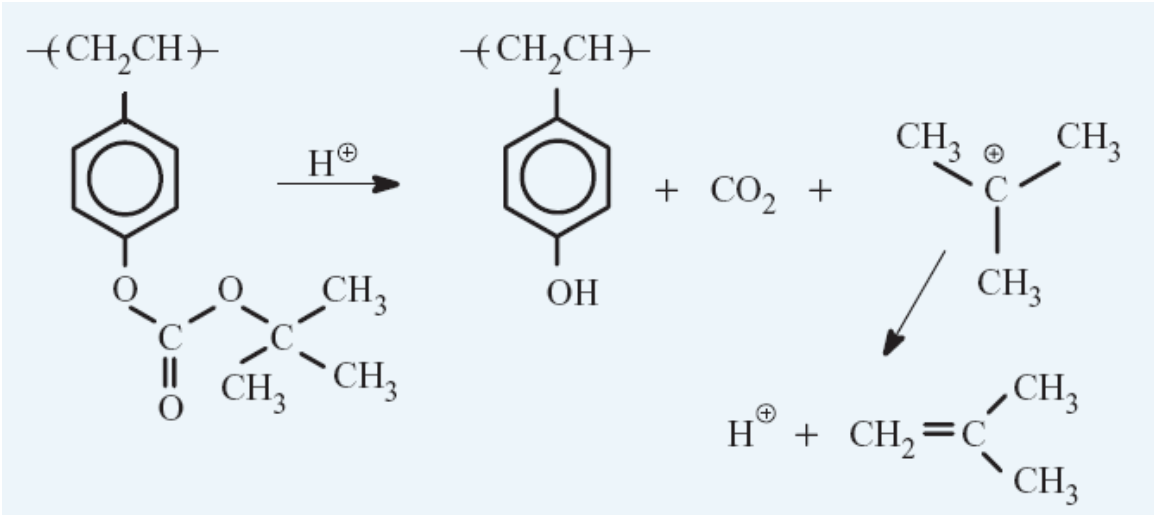

Figure 1.6: PHOST-tBOC undergoes an acid catalyzed reaction to become PHOST which is soluble in basic solution. In addition the acid is regenerated.

PHOST is soluble in basic solutions, but the tBOC attachment inhibits the dissolution. Between 10-30% of PHOST has tBOC protection[6]. The main benefit of the chemically amplified photoresist is that the acid is regenerated and thereby can catalyze more reactions. For comparison, the overall processes are shown in Figures 1.7 and 1.8 for novolak/DNQ and PHOST-tBOC, respectively[11].

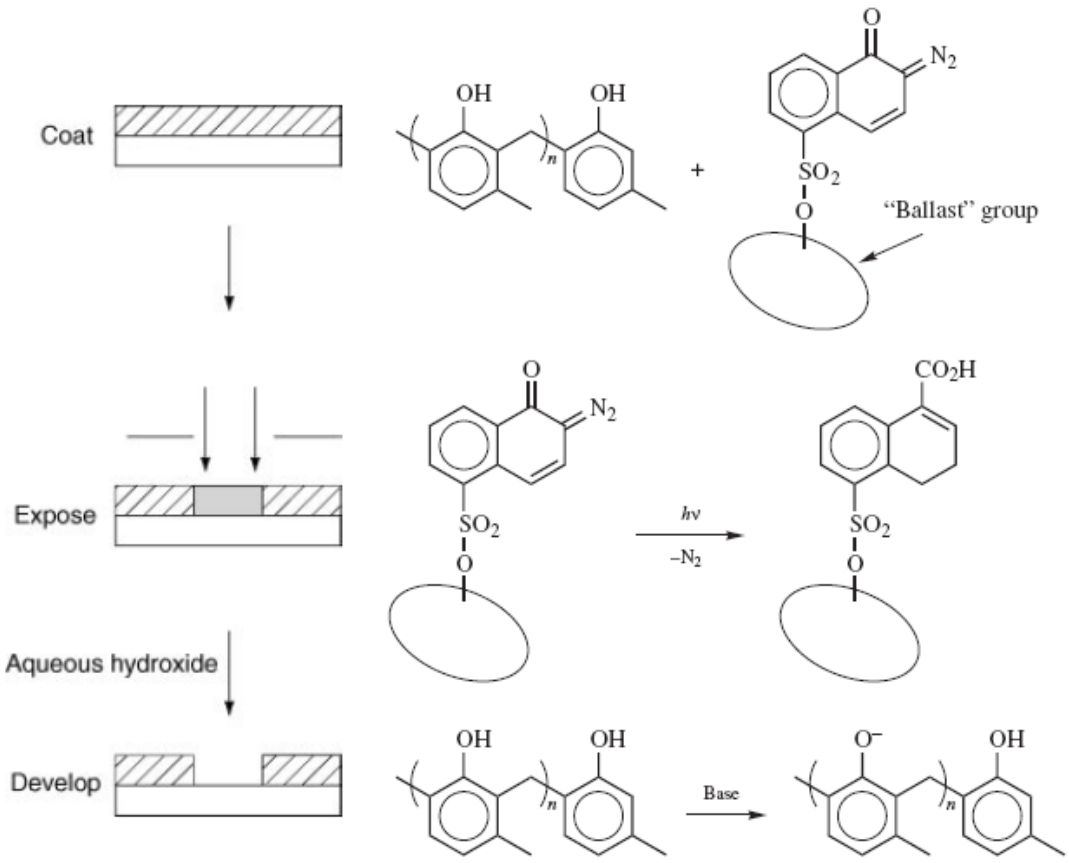

Figure 1.7: Processing sequence for DNQ/novolak.

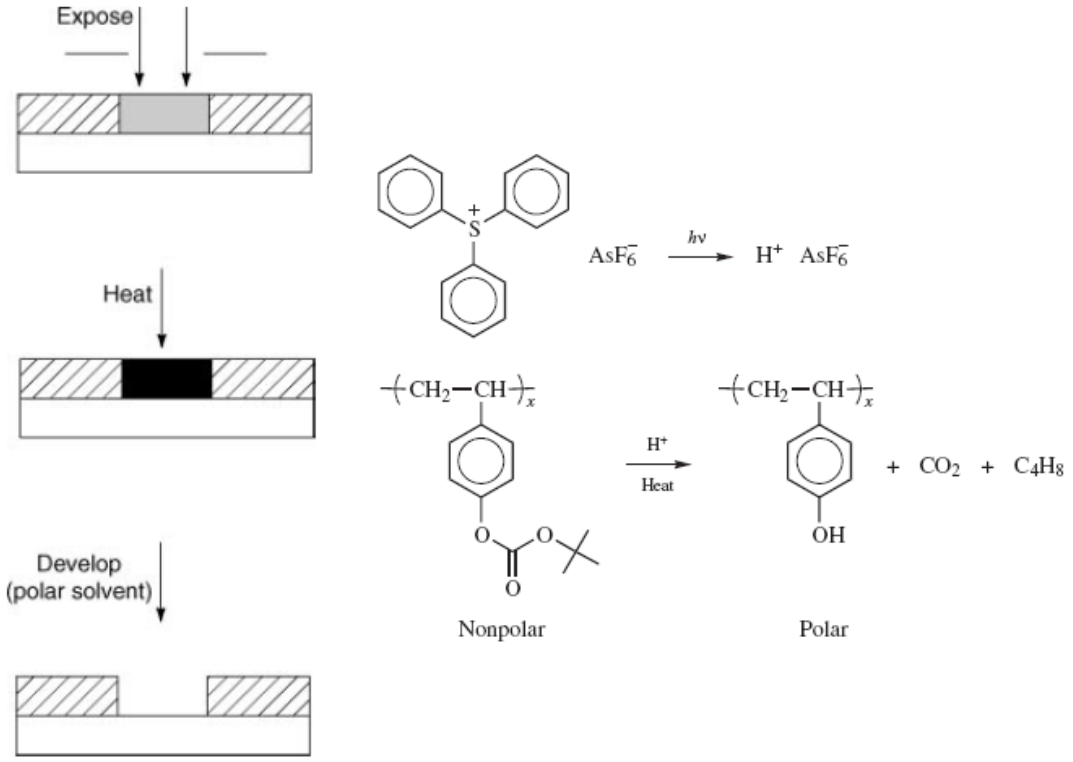

Figure 1.8: Processing steps for PHOST-tBOC.

After the photoresist film has been developed, the film is exposed to either a liquid wet etch or dry plasma etch process. A plasma is a highly reactive ionized gas formed when a voltage is applied to a gas across two parallel plates. The plasma phase is highly reactive due to the free radicals and ions created by the electrical discharge formed between the parallel plates[12]. During the dry etch process, the plasma not only etches the film not protected by the photoresist but also reacts with the photoresist; the combination of photoresist fragments and partially reacted etch products form etch residues that deposit on feature sidewalls and at the bottom of the trench that is formed. Plasmas using CF_4, C_2H_6, CHF_3, C_4F_8, NF_3, SF_6, $CFCl_3$, CF_3Cl, or CF_2Cl_2 are used to etch SiO_2 by reacting fluorine atoms with SiO_2, forming volatile etch products such as SiF_4 and CO_2 and generating a tough crust-like fluorinated film on top of the photoresist[13].

Cleaning Processes in FEOL and BEOL

The manufacture of an integrated circuit can be divided into two segments, designated front end of the line (FEOL) and back end of the line (BEOL). FEOL refers to the process steps prior to interconnect (conductor) film deposition whereas BEOL refers to the subsequent steps. Different types of cleaning steps are involved in each segment, but both segments must remove organic contaminants, metallic particles, oxide films, photoresist films, and etch residues. Figure 1.9 shows a schematic diagram of post-etched (pre-cleaned) and cleaned portions of a cross section of an integrated circuit[14]. In addition, Figure 1.9 illustrates the various types of residues present, including sidewall, top, and Cu-rich.

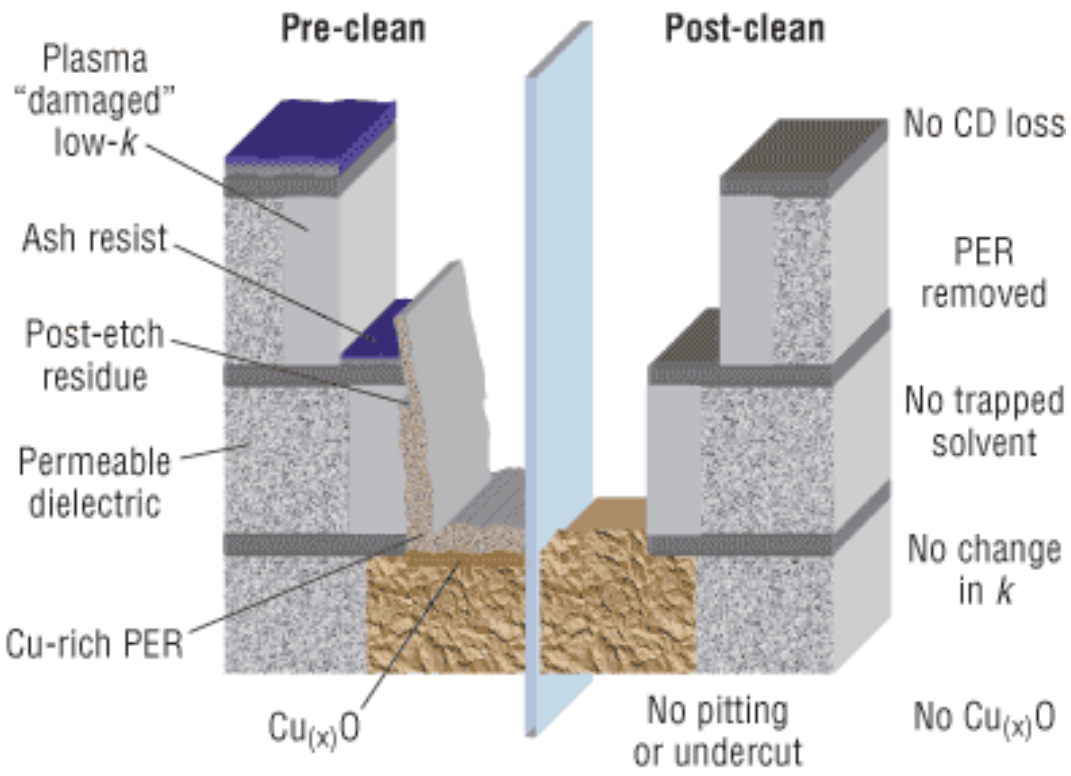

Figure 1.9: Diagram of pre-clean and post-clean. CD is critical dimension. PER is post etch residue.

In FEOL, the standard RCA (Radio Corporation of America) clean is generally implemented since this procedure is an effective clean. The RCA clean process has three parts: SC-1 (standard clean 1), a solution of H_2O, H_2O_2, and NH_4OH in a ratio of 5:1:1 that removes organic contaminants; SC-2 (standard clean 2), a solution of H_2O, H_2O_2, and HCl in a ratio of 6:1:1 that removes metallic contaminants; and a diluted 50:1 HF solution that removes the native silicon oxide film [15]. Variations on the RCA clean include the use of megasonics, ozonated water, and piranha solutions comprised of H_2O, H_2O_2, and H_2SO_4[15]. In order to reduce the use of de-ionized (DI) water and other chemicals, the immersion RCA steps can be replaced with spray tools and vapor phase cleaning[15]. A system called single-wafer spin cleaning with repetitive use of ozonated water and dilute hydrogen fluoride (SCROD) has been reported to be more effective in removing the organic and metallic contaminants in addition to reducing the amount of DI

water and chemicals used[16]. However, due to the simplicity, effectiveness, and low cost of the RCA immersion clean, the RCA process has not changed radically in the past 40 years.

In FEOL, photolithography is used to define the n and p-doped silicon regions. The dopants are added via ion implantation into the exposed areas and onto the protective photoresist. Oxygen plasma oxidizes the photoresist and creates volatile products which are pumped out of the system. After deposition of the high k gate dielectric and the first layer of metal interconnects, a low k interlevel dielectric is deposited by CVD. Contact holes are etched into the interlevel dielectric using a fluorocarbon plasma; subsequent processes comprise BEOL.

In BEOL, a fluorocarbon plasma is used to etch a low-k dielectric film, but in addition this process creates a thin fluorocarbon crust on top of the photoresist and along the sidewalls of the via[17]. Low-k dielectric film is the insulating layer between the metal layers. The residue ensures the generation of an anisotropic etch profile, but must be removed before subsequent processing. Unlike the situation in FEOL, the photoresist film cannot be removed using oxygen plasmas because the plasma will react with the organic groups in the low k dielectric and alter the dielectric constant. Alternatively, inorganic low k dielectrics such as carbon doped SiO_2 can be substituted instead[18]. Rather than an oxidative plasma, a reducing plasma such as H_2 or H_2/N_2 can remove the fluorocarbon residue. However, complete removal is inhibited, thereby requiring an additional liquid cleaning step[19].

In addition to the complexities caused by the low k dielectric, another concern is the corrosion of metal lines in BEOL. In the past, aluminum was used as the interconnect

material. At that time, hydroxylamine-based cleaning formulations were effective in removing the post plasma etch residue but did not damage the aluminum lines. However, technology has shifted toward the use of copper due to copper's superior electrical conductivity. Dual damascene processes for copper patterning involve etching of the dielectric rather than the copper, and then the copper is electrochemically deposited to form conductor patterns[20]. Although hydroxylamine solutions are compatible with copper, semi-aqueous fluoride chemistries require shorter processing times and use lower temperatures, and are therefore often preferred for cleaning purposes[21]. Hydroxylamine solutions perform best between 60°C-70°C whereas semi-aqueous fluoride chemistries can function at room temperatures and due to the lower temperatures, less DI water is evaporated[22]. The DI water present in the hydroxylamine and semi-aqueous fluoride solutions presents a possible a corrosion scenario but an isopropyl alcohol rinse can minimize corrosion[21]. Semi-aqueous fluoride solutions cause large critical dimension (CD) losses because they etch the dielectric sidewalls at contact lines present in patterned wafers.

Another alternative to the use of oxygen plasmas for cleaning is the application of densified ammonia after a microwave downstream plasma to remove the post etch residue and post etch residue rich with metal, but any moisture in the ammonia can cause metal corrosion[23]. Yet another cleaning approach uses a sulfur trioxide gas cleaning solution, but displays similar concerns with moisture content since corrosive sulfuric acid may form. In this process,the sample to be cleaned is exposed to sulfur trioxide gas at temperatures ~100°C and then rinsed using DI water[24]. Ozonated DI water has also been investigated as a removal solution. Although it is not very effective, the inclusion of

small concentrations of HF has improved its removal capability[25]. Companies such as ATMI and EKC have proprietary solvents that are able to remove photoresist and etch residues in BEOL but these formulations are expensive. As a result, spray tool companies such as Semitool have considered extremely dilute HF (1:1000) which is a significantly cheaper alternative albeit not as effective. Another means of facilitating photoresist and etch residue removal is the addition of mechanical energy to the substrate surface; this is generally accomplished by applying megasonic energy to the cleaning solution[26].

Frequently ashing, which uses oxygen plasmas as a dry removal step, is used in conjunction with a wet removal step to ensure effective cleaning[27]. The plasma can often partially remove the residue by oxidizing the hydrocarbon photoresist film and thus allow the liquid solvent to better penetrate the film to dissolve or lift it off. Instead of switching between two pieces of equipment, supercritical fluid (SCF) systems are able to clean and rinse/dry in the same chamber and thereby save space and lab costs[28]. Processes using supercritical CO_2 with tetramethyl ammonium hydroxide cosolvent have been demonstrated to remove photoresist and etch residues[29, 30]. Other high pressure approaches such as ammonium fluoride with supercritical CO_2 were able to remove these residues as well[31]. Rather than employ supercritical CO_2 conditions, IMEC has partnered with Eco-snow to develop a cryogenic CO_2 cleaning system[32].

Organization of Thesis

The prior sections described current approaches to removing photoresist and etch residue. The two key points that GXLs address are reduction of liquid solvent usage and penetration into smaller vias in integrated circuit devices. Because of these two

advantages, the use of GXLs for photoresist and etch residue removal may offer important advantages. Prior work by Spuller laid the foundation for fundamental studies of GXLs for photoresist and etch residue removal such as wetting and solvent usage[33]. This thesis intends to explore the role of CO_2 in GXLs for photoresist and etch residue removal by investigating the effectiveness and controlling attributes of GXLs for cleaning of device wafers obtained from industrial firms, and by studying the effect of GXLs on newly implemented film materials currently used in IC fabrication.

Chapter 1 describes the microelectronic device fabrication process and the importance of the photoresist and etch residue removal step. In addition, justification for this research and significance of GXLs in this specific processing step are presented. Chapter 2 describes the nature of GXLs by explaining how they are created and what specific characteristics are beneficial for the particular cleaning application we are considering. Furthermore, GXLs are compared to other fluids such as supercritical fluids, liquids, and gases in order to show the advantages of GXLs. In Chapter 3 the analytical techniques used to characterize the GXL processed materials are described. The techniques detailed include x-ray photoelectron spectroscopy (XPS), goniometry, ellipsometry, Fourier transform infrared spectroscopy (FTIR), quartz crystal microbalance (QCM), and electrical characterization methods such as current-voltage (IV) and capacitance-voltage (CV). Chapter 4 describes studies that evaluate the use of GXLs for cleaning industrially-generated device samples, since previous photoresist removal experiments using GXLs were only applied to model films generated in our laboratory. Two different gases, CO_2 and C_2H_6, were used as gases for the liquid expansion. These two gases have many similar properties except that C_2H_6 lacks the

quadrupole moment characteristic of CO_2. Both gases demonstrated that the film can be removed at elevated temperatures (90^oC) and pressures (>1000psi). However, fundamental differences between the mechanism by which each gas removed photoresist and etch residue mechanisms were not clearly identified because CO_2 reacts with TMAH whereas C_2H_6 does not. This reaction changes the composition of the GXL. The CO_2 GXL is dominated by bicarbonate whereas the C_2H_6 GXL has more hydroxide concentration which may be the cause of the different removal conditions. In Chapter 6 CO_2 and C_2H_6 were investigated without the reactive cosolvent. The absorption of these gases into polystyrene (PS) and polyhydroxystyrene (PHOST) were investigated using QCM. The hydroxyl group in PHOST may have interacted more with CO_2 through a Lewis acid-base interaction as indicated by the higher ratio of CO_2/C_2H_6 absorbed by PHOST compared to PS. In addition dissipation measurements suggested that the films had become less rigid due to swelling. Current microelectronic device fabrication technology incorporates low k dielectric materials. Since, these materials must be compatible with the GXL processes in order to consider use in IC processing, compatibility issues were investigated in Chapter 5. Chapter 7 summarizes the conclusions of this work and Chapter 8 provides future work that focuses on swelling investigations and possible gas and liquid alternatives to CO_2 and methanol.

References

1. Moore, G. E., Cramming more components onto integrated circuits. *Electronics* April 19, 1965.

2. Intel's Transistor Technology Breakthrough Represents Biggest Change to Computer Chips in 40 Years. www.intel.com (January 27, 2007) (09/2007).

3. Ramanathan, R. M.; Willoner, R. Silicon Innovation Leaping: from 90nm to 65nm. www.intel.com (09/2007).

4. Intel Unveils World's Most Advanced Chip-Making Process. http://www.intel.com/pressroom/archive/releases/20020813tech.htm (09/2007).

5. Association, S. I., International Technology Roadmap for Semiconductors 2006 update. **2006**.

6. Mack, C. A., *Inside Prolith: A Comprehensive Guide to Optical Lithography Simulation*. Finle Technologies: Austin, TX, 1997; p 72-78.

7. http://www.chbe.gatech.edu/henderson/ (09/2007).

8. May, G. S.; Sze, S. M., *Fundamentals of Semiconductor Fabrication*. John Wiley and Sons: Hoboken, NJ, 2004; p 68-69.

9. Helbert, J. N.; Daou, T., Resist Technology—Design, Processing, and Applications. In *Handbook of VLSI Microlithography - Principles, Tools, Technology and Applications*, 2nd ed.; Helbert, J. N., Ed. William Andrew Publishing/Noyes: New York City, NY, 2001; p 96.

10. Leuschner, R.; Pawlowski, G., Photolithography. In *Handbook of Semiconductor Technology*, Jackson, K. A.; Schröter, W., Eds. John Wiley and Sons: New York City, NY, 2004; Vol. 2, p 84.

11. Hinsberg, W. D.; Wallraff, G. M., Lithographic Resists. In *Kirk Othmer Encyclopedia of Chemical Technology*, John Wiley and Sons: New York City, NY, 2001; Vol. 15, pp 35, 37.

12. Flamm, D. L.; Herb, G. K., Plasma Etching Technology - An Overview. In *Plasma Etching - An Introduction*, Manos, D. M.; Flamm, D. L., Eds. Academic Press: New York Ciyt, NY, 1989; p 14.

13. Fraser, D. B.; Westwood, W. D., Techniques for IC Processing. In *Handbook of Plasma Processing Technology - Fundamentals, Etching, Deposition, and Surface Interactions*, Rossnagel, S. M.; Cuomo, J. J.; Westwood, W. D., Eds. William Andrew Publishing/Noyes: New York City, NY, 1990; p 12.

14. Hiraga, T.; Reid, C.; Suzuki, T., Rapid and selective post-etch residue removal for Cu and low-k devices. *Solid State Technology* 2005.

15. Kern, W., Overview and Evolution of Semiconductor Wafer Contamination and Cleaning Technology. In *Handbook of Semiconductor Wafer Cleaning Technology - Science, Technology, and Applications*, Kern, W., Ed. William Andrew Publishing/Noyes: 1993.

16. Hattori, T., Implementing a single-wafer cleaning technology suitable for minifab operations. *Micro* 2003.

17. Oehrlein, G. S.; Kurogi, Y., Sidewall Surface Chemistry in Directional Etch Processes. *Materials Science and Engineering* **1998,** 24, 153-183.

18. Maex, K.; Baklanov, M. R.; Shamiryan, D.; Iacopi, F.; Brongersma, S. H.; Yanovitskaya, Z. S., Low dielectric constant materials for microelectronics. *Journal of Applied Physics* **2003,** 93, (11), 8793-8841.

19. Louis, D.; Lajoinie, E.; Pires, F.; Lee, W. M.; Holmes, D., *Microelectronics Engineering* **2002,** 41-42, 415.

20. Van Zant, P., *Microchip Fabrication*. 5th ed.; McGraw-Hill: New York City, NY, 2004; p 411.

21. Song, J.-I.; Novak, R., Using an immersion-type BEOL cleaner with hydroxylamine and fluorine chemistries. *Micro* 2003.

22. Radzewich, C., personal communication. In Hayward, CA, 2006.

23. Beery, D.; Reinhardt, K.; Smith, P. B.; Kelley, J.; Sivasothy, A. In Proceedings of the IEEE International Interconnect Technology Conference, 1999; 1999; p 140.

24. Pawsat, S., White Paper on Novel Wafer Cleaning Technologies. *Electrochemical Society Proceedings* **2001,** 2001-6, 94-113.

25. Semitool, Advances in BEOL Cleans Cu Interconnects/ Al Interconnects. In U.S. Technical Seminar Tour June 8 - July 21, 2005: San Jose, CA, 2005.

26. Singer, P., Wafer Cleaning and Surface Prep: Evolution to Revolution. *Semiconductor International* April 1, 2007.

27. Donohoe, K. G.; Turner, T.; Jackson, K. A., Etching Processes in Semiconductor Manufacturing. In *Handbook of Semiconductor Technology*, Jackson, K. A.; Schroter, W., Eds. John Wiley and Sons: New York City, NY, 2004; Vol. 2, p 331.

28. Biberger, M. A.; Schilling, P.; Frye, D.; Mills, M. E., Photoresist and Photoresist Residue Removal with Supercritical CO_2 - A Novel Approach to Cleaning Wafers. *Semiconductor Fabtech* 2005, pp 239-243.

29. Myneni, S.; Hess, D. W., Post Plasma Etch Residue Removal Using CO_2-Based Mixtures: Mechanistic Considerations. *Journal of The Electrochemical Society* **2005,** 152, (10), G757-G765.

30. Myneni, S.; Hess, D. W., Post-Plasma-Etch-Residue Removal Using CO_2-Based Fluids. *Journal of The Electrochemical Society* **2003,** 150, (12), G744-G750.

31. Korzenski, M. B.; Ghenciu, E. G.; Xu, C.; Baum, T. H. Removal of particle contamination on patterned silicon/silicon dioxide using supercritical carbon dioxide/chemical formulations. US Patent Number 6,943,139, 2002.

32. Eco-Snow Systems and IMEC to Develop and Study Photoresist and Particle Removal Technology. *Business Wire* July 17, 2007.

33. Spuller, M. Resist and Residue Removal Using Gas Expanded Liquids. PhD, Georgia Institute of Technology, Atlanta, 2003.

CHAPTER 2

GAS EXPANDED LIQUIDS (GXLS)

Introduction

As the feature sizes of integrated circuits (ICs) decrease, transport of liquid solvents (cleaning solutions) into and out of the vias and trenches becomes more difficult due to surface tension[1]. Vias are high aspect ratio holes that vertically connect the metal layers in an integrated circuit whereas trenches horizontally connect the various transistors and other devices. The vias and trenches are later filled with metal lines during dual damascene processes for copper. Surface tension during cleaning and drying operations using liquids generates capillary forces that can cause feature collapse[2]. Possible alternatives to liquids are supercritical fluids (SCFs) and gas expanded liquids (GXLs) which have lower surface tensions. Another reason to consider these alternatives relative to atmospheric pressure liquids relates to environmental concerns with the large volumes of hazardous chemicals and DI water used by the microelectronics industry. Increased legislative restrictions on the use of many liquids currently employed may force companies to invoke GXLs or SCFs for photoresist and etch residue removal process as well as rinsing and drying steps, since they require lower volumes of liquids.

Carbon Dioxide in SCFs and GXLs

The need for a fluid that can penetrate into the small geometries that will be used in future microelectronic devices and that can meet the environmental regulations on toxic chemicals and water has generated an interest in SCFs and GXLs. SCFs and GXLs both utilize fluids at high pressures (>1000 psi) and moderate to high temperatures

(>50°C). The gas used in both fluids is currently CO_2 because it is benign in nature, relatively environmentally friendly, not explosive, non-flammable, inexpensive, and readily available. In addition, it has an easily attainable supercritical condition due to its low critical temperature of 31°C and reasonable critical pressure of 1070psi. A SCF is a fluid at conditions above its critical temperature and pressure. The SCF has characteristics of both a gas and liquid and properties that lie between these extremes as indicated in Table 2.1.

Table 2.1: Gas, liquid, and supercritical properties of a typical organic fluid[3].

	Density (g/ml)	Diffusivity (cm^2/s)	Dynamic Viscosity (g/cm-s)
Gas	1×10^{-3}	1×10^{-1}	1×10^{-4}
Liquid	1.0	5×10^{-6}	1×10^{-2}
Supercritical Fluid	3×10^{-1}	1×10^{-3}	1×10^{-4}

Although pure CO_2 at supercritical conditions is a relatively poor solvent, supercritical CO_2 (SCCO2) with additives can serve as a potent solvent. $SCCO_2$ functions as a nonpolar solvent and thus displays moderate solubility for organic species. In addition, CO_2 can behave as a Lewis base or acid[4]. $SCCO_2$ is used in conjunction with a cosolvent in various chemical extraction and purification processes[5]. One well known process is the decaffeination of tea and coffee. Only the caffeine is selectively removed in the $SCCO_2$-based mixture and after decompression the CO_2 can be recycled as an added benefit[6].

SCFs have one phase whereas GXLs have two phases, liquid and gas. However, only the liquid phase in a GXL is used as the solvent in contact with the material to be solubilized. In comparison to SCFs, GXLs have lower operating pressure conditions and a higher liquid fraction is present. Due to the inclusion of more liquid, GXLs have

inferior transport properties compared to SCFs but have superior solvent capabilities. Figure 2.1 illustrates the transport ability and solvent power differences between the gases, SCFs, GXLs, and liquids.

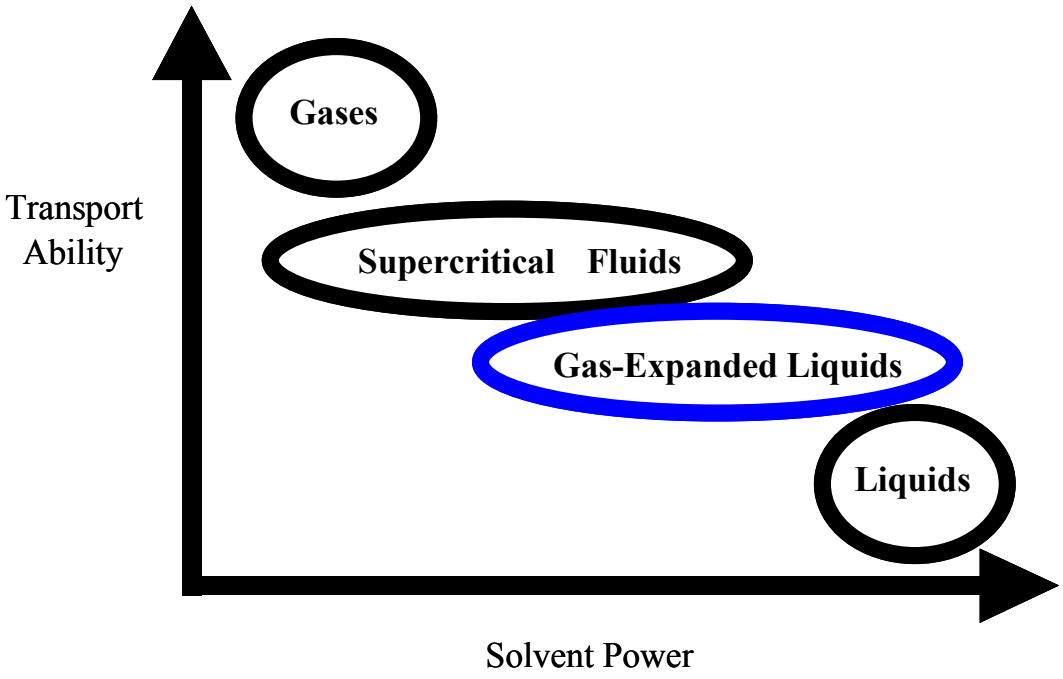

Figure 2.1: Diagram of transport ability and solvent power of gases, SCFs, GXLs, and liquids[7].

As is evident from Table 2.1, gases and SCFs have higher diffusivities and lower viscosities than GXLs, so their transport properties are enhanced relative to those of GXLs. However, liquids and GXLs with their larger liquid solvent content have better solvent power for photoresist and etch residue removal applications.

Unique Characteristics of GXLs

In GXLs, the liquid/gas combination allows increased tunability of physical properties such as viscosity and density. Furthermore, the key attributes of tunability and reduced volumetric use of liquids with the incorporation of CO_2 make GXLs an excellent choice for removing photoresists and etch residues. In addition, because GXLs require

lower pressures, the elevated pressure equipment is less expensive and the transition from a liquid system to a GXL system should be somewhat easier as compared to a liquid to SCF transition.

Although SCFs have been intensively investigated, GXLs have not garnered as much support. However, GXLs have been employed for crystallization[8], separation processes[9-11], and amine formation and separation[12]. The use of GXLs in microelectronics processing has been initially investigated by Spuller with respect to general feasibility and the identification of fundamental concerns[13]. In order to demonstrate the tunability of GXLs, Spuller derived expressions for the dependence of viscosity and diffusivity on GXL composition GXLs by fitting experimental data and using literature correlations[14]. Equation 2.1 describes viscosity and Equation 2.2 describes density in GXLs with varying gas mole fraction.

$$\frac{\mu_{GXL}}{\mu_L} = \mu_{CO_2}^{1-x}\,\mu_L^{x-1} \qquad (2.1)$$

where μ = viscosity (g/cm-s)

x = mole fraction of liquid in GXL

$$\frac{D_{GXL}}{D_L} = \left[\left(\frac{\phi_{CO_2}}{\phi_L}(1-x)+x\right)\left(\frac{M_{CO_2}}{M_L}(1-x)+x\right)\right]^{0.5}\frac{\mu_L}{\mu_{GXL}} \qquad (2.2)$$

where D = diffusivity (cm^2/s)

ϕ = solvent association factor

x = mole fraction of liquid in GXL

μ = viscosity (g/cm-s)

M = molecular weight (g/mole)

These equations demonstrate that GXL properties such as viscosity and diffusivity can be tuned by varying the mole fraction of gas dissolved in the GXL; mole fraction variation can be achieved by changing the pressure. Other properties that can be tuned are density and surface tension. Density and pressure change with mole fraction of CO_2 in methanol is portrayed in Figure 2.2.

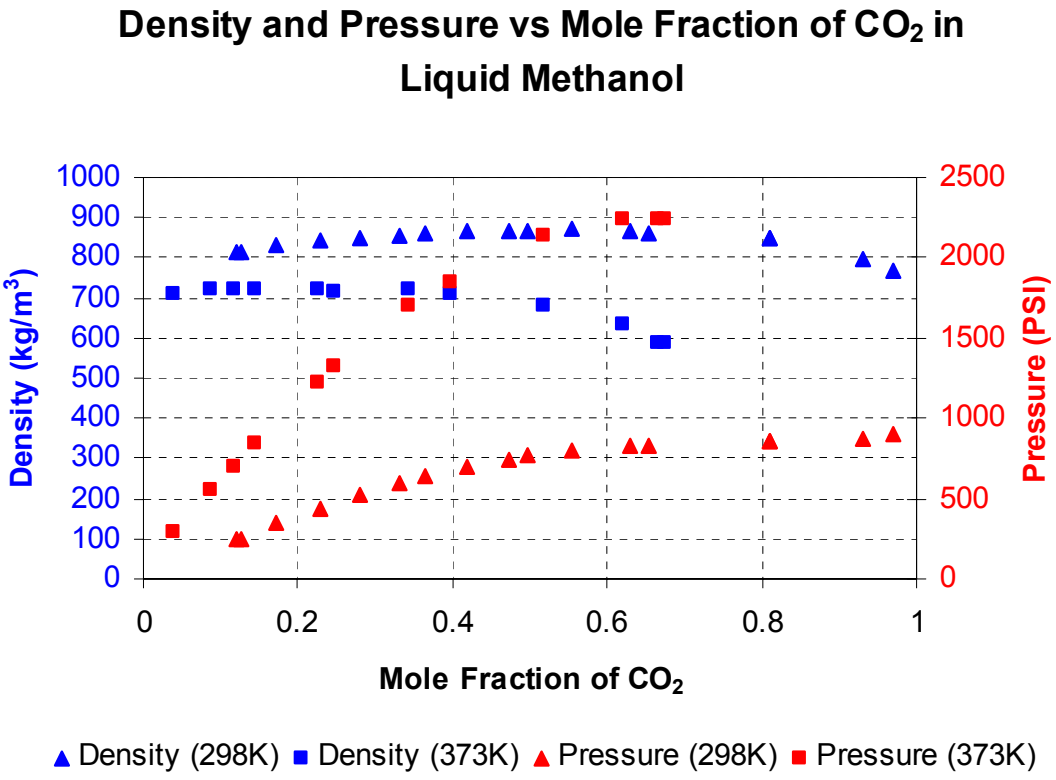

Figure 2.2: Pressure and density values as a function of CO_2 mole fraction in methanol [15].

Figure 2.3 shows the decrease in surface tension for ethanol when CO_2 has been added at different temperatures.

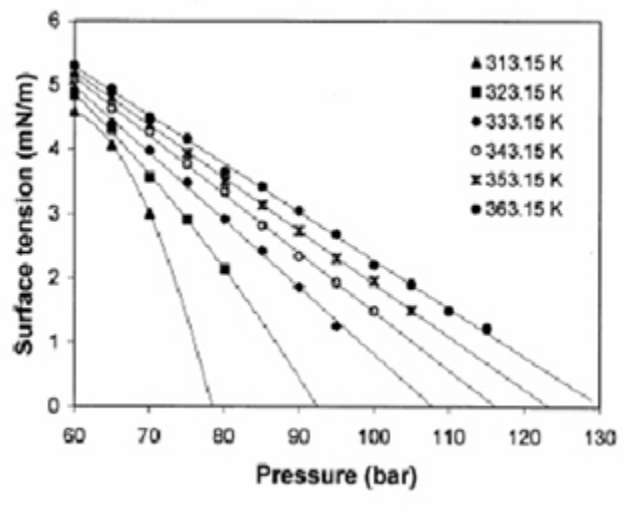

Figure 2.3: Surface tension of liquid ethanol as a function of CO_2 pressure at different temperatures [16].

SCFs and GXLs function in a similar manner for photoresist and etch residue removal in that swelling by CO_2 facilitates penetration of the photoresist/residue by the cosolvents and additives. However, the role of CO_2 in the GXL is not well understood because CO_2 may simply act as a diluent but more likely plays a more important role. The combination of the liquid in GXL and the CO_2 dissolved in it behaves differently from a one phase supercritical system. CO_2 swells polymeric films such as photoresist, especially if the temperature is above the glass transition temperature (T_g) of the film[17]. Film swelling decreases polymer-polymer and polymer-substrate interactions and thereby aids in removal. In addition, mechanical pulsing of CO_2 pressure facilitates film swelling and can even crack the photoresist film[17]. In conjugation with swelling and mechanical destruction of the photoresist film by high pressure CO_2, the cosolvent can penetrate underneath the film in order to lift it from the surface. Various cosolvents have been investigated such as tetramethylammonium hydroxide (TMAH)[18], propylene carbonate (PCO_3)[19], nitrogen-containing bases[19], and ozonated water[20]. In most cases, the cosolvent is only 5 wt% of the fluid[21]. However, for GXLs the cosolvent amount is much higher,

and the CO_2 is dissolved in the cosolvent rather than the cosolvent dissolved in the CO_2. Due to the higher solvent power of GXLs and the ability to tune their properties, this class of fluids offers the potential of high effectiveness for photoresist and etch residue removal in IC processing.

References

1. Spuller, M. T.; Hess, D. W., Incomplete wetting of nanoscale thin-film structures. *J. Electrochem. Soc.* **2003,** 150, G476-G480.

2. Weibel, G. L.; Ober, C. K., An overview of supercritical CO_2 applicatons in microelectronics processing. *Microelectronics Engineering* **2003,** 65, 145-152.

3. Manivannan, G.; Sawan, S. P., The Supercritical State. In *Supercritical Fluid Cleaning Fundamentals, Technology, and Applications*, McHardy, J., Ed. Noyes Publications: Westwood, NJ, 1998.

4. Mount, D. J.; Rothman, L. B.; Robey, R. J.; Ali, M. K., The technology behind cleaning with supercritical fluids. *Solid State Technology* 2002, pp 103-105.

5. Suzuki, I., Application of supercritical fluid for food processing. *Reito* **2006,** 81, (949), 922-927.

6. Park, H. S.; Lee, H. J.; Shin, M. H.; Lee, K.-W.; Lee, H.; Kim, Y.-S.; Kim, K. O.; Kim, K. H., Effects of cosolvents on the decaffeination of green tea by supercritical carbon dioxide. *Food Chemistry* **2007,** 105, (3), 1011-1017.

7. Hallett, J.; Kitchens, C.; Hernandez, R.; Liotta, C. L.; Eckert, C. A., Probing the Cybotactic Region in Gas-Expanded Liquids (GXLs). *Acc. Chem. Res.* **2006,** 39, 531-538.

8. Bertucco, A., Precipitation and Crystallization Techniques. In *Chemical Synthesis Using Supercritical Fluids*, Jessop, P. G.; Leitner, W., Eds. Wiley-VCH: New York City, NY, 1999.

9. Lee, S. T.; Olesik, S. V.; Fields, S. M., *Journal of Microcolumn Separations* **1995,** 7, 477-483.

10. Chang, C. J.; Randolph, A. D., *Biotechnology Progress* **1991,** 7, 275-278.

11. Eckert, C. A.; Bush, D.; Brown, J. S.; Liotta, C. L., *Ind. Eng. Chem. Res.* **2000,** 39, 4615-4621.

12. Xie, X.; Liotta, C. L.; Eckert, C. A., CO_2- Protected Amine Formation from Nitrile and Imine Hydrogenation in Gas-Expanded Liquids. *Ind. Eng. Chem. Res.* **2004,** 43, 7907-7911.

13. Spuller, M. T.; Hess, D. W. Gas-expanded liquids, methods of use thereof, and systems using gas-expanded liquids for cleaning integrated circuits of photoresists. U.S. Pat. 6,786,977, 2004.

14. Spuller, M. Resist and Residue Removal Using Gas Expanded Liquids. PhD, Georgia Institute of Technology, Atlanta, 2003.

15. Brunner, E.; Hultenschmidt, W.; Schlichtharle, G., Fluid mixtures at high pressures IV. Isothermal phase equilibria in binary mixtures consisting of (methanol+hydrogen or nitrogen or methane or carbon monoxide or carbon dioxide. *J. Chem. Thermodynamics* **1987,** 19, 273-291.

16. Sun, Y.; Shekunov, B. Y., Surface tension of ethanol in supercritical CO2. *J. of Supercritical Fluids* **2003,** 27, 73-83.

17. King, J. W.; Williams, L. L., Utilization of critical fluids in processing semiconductors and their related materials. *Current Opinion in Solid State and Materials Science* **2003,** 7, 413-424.

18. Levitin, G.; Myneni, S.; Hess, D., Post Plasma Etch Residue Removal Using CO2-TMAHCO3 Mixtures: Comparison of Single-Phase and Two-Phase Mixtures. *Journal of the Electrochemical Society* **2004,** 151, (6), G380-G386.

19. Rubin, J. B.; Davenhall, L. B.; Taylor, C. M. V.; Sivils, L. D.; Pierce, T.; Tiefert, K., CO_2 Based Supercritical Fluids as Replacements for Photoresist-Stripping Solvents.

20. DeGendt, S.; Knotter, D.; Heyns, M.; Meuris, M.; Mertens, P. Method for removing organic contaminants from a semicondcutor surface. patent number 6551409, 2003.

21. Pawsat, S., White Paper on Novel Wafer Cleaning Technologies. *Electrochemical Society Proceedings* **2001,** 2001-6, 94-113.

CHAPTER 3

ANALYTICAL TECHNIQUES

In order to characterize and analyze films exposed to GXLs and other fluids, a broad spectrum of analytical techniques were implemented. Surface characterization was performed using x-ray photoelectron spectroscopy (XPS) and goniometry. Thicknesses were measured using ellipsometry. Bulk composition and bonding in films were characterized using Fourier transform infrared spectroscopy (FTIR). Mass uptake was measured using quartz crystal microbalance (QCM). Electrical characterization was interpreted through current-voltage (IV) and capacitance-voltage (CV) plots using a semiconductor parameter analyzer and CV analyzer.

X-ray Photoelectron Spectroscopy

Surface properties such as elemental composition and bonding structures are obtained using x-ray photoelectron spectroscopy (XPS). Elemental composition is important because photoresist and etch residue complete removal can be confirmed by atomic composition percentages. For example, a silicon atomic percentage above 22% represents complete removal of photoresist and etch residue[1] for the samples tested in Chapter 4. This removal was also confirmed via scanning electron microscopy (SEM). In addition to atomic percentage compositions, XPS signals are sensitive to bonding structures. For instance, etch residue that results from fluorocarbon plasma etching, contains carbon bonded to fluorine as C-F, C-F_2, C-F_3, or C-C-F_x[2]. Each of these bonds results in different peaks or binding energy shifts in the XPS spectrum as shown in Figure 3.1.

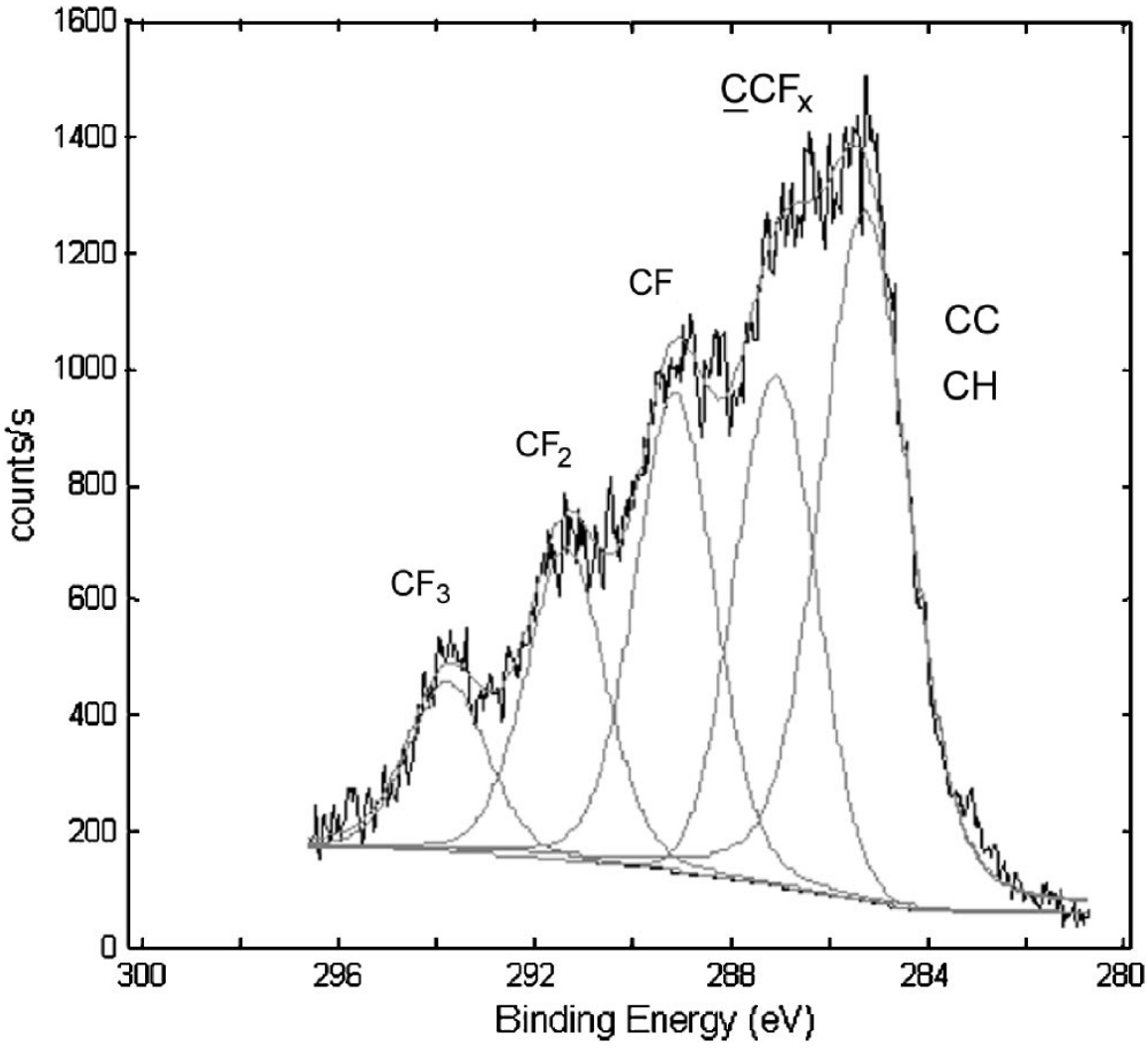

Figure 3.1: XPS spectra for fluorocarbon post etch residue. Different peaks for each bonding structure[2].

In XPS analysis, an x-ray impacts an atom and upon energy transfer to core electrons, the energized electrons escape the coulombic attraction from the nucleus. This transition is known as the photoelectric effect; Figure 3.2 shows a schematic photoelectric effect.

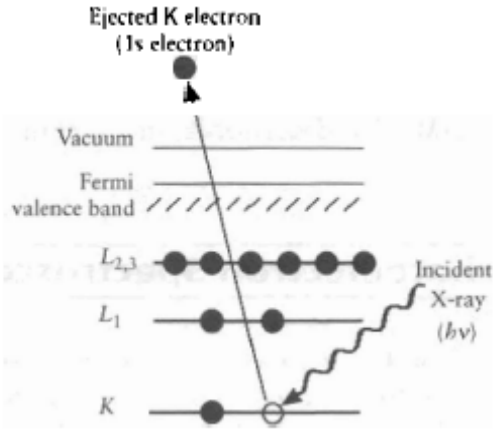

Figure 3.2: Photoelectric effect[3].

An ultra high vacuum environment ~10^{-9} torr is necessary to maximize the number of electrons that are detected and not lost by collisions with gas molecules in the XPS chamber. An electron spectrometer measures the velocity of the emitted electron in order to determine the kinetic energy and thereby calculate the binding energy of the electron (to the solid) which gives a unique signature for each element. Equation 3.1 is used to calculate the binding energy[3].

$$E_B = h\nu - E_K - W \qquad (3.1)$$

where E_B = binding energy (eV)

$h\nu$ = x-ray energy (eV)

E_K = kinetic energy (eV)

W = work function (eV)

The x-ray energy is known and is a function of the metal used to generate the x-ray. Our system uses an Al k alpha source which gives a photon energy range from 0 to 1486eV. Kinetic energy can be calculated from the known velocity of the escaped electron, while the work function is a known property of the spectrometer.

A typical XPS spectrum displays intensity along the ordinate and binding energy along the abscissa. Each element has a unique XPS spectrum because each electron escapes at a specific binding energy. XPS can detect atoms to a depth of ~10nm and our particular system averages over an area corresponding to an 800μm diameter spot. For general XPS analyses, a survey scan was performed at 187.85eV pass energy with a step size of 0.5eV and 50ms. The pass energy is the energy range allotted to the detector; a large pass energy allows higher electron counts at the expense of lower resolution. After survey scans, specific binding energy regions were scanned at the lower pass energy of 46.95eV with a step size of 0.025eV; 100ms/step was used for higher resolution studies.

A neutralizer or electron flood gun was used to neutralize charge build up on the insulating surfaces being analyzed. Neutralizer alignment was performed using carbon at 284.8eV as the reference peak. All samples contain adventitious carbon that arises from the exposure of samples to atmospheric conditions; adventitious carbon is indicated by a C-C bonding peak at 284.8eV[4]. The XPS system is a Phi model SCA 1600/3057. The software used for data collection is Phi PC Explorer version 3.4 while Multipak version 8.2B was used to deconvolute curves such as those in Figure 3.1. Gaussian and Lorentzian curves served as fits for the deconvolution.

Variable Angle Spectroscopic Ellipsometry

Thin films thicknesses measurements on the order of nanometers are performed using variable angle spectroscopic ellipsometry (VASE). Measurement of the film thickness before and after processing determines whether film etching or film growth has occurred. Ellipsometry measures the change in polarization and amplitude of a light beam after it reflects off a transparent film to establish the thickness (and refractive

index) of the specified film[5]. In addition, the angle of the incident light can varied to maximize sensitivity and accuracy[6]. Polarization of the light refers to the direction of the transverse electric field; the electric field is perpendicular to the magnetic field. The light is set to a known polarization state based on orientation and phase of the electric field vector. At this point in time the light is linearly polarized where the x and y components of the electric field are in phase with each other and have the same amplitude. After reflection from the film surface, the parallel (s) and perpendicular (p) components of the light beam are out of phase and have different amplitudes in the s and p planes[7], where s refers to the plane of incidence and p is perpendicular to the plane of incidence[5]. Figure 3.3 shows a schematic representation of this process[7].

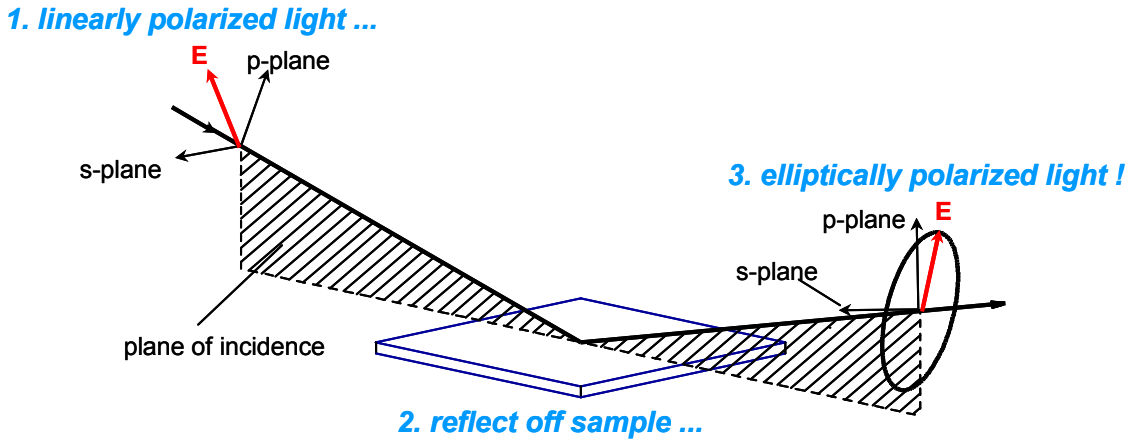

Figure 3.3: Sequence of polarized light reflecting off a sample film[7].

From the elliptically polarized light, the azimuth angle ψ and phase shift Δ can be obtained according to Figure 3.4.

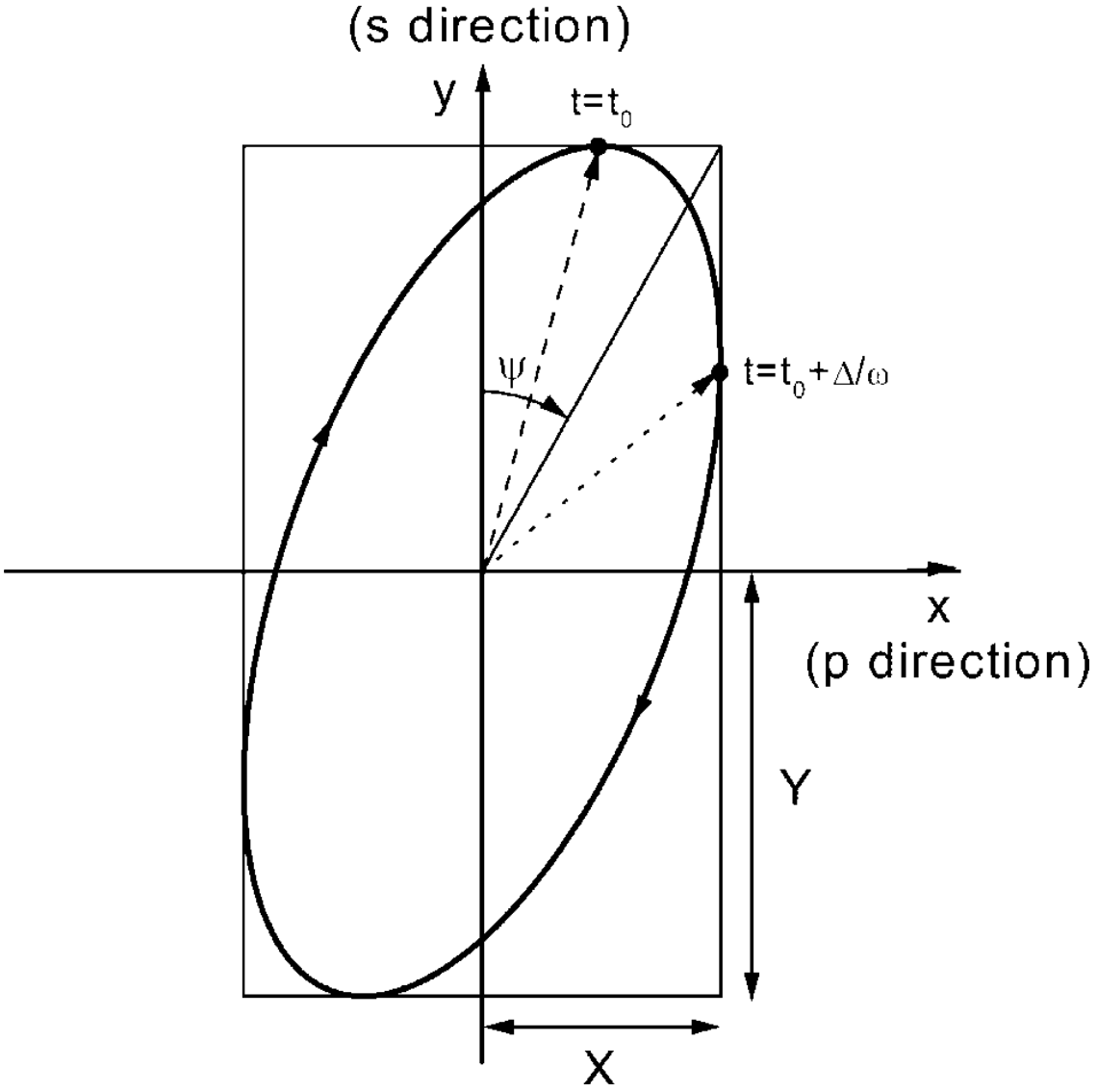

Figure 3.4: Elliptically polarized light where the light is propagating towards the reader[8].

The fundamental equation for ellipsometry uses ψ and Δ to calculate a ratio between total reflection coefficients according to Equation 3.2[5].

$$\frac{R^P}{R^S} = \tan(\psi)e^{i\Delta} \tag{3.2}$$

$$R^P = \frac{r_{12}^P + r_{23}^P \exp(-i2\beta)}{1 + r_{12}^P r_{23}^P \exp(-i2\beta)} \qquad R^S = \frac{r_{12}^S + r_{23}^S \exp(-i2\beta)}{1 + r_{12}^S r_{23}^S \exp(-i2\beta)}$$

$$r_{ab}^p = \frac{\widetilde{N}_b \cos\phi_a - \widetilde{N}_a \cos\phi_b}{\widetilde{N}_b \cos\phi_a + \widetilde{N}_a \cos\phi_b} \qquad r_{ab}^s = \frac{\widetilde{N}_a \cos\phi_a - \widetilde{N}_b \cos\phi_b}{\widetilde{N}_a \cos\phi_a + \widetilde{N}_b \cos\phi_b}$$

$$\widetilde{N} = n - ik$$

$$\beta = 2\pi\left(\frac{d}{\lambda}\right)\widetilde{N}_2 \cos\phi_2$$

where R = total reflection coefficient

r = Fresnel reflection coefficient

β = phase angle (^{o})

ϕ = incidence angle (^{o})

$\widetilde{N}$ = complex refractive index

n = refractive index

k = extinction coefficient

d = film thickness (nm)

λ = wavelength (nm)

Using this ratio in Equation 3.2 and the known or measured refractive indices, incidence angle, and extinction coefficients at specified wavelengths, the thickness of the film can be calculated. Figure 3.5 shows a diagram of a film with incident, reflected, and transmitted light beams labeled according to the parameters indicated above.

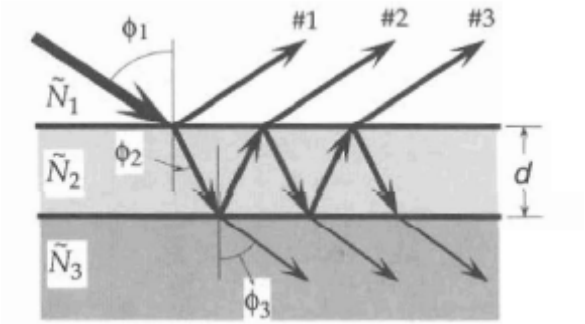

Figure 3.5: Arrows indicate direction of light. One film ($\widetilde{N}_2$) on a substrate ($\widetilde{N}_3$) exposed to air ($\widetilde{N}_1$)[5].

A Cauchy model, Equation 3.3, was used to relate refractive index as a function of wavelength in order to fit the data and thus calculate a thickness for low k dielectric films and photoresist films[5].

$$n(\lambda) = n_o + \frac{n_1}{\lambda^2} + \frac{n_2}{\lambda^4} \tag{3.3}$$

where $n(\lambda)$ = refractive index

n_o, n_1, n_2 = fitted Cauchy parameters

In order to ensure a reasonable fit, a range of wavelengths between 400-1000nm were used in addition to incident angles of 65°, 70°, and 75°. These angles were chosen because they are similar to the Brewster angles for glass at 56° and silicon at 75°, where the Brewster angle is the angle at which $\Delta = 90^o$, at which point the sensitivity is maximized[7]. A J.A. Woollam M-2000VI ellipsometer was used to perform all thickness measurements using WVASE32 version 3.632 for analysis and data fitting.

Goniometry

Goniometry or contact angle measurements were performed to measure the change in hydrophilicity or hydrophobicity of a film before and after GXL processing. Contact angle measurements are important because they can indicate surface changes that resulted from alteration of roughness or chemical bonding structures. Two different types of films were investigated: photoresist and low k dielectrics. For both films, the contact angle using water as the probe liquid is greater than 90° indicating hydrophobicity. However, after GXL processing the photoresist film is removed and the underlying SiO_2 has a contact angle of 25°. The decreased contact angle indicates that the photoresist film has been removed. In the case of low k dielectrics, the decrease in

contact angle may indicate etching of the film as discussed in detail in Appendix A. Young's equation (Equation 3.4) is used to calculate the contact angle[9].

$$\gamma_{lv}\cos\theta_Y = \gamma_{sv} - \gamma_{sl} \quad (3.4)$$

where γ_{lv} = surface tension between liquid and vapor interface (dynes/cm)

γ_{sv} = surface tension between solid and vapor interface (dynes/cm)

γ_{sl} = surface tension between solid and liquid interface(dynes/cm)

θ_Y = contact angle (^{o})

Figure 3.6 illustrates these variables.

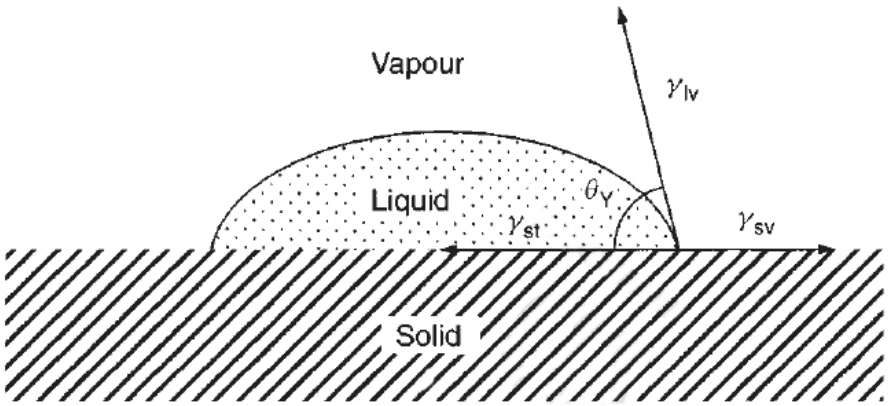

Figure 3.6: Illustration of surface tension between different phases[9].

Although these surface tensions can be calculated or measured in order to calculate contact angle, the contact angle is directly measured by taking a picture of the drop and drawing lines tangent to the drop at the surface to measure the contact angle as shown in Figure 3.7.

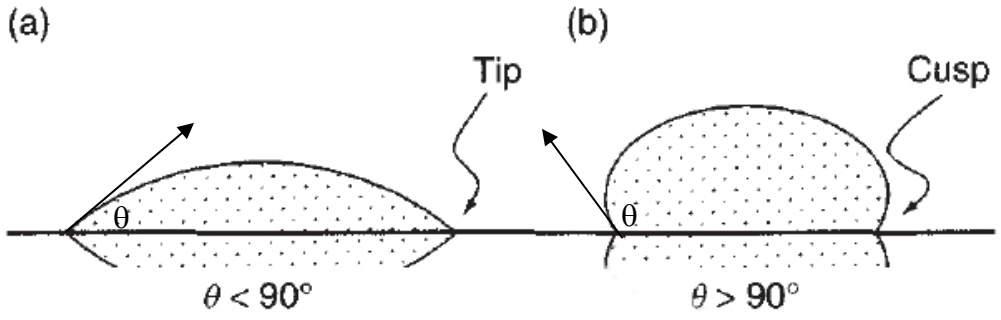

Figure 3.7: A) hydrophilic surface and B) hydrophobic surface.

An AST Products Video Contact Angle System 2500XE was used to measure the contact angles and VCA version 1.52 was used to calculate the contact angles. Contact angle measurements were performed for both the left and right side of the droplet and at least three measurements were averaged. The droplet size was 2μL.

Fourier Transform Infrared Spectroscopy

Like XPS, Fourier transform infrared (FTIR) spectroscopy gives information about chemical bonds and chemical composition, although FTIR probes vibrational modes of bonding structures[10]. Through the use of FTIR spectra we can determine the specific types of chemical bonds present in the bulk film, whereas XPS is sensitive only to surface and near surface bonds. FTIR can detect ~10^{13} bonds/cc with accuracy around 5%[10]. Specifically, FTIR was used in conjunction with XPS to determine bonding changes in low k dielectric films before and after GXL processing.

FTIR uses an infrared radiation source that is transmitted through the film and substrate. The intensity of the beam is measured before and after transmission through the film. The transmission ratio is defined in Equation 3.5.

$$T_w = (I_t/I_o) \qquad (3.5)$$

where T_w = fraction of light transmitted

I_t = transmitted light intensity

I_o = original light intensity

In our studies, absorbance has been measured, where absorbance is the negative log of transmission. The absorbance intensity is measured at different frequencies to create an infrared spectrum as shown in Figure 3.8[10].

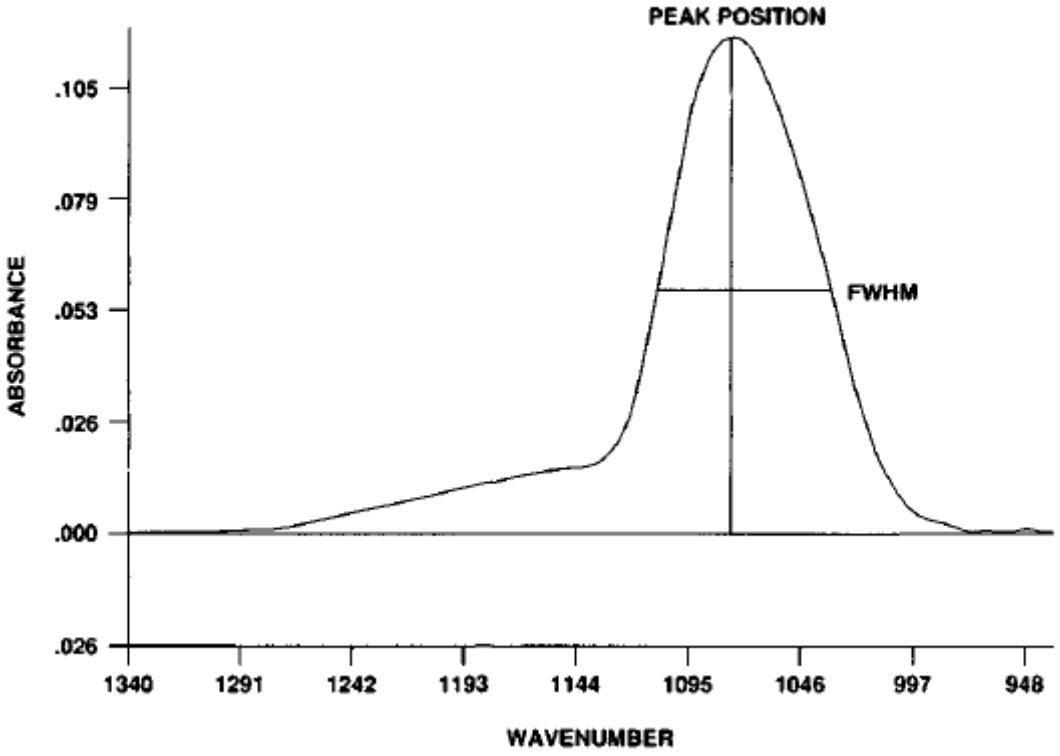

Figure 3.8: Infrared spectrum. FWHM is the full width half maximum. Wavenumbers are typically in units of cm^{-1}.

Fourier transform IR is necessary to change from the intensity-time domain output of the interferometer to the intensity-frequency domain[10]. The infrared beam causes the chemical bonds to vibrate in various ways. Figure 3.9 illustrates typical bond movements.

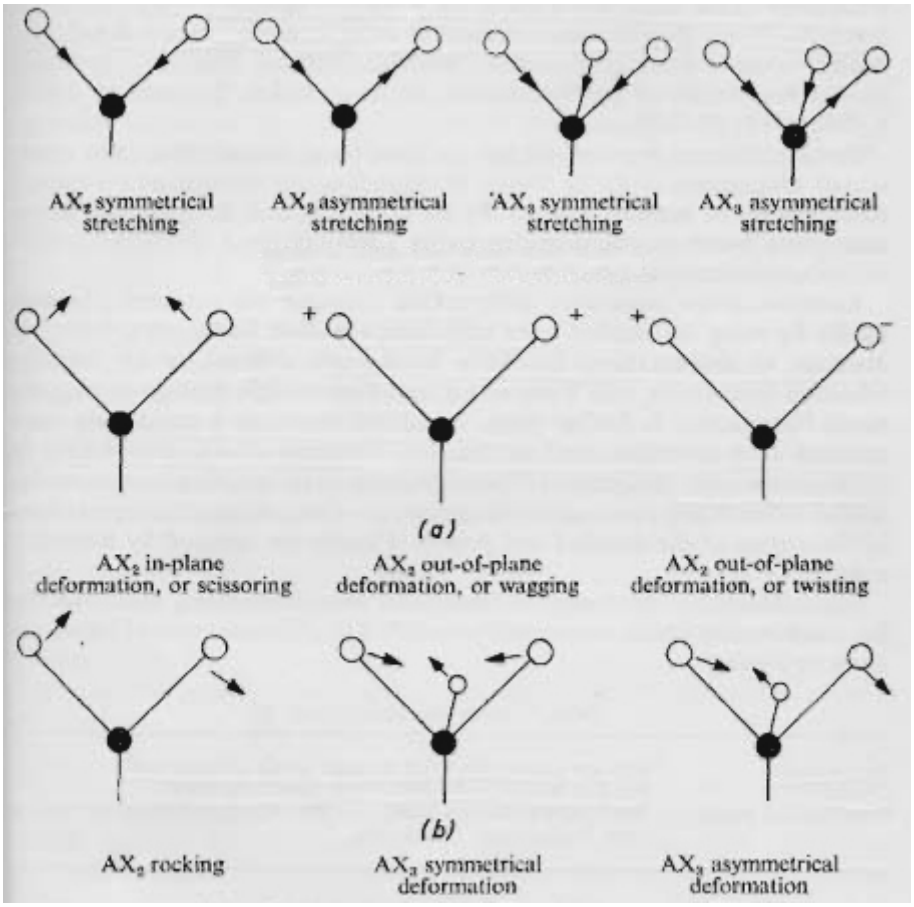

Figure 3.9: Different modes of stretching, vibrating, and deformations of bonds[11].

A Bruker IFS66v/S FTIR was used in conjunction with Opus version 3.1 to analyze the data. The frequency step size was $4cm^{-1}$ and 256 scans were performed for the background sample or substrate and 128 scans were performed for the film with the substrate. The sample chamber was evacuated to 1mbar and purged with nitrogen to reduce moisture.

Quartz Crystal Microbalance

Mass absorption in thin films was measured using a quartz crystal microbalance (QCM). Due to the thin films and small amount of gas absorbed, a very sensitive mass balance such as a QCM is required which can measure on the order of 10^{-9}g. QCM uses a quartz crystal as the substrate onto which a film is deposited. The crystal is sandwiched

between two gold electrodes. Quartz is a piezoelectric material which means that when a mechanical stress (e.g., mass) is applied to the crystal, an electric charge is created but in a closed loop this causes the appearance of a potential difference or voltage. In addition, when a voltage is applied to the crystal, the crystal responds by changing the vibration frequency[12]. The change in frequency can be related to the change in mass using the Sauerbrey equation shown in Equation 3.6[13, 14].

$$\Delta F = F - F_o = \Delta F_m + \Delta F_p + \Delta F_n \qquad (3.6)$$

$\Delta F_p = F_o \alpha P$ $\quad F_o\alpha = 0.43 Hz/psi$ [15] (frequency change due to pressure)

$\Delta F_n = -0.5 C_m (\pi F_o)^{-1/2} (\rho_f \eta_f)^{1/2}$ (frequency change due to viscosity)

$C_m = -2F_o^2/(\mu_q \rho_q)^{1/2}$

$\mu_q = 2.947 \times 10^{11}$ g/cm-s^2

$\rho_q = 2.648$ g/cm^3

$\Delta F_m = -2F_o^2 \Delta m/(\mu_q \rho_q)^{1/2} = -C_m \Delta m/A$ (frequency change due to mass)

$A = 1.53$ cm^2

where F = current frequency (Hz)

F_o = original frequency (Hz)

ΔF_m = frequency change due to mass (Hz)

ΔF_p = frequency change due to pressure (Hz)

ΔF_n = frequency change due to viscosity (Hz)

α = pressure correction factor

C_m = mass sensitivity constant $\left(\frac{Hz^2}{g/cm^2 s} \right)$

ρ_f = density of fluid (g/cm^3)

n_f = viscosity of fluid (g/cm-s)

μ_q = shear modulus of crystal ($g/cm\text{-}s^2$)

ρ_q = density of crystal (g/cm^3)

A = area of crystal (cm^2)

Simply, when mass is loaded onto the quartz crystal, the frequency of the crystal decreases. Different overtones above the fundamental resonant frequency can be measured. For 6MHz crystal, the fundamental frequency is 6MHz and the 3rd and 5th overtones occur at 18MHz and 30MHz. The higher frequencies are more sensitive and measure the mass uptake closer to the crystal substrate[16]. The higher frequencies are more sensitive because a smaller change in mass is reflected in a larger change in frequency. The range used for higher frequencies is greater than the measurement range used for lower frequencies. The overtones measure the mass uptake closer to the film because higher frequencies dissipate faster through the film and hence the resonant wave does not propagate through the entire film[17]. Figure 3.10 demonstrates this phenomena for a thin film[17].

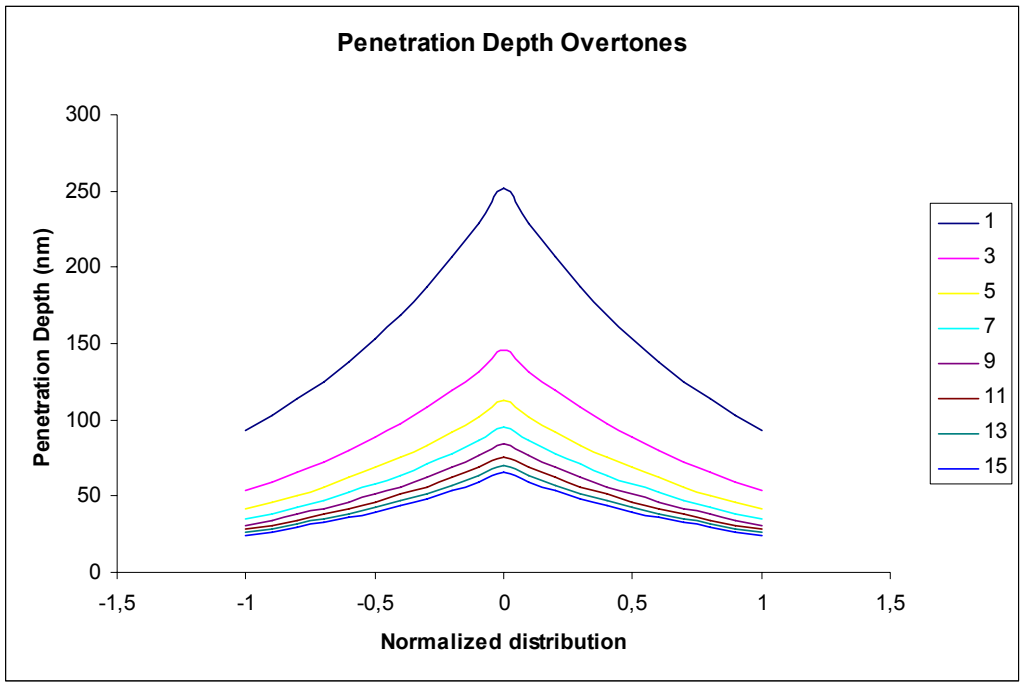

Figure 3.10: Depth profiling using overtones. The numbers in the legend are the overtone numbers[18, 19].

A Maxtek RQCM with RQCM Data Logging Software version1.8.8 and Q-Sense QCM-D with QSoft 301 version1.6.14.47 were used to collect and analyze the QCM data. The Q-Sense QCM-D can also process multiple overtones and measure film dissipation as well. Frequency and dissipation data were collected every 2 seconds.

Electrical Measurements

In order to measure the capacitance-voltage (CV) and current-voltage (IV) curves, an MIS (metal-insulator-semiconductor) structure was fabricated. Silicon substrates were p-type (100) 4" test wafers from Nova Electronic Materials with a boron concentration of 10^{16} to $5.5x10^{14}$ atoms/cm^3 corresponding to resistivities between 1 and 25 ohm-cm. A parallel plate capacitor in Figure 3.11 was created for the electrical characterization measurements.

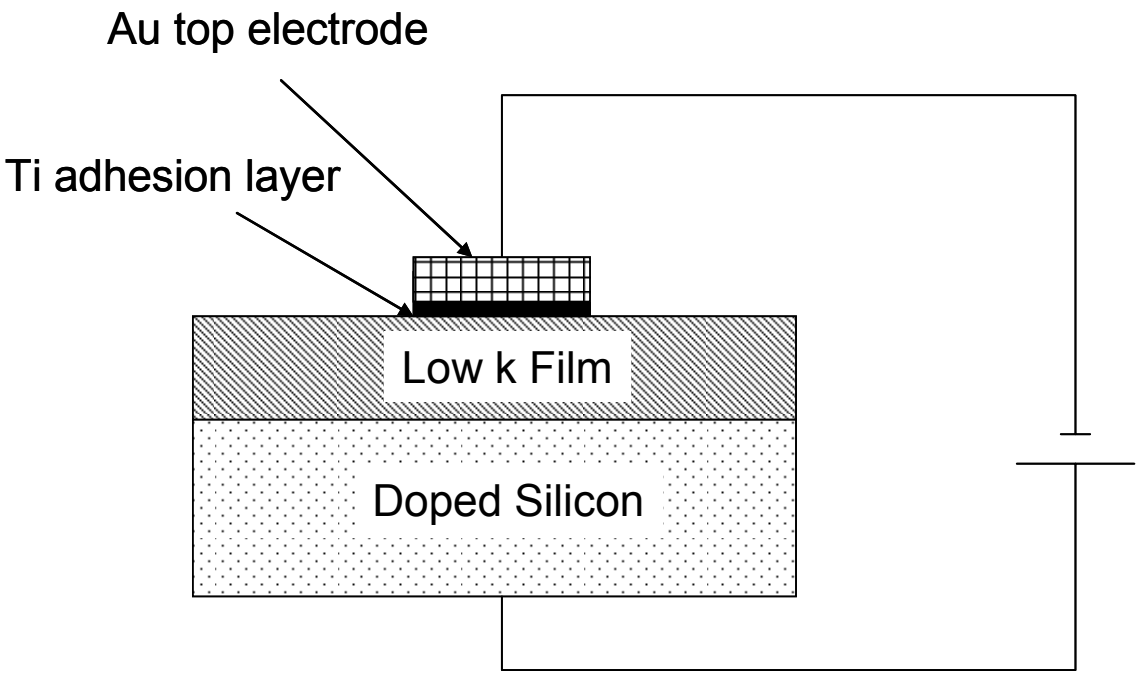

Figure 3.11: Schematic of parallel plate capacitor.

The metal used as the top electrode was gold, the insulation layer was the methylsilsesquioxane (MSQ) film, and the semiconductor was boron-doped silicon as described above. A shadow mask with 2mm diameter holes was used to pattern the top electrodes. Using a CVC e-beam evaporator, 300A of Ti was deposited at 3A/s as an adhesion layer between the MSQ and the subsequent 3000A of Au deposited at 3A/s. Electrode deposition onto the silicon wafer backside was not necessary because of the doped silicon substrate. Metal depositions were performed in a class 1000 cleanroom at the MIRC (Microelectronics Research Center) at Georgia Tech.

Current – Voltage (IV) Curves

IV curves were obtained to measure leakage currents or currents passed through a dielectric material. The low k dielectric films behave as insulators; however, upon application of high voltages the film begins to conduct current. This voltage is known as the breakdown voltage. The breakdown voltage depends on film thickness so instead,

electric field breakdown which is voltage per unit length will be referenced. At this point, the circuit is "open" in that the current passes directly through the dielectric from the top electrode to the bottom electrode. The dielectric has failed because it is no longer behaving as an insulator and storing a charge. Instead, the high voltage has caused ionization of electrons from atoms in the solids and the electric field causes current or electron transport through the film[20]. A HP 4156A Precision Semiconductor Parameter Analyzer was used with a voltage step size of 0.1V for a range between -20V and 20V.

Capacitance – Voltage (CV) Curves

In addition to IV curves, CV curves were obtained which were used to calculate dielectric constants for the low k films via Equation 3.7.

$$k = \frac{cd}{A\varepsilon} \tag{3.7}$$

where k = dielectric constant

c = capacitance (F)

d = film thickness (m)

A = area of electrode (m^2)

ε = permittivity in a vacuum (8.854×10^{-12} F/m)

The capacitance was measured in the accumulation region of the CV curves. An accumulation region is established when the majority carriers in a semiconductor are attracted to the surface by an applied field[21]. A p-type silicon wafer has a higher concentration of holes relative to the concentration of electrons, so that holes are the majority carriers and electrons are the minority carriers. When a negative potential is applied to the top metal electrode, this attracts holes to the semiconductor surface where

they begin to "concentrate" or accumulate. As the applied potential changes from negative to positive, the holes begin to move away from the silicon surface and the positive potential attracts the electrons instead at which point inversion has occurred[21]. For p-type silicon, accumulation of holes at the surface occurs when a more negative voltage is applied. Likewise for n-type silicon, accumulation of electrons at the surface occurs when a more positive voltage is applied. Band diagrams indicating accumulation, depletion, and inversion are shown in Figure 3.12

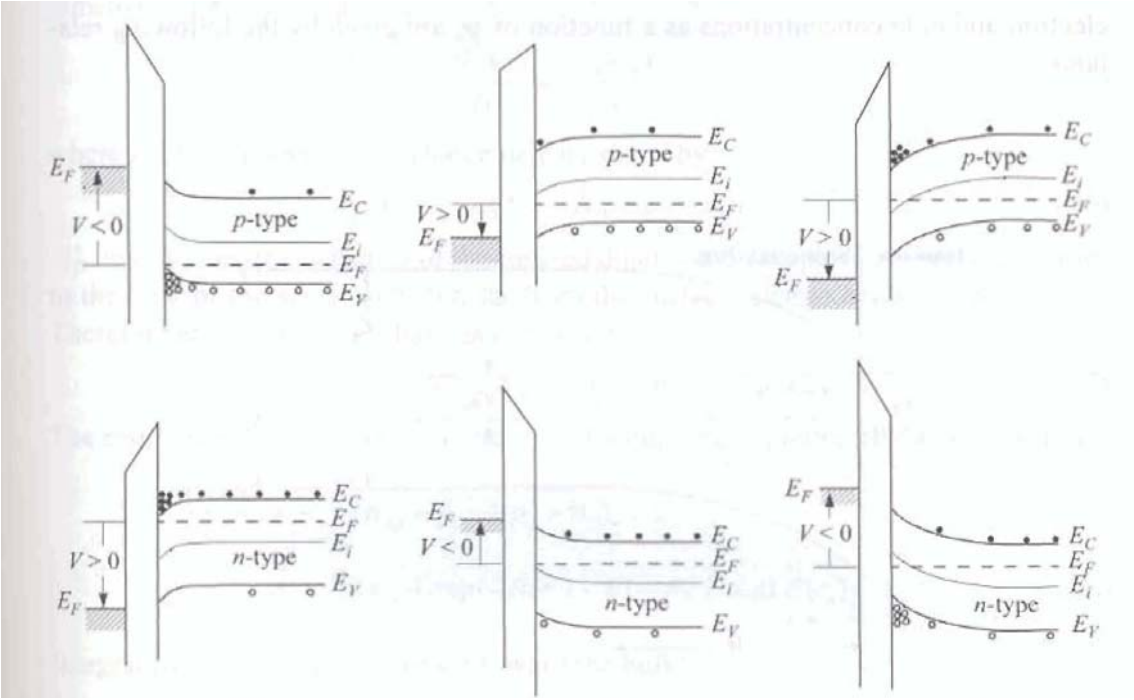

Figure 3.12: Accumulation, depletion, and inversion in p and n-type wafers. Black dots are electrons and white dots are holes. E_F = Fermi energy band, E_C = conduction energy band, E_i = intrinsic energy band, and E_V = valence energy band[22].

In the accumulation region, the capacitance is measured for the dielectric constant calculation because the thickness of the depletion region is effectively zero in the accumulation regime. The depletion region has zero thickness under accumulation because the majority carriers are attracted to the semiconductor surface. However, at

inversion the surface depletion region thickness is the largest which adds an additional capacitor to the overall dielectric film thickness. If the resulting capacitance was used to calculate the dielectric constant an incorrect value would be calculated[21]. Figure 3.13 and Figure 3.14 illustrate the different regions for a CV curve for p-type and n-type silicon wafers, respectively.

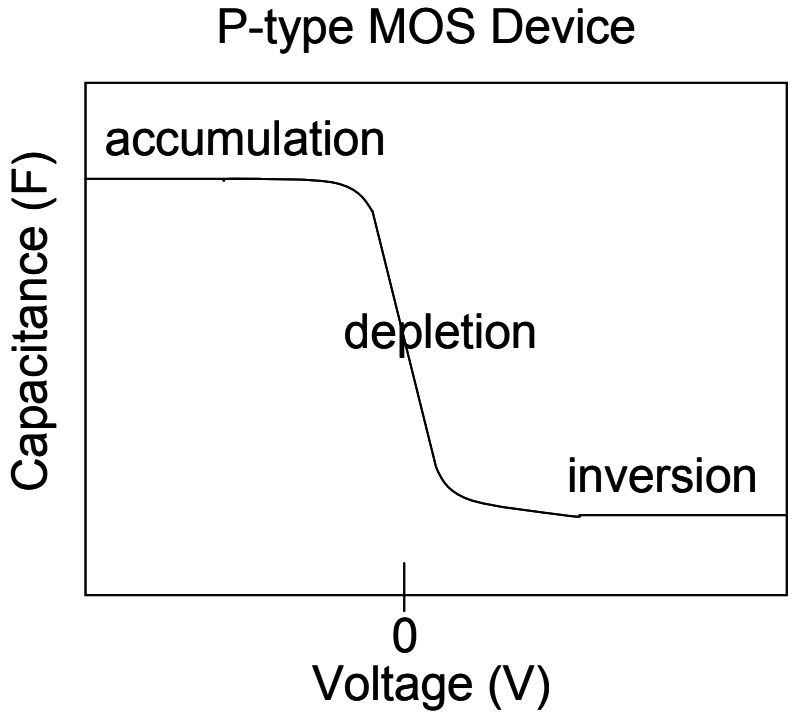

Figure 3.13: CV curve for p-type silicon wafer.

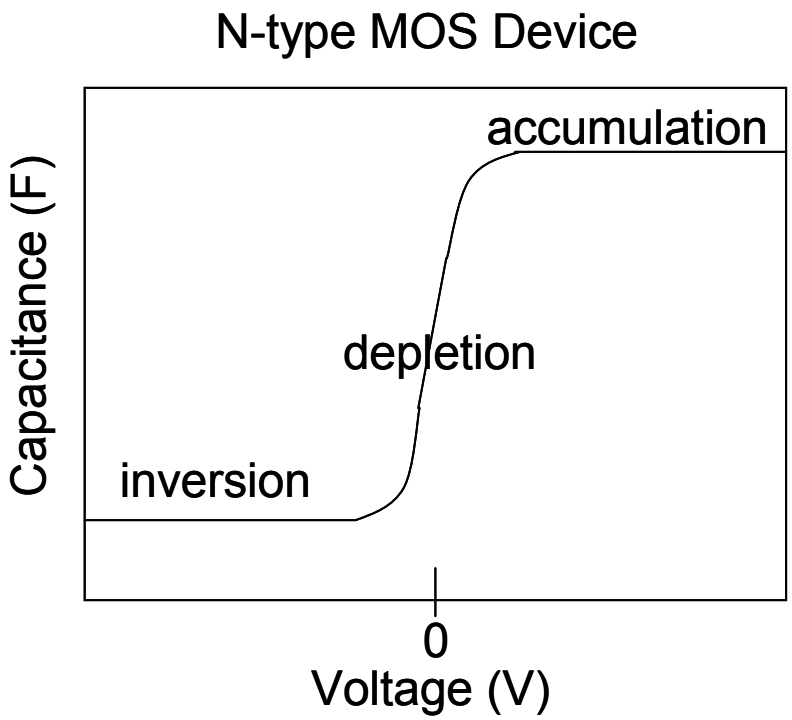

Figure 3.14: CV curve for n-type silicon wafer.

A Keithley 590 CV Analyzer with Labview version 6.1 was used to collect and analyze the CV data. The step size used was 0.1V from -20V to 20V at 100kHz.

References

1. Myneni, S.; Hess, D. W., Post-Plasma-Etch-Residue Removal Using CO_2-Based Fluids. *Journal of The Electrochemical Society* **2003,** 150, (12), G744-G750.

2. Timmons, C. L.; Hess, D. W., Electrochemical Cleaning of Post-Plasma Etch Fluorocarbon Residues Using Reductive Radical Anion Chemistry. *Electrochemical and Solid-State Letters* **2004,** 7, (12), G302-G305.

3. Watts, J. F.; Wolstenholme, J., *An Introduction to Surface Analysis by XPS and AES*. John Wiley and Sons: New York City, NY, 2003; p 1-8.

4. Barr, T. L.; Seal, S., Nature of the use of adventitious carbon as a binding energy standard. *Journal of Vacuum Science & Technology, A: Vacuum, Surfaces, and Films* **1995,** 13, (3, Pt. 2), 1239-1246.

5. Tompkins, H. G.; McGahan, W. A., *Spectroscopic Ellipsometry and Reflectometry: A User's Guide*. John Wiley and Sons: New York City, NY, 1999; p 18-20, 28.

6. Woollam, J. A.; Snyder, P. G., Variable Angle Spectroscopic Ellipsometry. In *Encyclopedia of Materials Characterization*, Brundle, C. R.; Charles A. Evans, J.; Wilson, S., Eds. Butterworth-Heinemann: Boston, MA, 1992; pp 401-414.

7. Synowicki, R., Fundamentals and Applications of Spectroscopic Ellipsometry. In J.A. Woollam: Atlanta, GA, 2007.

8. Josef, H., Polarized Light and Ellipsometry. In *Handbook of Ellipsometry*, Tompkins, H. G.; Irene, E. A., Eds. William Andrew Publishing: Norwich, NY, 2005; pp 3-13.

9. Lam, C. N. C.; Lu, J. J.; Neumann, A. W., Measuring Contact Angle. In *Handbook of Applied Surface and Colloid Chemistry*, Holmberg, K., Ed. John Wiley and Sons: New York City, NY, 2002; Vol. 1-2, pp 252-254.

10. Cox, J. N., FTIR: Fourier Transform Infrared Spectroscopy. In *Encyclopedia of Materials Characterization*, Brundle, C. R.; Jr., C. A. E.; Wilson, S., Eds. Butterworth-Heinemann: Boston, MA, 1992; pp 416-421.

11. Cross, A. D., *An Introduction to Practical Infrared Spectrscopy*. Butterworths Scientific Publications: London, UK, 1960; p 3.

12. Fairweather, D.; Richards, R. C., *Quartz Crystals as Oscillators and Resonators*. Marconi's Wireless Telegraph Co.: Chelmsford, Essex, UK, 1957; p 3.

13. Sauerbrey, G., The use of quartz oscillators for weighing thin layers and for microweighing. *Zeitschrift fuer Physik* **1959,** 155, 206.

14. Zweber, A. E.; Carbonell, R. G., Monitoring photoresist dissolution in supercritical carbon dioxide using a quartz crystal microbalance. *Proceedings of SPIE-The International Society for Optical Engineering* **2006,** 6153, (Pt. 2, Advances in Resist Technology and Processing XXIII), 61534C/1-61534C/9.

15. Stockbridge, C. D., Effect of hydrostatic pressure on rotated Y - cut quartz crystal resonators. *Vacuum Microbalance Techniques* **1966,** 5, 179-191.

16. Hussey, S., In Q-Sense: 2006.

17. http://www.q-sense.com/ (09/2007).

18. Poggi, M., In Q-Sense: 2007.

19. Kanazawa, K. K.; Gordon, J. G., *Anal. Chem.* **1985,** 57, 1770-1771.

20. Sergent, J. E., Materials and Processes for Hybrid Microelectronics and Multichip Modules. In *Electronic Materials and Processes Handbook*, 3rd ed.; Harper, C., Ed. McGraw Hill: New York City, NY, 2004; pp 8.16-8.17.

21. Grove, A. S., *Physics and Technology of Semiconductor Devices*. John Wiley and Sons: New York City, NY, 1967; p 265.

22. Sze, S. M.; Ng, K. K., *Physics of Semiconductor Devices*. 3rd ed.; John Wiley and Sons: Hoboken, NJ, 2007; p 199-200.

CHAPTER 4

PHOTORESIST AND ETCH RESIDUE REMOVAL USING GAS-EXPANDED LIQUIDS

Introduction

Rapid technology development and demands for state-of-the-art generations of integrated circuits bring new challenges to microelectronic device manufacturing. Specifically, decreasing dimension sizes may limit the effectiveness of liquid based removal of photoresist and plasma etch residues. In addition, the hazardous solvents currently in use pose environmental concerns. Gas expanded liquids (GXLs) and supercritical fluids may offer cleaning or residue removal approaches that overcome some of the drawbacks of current surface preparation methods.

The chemically reactive additives for the GXL investigations described below have been selected as a result of previous studies which demonstrated that mixtures of tetramethylammonium bicarbonate ($TMAHCO_3$) diluted in CH_3OH and CO_2 can remove fluorocarbon-based plasma etch residues at pressures of 3000 psig and temperatures >50^oC where the mixture was either a two phase gas with liquid droplets or a single phase[1]. The current study is distinct from our previous work in that the cleaning mixture is a single liquid phase with gas dissolved in the liquid. That is, in a GXL, the active cleaning phase is liquid expanded by CO_2 which offers higher fluid density at lower pressures than supercritical fluids. Based on the phase behavior of various $CO_2/TMAHCO_3/CH_3OH$ mixtures at different temperatures and pressures, the use of pressures between 1000 and 2000 psig should generate a GXL suitable for photoresist and etch residue cleaning[1]. In this study, we demonstrate that GXLs with a high mole

fraction of CO_2 can effectively remove polyhydroxystyrene (PHOST) films. Furthermore, the feasibility of using selected GXLs for the removal of post plasma etched residue films is also investigated. Specifically, the effect of CO_2 pressure or mole fraction dissolved in the solvent on residue removal is examined. Transport enhancement, environmental impact, and solvent strength of GXLs are shown to be functions of the extent to which a conventional solvent is expanded with CO_2. In addition, C_2H_6 is also investigated as an expansion gas in order to compare the quadrupolar nature of CO_2 to the non-polar C_2H_6. Polarity may be a factor in swelling the photoresist which aids in removal because novolac and PHOST resin have hydroxyl groups that the CO_2 quadrupole may interact with. As evident in Table 4.1, C_2H_6 was selected because other than polarity CO_2 and C_2H_6 have similar physical properties.

Table 4.1: Properties of ethane and carbon dioxide.

	Ethane	**Carbon Dioxide**
Molecular Weight	**30**	**44**
Critical Temperature (^oC)	**32.17**	**31.06**
Critical Pressure (PSI)	**706**	**1070**
Liquid Molar Volume (mL/mol)	**55.2**	**37.3**
Solubility Parameter $(J/cc)^{1/2}$	**12.4**	**14.56**
Dipole Moment	**0**	**0**
Liquid Density at 298K (g/cc)	**0.316**	**0.716**
Viscosity at 298K (Pa-s)	**3.73E-05**	**6.43E-05**
Surface Tension at 298K (N/m)	**8.60E-04**	**5.85E-04**

Experimental

The reactor used in this study consisted of a 0.75 inch 316 stainless steel four-way cross rated for 3500 psig; samples of approximately $1cm^2$ can be processed. One arm of the cross was equipped with a sapphire window. This window allowed direct observation of the phase, phase boundary of fluids, and overall film modification (e.g., peeling, cracking) during cleaning or surface treatment. In addition, the window permitted the use of an interferometer system for measurement of GXL refractive indices and thus fluid composition estimates, as well as the thickness and refractive index of dissolving films *in situ*[2].

Solvents and CO_2 were introduced into the reactor from two high pressure syringe pumps (ISCO, Inc.). Figure 4.1 shows a diagram of the experimental setup.

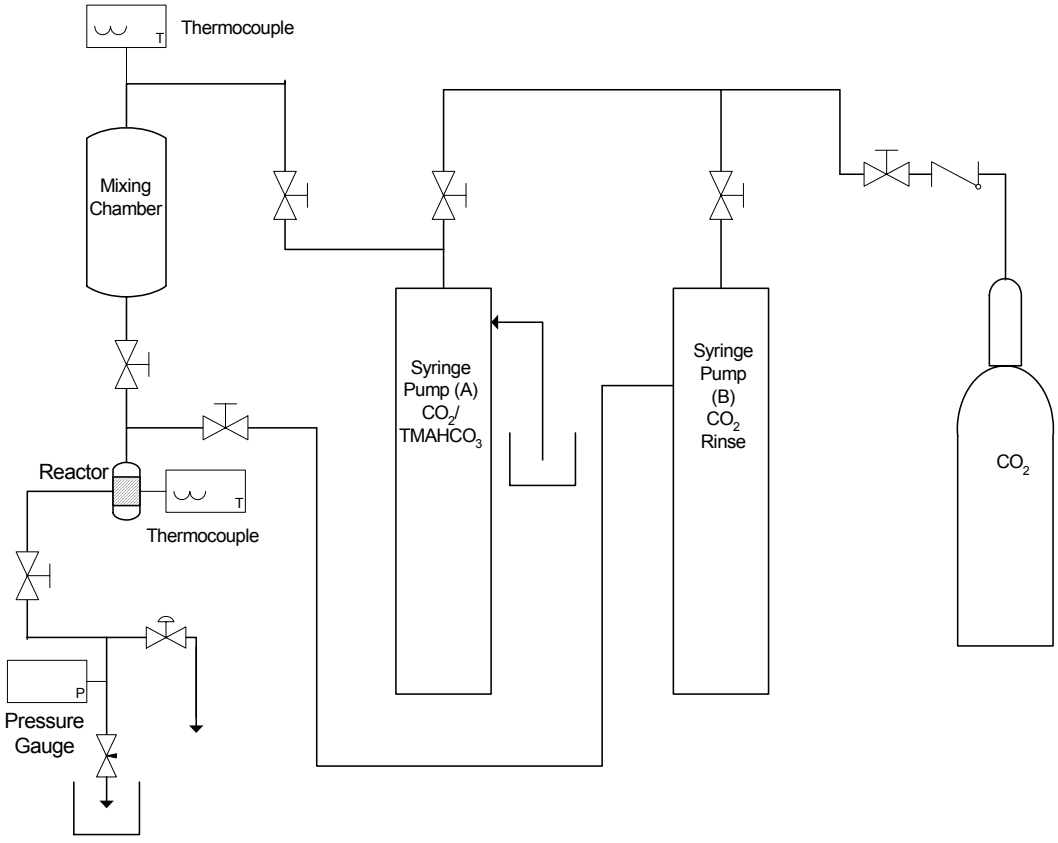

Figure 4.1: Experimental setup for GXL studies.

One pump (A) was operated in constant pressure mode to maintain the pressure setpoint (and thus composition) while the second pump (B) was operated in constant flow mode in order to control liquid delivery rate. A mixing chamber was employed to ensure adequate mixing of CO_2 and solvent at the temperature and pressure of interest so that liquid composition was controllable and could be estimated from equilibrium data.

Pump B was first loaded with the solvent to be studied. The liquid inlet valve was then closed and the pump contents delivered to the liquid mixing chamber. To pressurize the system with CO_2, pump A was filled with CO_2 to a sufficient volume for continuous introduction during the experiment and for GXL equilibration. A check valve was used to prevent backflow into the CO_2 cylinder and a 10μm filter eliminated small particles. After the pump was filled, the mixing chamber was pressurized and pump A operated in a constant pressure mode at the chosen setpoint. To establish adequate mixing of solvent with CO_2, the mixing chamber was periodically agitated over several hours. The fluid flowed between the reactor system components through Swagelok ¼" tubing outfitted with HiP straight valves.

Control of the vapor-liquid phase equilibrium concentrations was ensured by control of the fluid mixture temperature and pressure. K type Omega thermocouples were used for temperature measurements. An Omega multi-zone controller supplied power to the heating tape surrounding the mixing and reactor chambers. At the reactor exit, a Hoke metering valve attached to a Wika pressure gauge was used to maintain a specific pressure during constant flow by the ISCO pump. Composition of the GXL was assumed to be at equilibrium; thus, a vapor liquid phase diagram based on CO_2 and the particular additive allowed determination of the fluid composition[3].

Thin films for removal studies were formed on silicon wafers by spin casting from a poly-hydroxystyrene (PHOST) solution (15 wt% by mass in propylene glycol methyl ether acetate (PGMEA), MW=12000, PDI=6.4) at 800 RPM. Prior to spin casting, the silicon wafer was cleaned by immersion in dilute (1:50) hydrofluoric acid (HF) to remove the native oxide layer. The PHOST film was subsequently baked on a hotplate at 120°C for 5 minutes. Optical constants and thickness of the film were determined using a variable angle spectroscopic ellipsometer (J.Woollam, Lincoln, NE).

CO_2 was purchased from Airgas (SFC grade, 99.9995% with eductor tube). C_2H_6 was also purchased from Airgas (CP grade, 99% with eductor tube). The eductor tube was necessary to draw liquid from the bottom of the cylinder. The liquid allowed higher pressures when compressed. For operating pressures other than those of the CO_2 cylinder, an ISCO 1000 D syringe pump was used to both attain and maintain the pressure setpoint. For pressures above 2000 psig, 500HP and 260D ISCO pumps were used.

Films were treated in the high-pressure reactor with CO_2-expanded liquids. Samples were mounted on a customized sample holder and loaded into the chamber. The system was then pressurized with pure CO_2; simultaneously, GXLs were formulated as described above. The films were monitored both prior to and during liquid immersion by interferometry[2]. The samples were then removed from the chamber and analyzed by x-ray photoelectron spectroscopy (XPS) and scanning electron microscopy (SEM). The ability of a process to remove photoresist can be evaluated by XPS measurements of the Si atomic composition on the treated surface. From XPS analysis, a silicon atomic percentage above 22% indicates that the photoresist has been effectively removal[4].

Photoresist-coated silicon wafers yield a significantly different XPS spectrum, in that the underlying silicon is not detectable if photoresist or other material of thickness greater than ~10 nm is present.

In addition to PHOST samples, low dielectric constant (low-k) films of Coral™ that had been patterned with a fluorocarbon-based plasma were treated with GXLs. These samples, supplied by Novellus Inc., contained vias of 130 and 250 nm width and aspect ratios between 3 and 4. The film stack was composed of 625 nm of photoresist, 60 nm BARC, 50 nm SiO_2, 1000 nm Coral™, 70 nm SiC, and 500 nm SiO_2. Due to the plasma etch process, a hardened crust of photoresist residue existed on the photoresist surface[1]. Plasma etched samples were exposed to the $TMAHCO_3/CH_3OH$ solution expanded with CO_2 at pressures from atmospheric to 2200 psig at 90°C. Samples were exposed to the GXL for 40 minutes followed by a rinse in supercritical CO_2 at 2200psi and 90°C for 30 minutes.

The $TMAHCO_3/CH_3OH$ solution was created by bubbling CO_2 into a 25wt% TMAH in methanol solution from Sigma Aldrich. The 25wt% TMAH in methanol contained ~5.5% water as well[5]. After bubbling excess CO_2, the TMAH became tetramethyl ammonium bicarbonate with a small amount of hydroxide ions ($5.65x10^{-5}$M) in equilibrium according to pH measurements using voltage differences[6]. This solution was then further diluted 4 times by methanol.

Between four and nine XPS measurements were obtained on etched wafer samples at each pressure investigated. The 90% confidence intervals calculated incorporate both the standard deviation and the total number of data points. A larger number of data points were recorded for samples that displayed non-uniform removal in

order to reduce the confidence intervals; fewer points were necessary for samples where complete film removal was achieved. The number of data points taken in relatively clean versus incompletely clean areas thus reflects the removal uniformity.

Results and Discussion

PHOST Removal

Initially, PHOST samples were treated with CO_2-expanded ethanol. Although ethanol is an excellent solvent for removal of the hard baked PHOST films, CO_2 alone is not. As shown in Figure 4.2, single wavelength interferometry indicates that the film begins to swell significantly upon exposure to ethanol/CO_2 vapor.

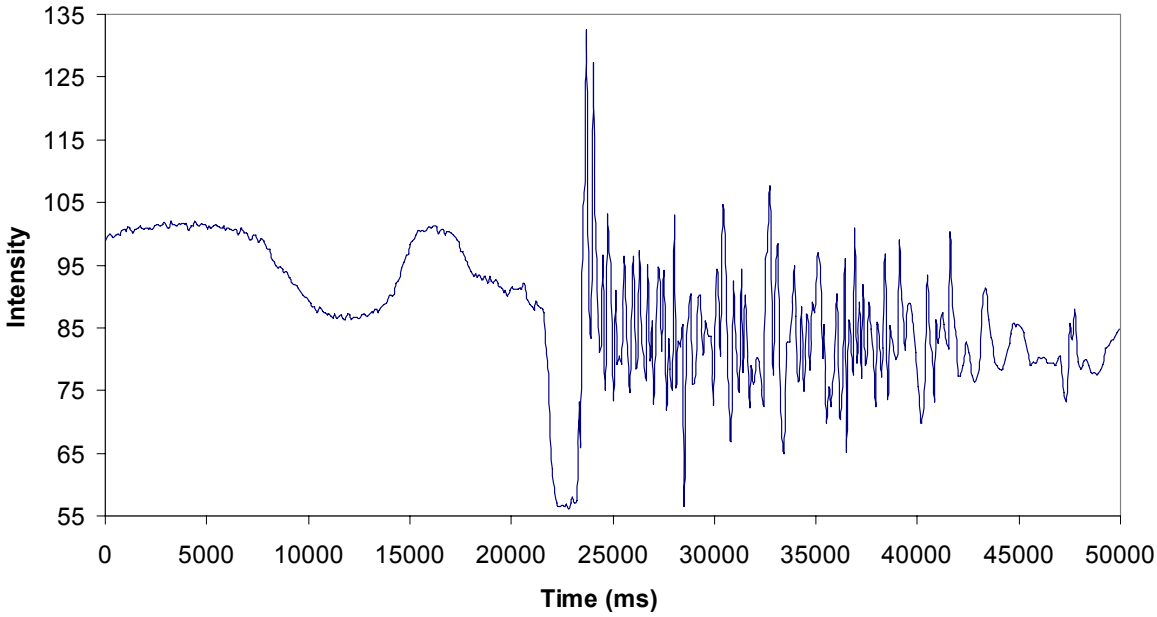

Figure 4.2: Single wavelength interference spectrum for PHOST exposed to CO_2-expanded ethanol at 725 psig. The liquid contacts the sample at t = 22 sec, at which time the intensity drops significantly due to interference with the meniscus. Swelling occurs prior to liquid exposure, characterized by the oscillation of the intensity. No film is detectable after liquid submersion, likely due to rapid dissolution.

The changes in light intensity with exposure time demonstrate film swelling, which allows ethanol to more easily penetrate the PHOST film and ultimately dissolve it. The relationship between swelling and the mechanism of film removal is clarified in the following section on post plasma etch residue removal and by previous results[7]. After exposure to the liquid (at t = 24000 ms), no interference pattern is detected. This observation can be attributed to either complete film removal or film cracking, which leads to significant scattering of the light beam. SEM and XPS were used to determine which of these possibilities occurred in particular samples. When GXLs incompletely removed PHOST films, partial dissolution yielded a rough, nonuniform layer and surface. Scattering from this surface prevented acquisition of an interferogram; thus, real time dissolution rate data in GXLs was not possible for this particular film. However, in the case of complete removal the dissolution rate can be examined as illustrated in Figure 4.1, but the dissolution occurs immediately upon contact with the liquid.

XPS analysis was performed on the cleaned samples to determine their surface compositions. As expected, XPS results indicate that the amount of residual polymer on the substrate surface is inversely related to the concentration of ethanol in the GXL. Figure 4.3 depicts the atomic percentages detected at the surface after treatment with GXLs with various CO_2 mole fractions.

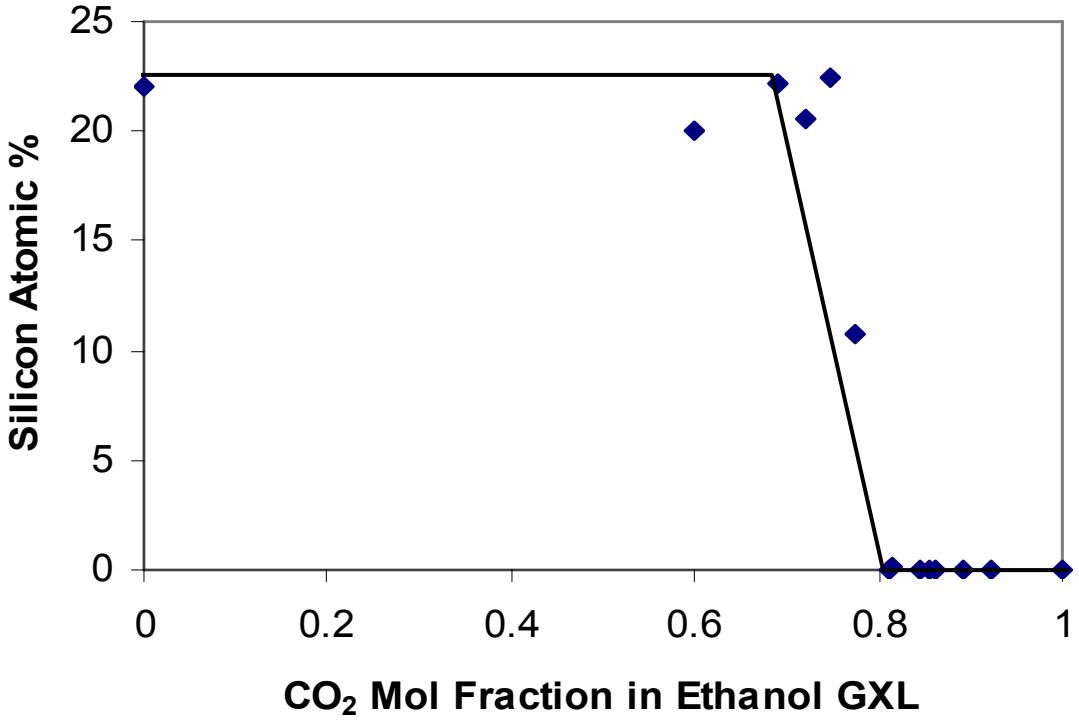

Figure 4.3: Surface composition after exposure to CO2 expanded ethanol at various mole fractions of CO2. Even at 0.75 mol fraction of CO2 or 700 psig, the GXL removed the PHOST.

Silicon is observed when sufficient film/residue is removed so that XPS detects the SiO_2 underneath the PHOST film; carbon is observed primarily due to the presence of the PHOST film. No silicon was detected at CO_2 mole fractions above 0.8 confirming that PHOST remained above the SiO_2 layer. However, mole fractions up to 0.75 CO_2 or 700 psig removed the photoresist indicating that ethanol was effective for dissolution of PHOST even at these diluted levels. Such observations suggest that reduced solvent

usage and lowered flammability should be possible with GXLs while maintaining solvent strength and thus cleaning ability. In addition to XPS, SEM images were taken in order to visually confirm PHOST removal. The image showed film cracking and peeling resulting from the stress developed due to CO_2 induced swelling.

PHOST films were also treated with CO_2-expanded NMP. Similar behavior to that of ethanol is observed, in which mixtures too rich in CO_2 do not remove PHOST layers. As shown in Figure 4.4, mixtures up to 725 psig, or correspondingly 70% CO_2, remove PHOST films analogous to the results obtained with pure liquid NMP[8].

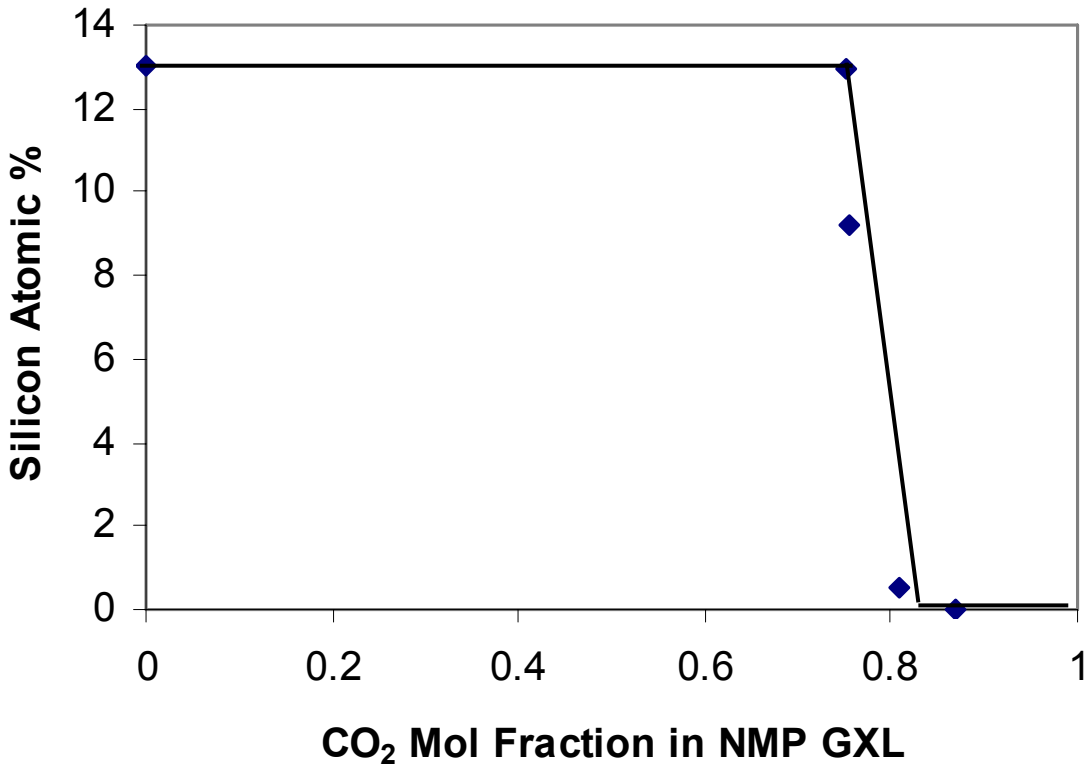

Figure 4.4: Surface concentration following treatment of PHOST films with CO2-expanded NMP of different composition.

Post Plasma Etch Residue Removal Using CO_2

Plasma etch residue samples were exposed to pressures ranging from atmospheric to 2200 psig at 90°C using CO_2 and a solution containing $TMAHCO_3/CH_3OH$ with a molar ratio of 0.020; these mixtures have been previously demonstrated to effectively remove photoresist and etch residues at higher pressures where two-phase or dense fluid phases exist[1, 5]. Clearly, the XPS results in Figure 4.5 demonstrate that at pressures below 100 psig and above 1000 psig cleaning is achieved.

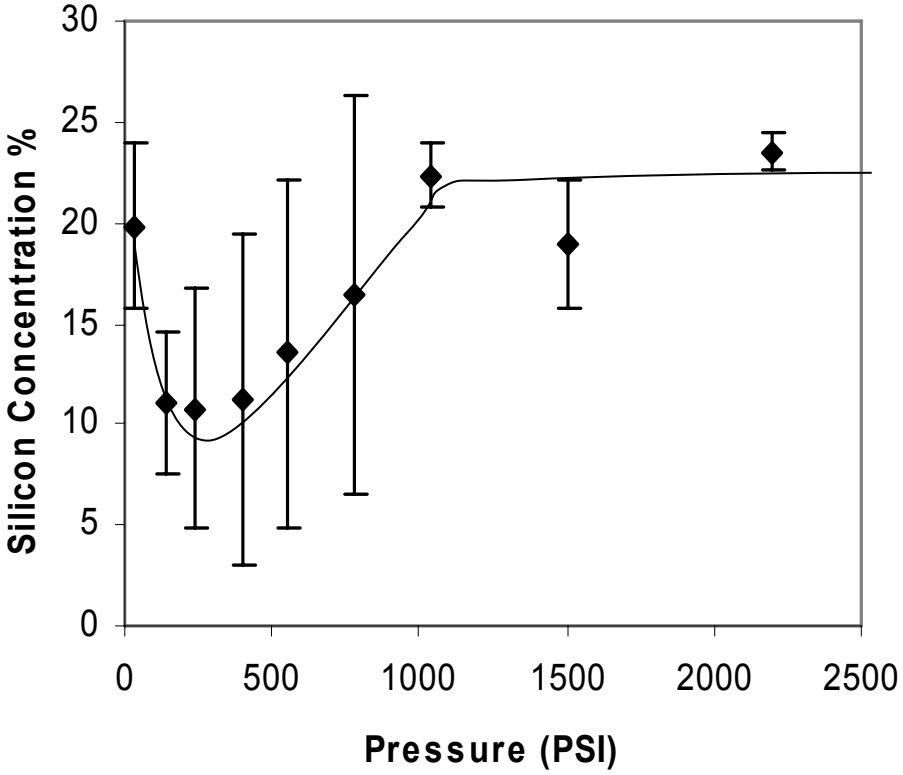

Figure 4.5: Cleaning of a plasma etch residue sample occurs at pressures below 100 psig and above 1000 psig where the atomic silicon concentration is above 20%. The cleaning solution was CO_2 expanded $TMAHCO_3/CH_3OH$ with a molar ratio of 0.020 at pressures ranging from atmospheric to 2200 psig at 90°C. The solid line is not the result of a model but rather is presented to serve as a guide to the overall trend in data points.

As described in the Experimental Section, at least four XPS measurements on multiple samples were performed at each pressure. The patterned wafer samples contained flat areas (unpatterned) and areas with 130 or 250 nm vias. Under all removal conditions,

some of the etch residue was removed from the flat areas; however, only for pressure conditions below 100 psig or above 1000 psig was the residue film in areas with a high density of vias (130 nm) removed. Samples with larger confidence intervals (error bars) processed at pressures between 100 and 1000 psig showed non-uniform removal; that is, both clean flat areas and incompletely clean areas that contain vias were present. The large difference in atomic silicon percentage between the two areas results in the larger confidence intervals, while the confidence intervals are smaller in regions above and below these pressure limits because the film is completely removed.

At low pressures (<100 psig), only a small amount of CO_2 is soluble in the $TMAHCO_3/CH_3OH$ solution (liquid) due to the high temperature. In this limit, liquid $TMAHCO_3$ is responsible for sample cleaning. As the pressure increases, more CO_2 is incorporated into the GXL, thereby decreasing the mole fraction of chemically reactive $TMAHCO_3$ in the liquid phase and reducing removal efficiency. However, at pressures exceeding 600 psig, the GXL density apparently decreases sufficiently to enhance mass transport to the SiO_2 layer beneath the photoresist and BARC films to permit removal of both layers by a lift-off mechanism. The enhanced mass transport likely results from the combined effects of the less dense GXL and the CO_2 induced swelling of the photoresist film, thereby facilitating mass transport through the film. This conclusion is based on previous studies of CH_3OH and CO_2 mixtures at 373K, where the density of the liquid mixture increases initially as the pressure is increased, but at pressures above ~850 psig, the density decreases[9]. Although more CO_2 is incorporated into the liquid solution at higher pressures, the GXL density initially increases and then decreases at temperatures above 373K. Indeed, previous studies of methanol/CO_2 mixtures support this

conclusion[9]. In our studies, the $TMAHCO_3$ mixture contains a salt that can affect density; the dependence of fluid density on pressure and salt concentrations for these salt mixtures is currently under investigation. Nevertheless, if the density trends for CH_3OH/CO_2 mixtures are indicative of those for $TMAHCO_3/CH_3OH/CO_2$ mixtures, then the cleaning efficiency depends inversely on the mixture density in this pressure regime. Moreover, this implies that at a sufficiently high density, cleaning does not occur whereas at lower densities removal is observed. Such conclusions suggest that the presence of CO_2 at high pressures assists photoresist and residue removal through photoresist swelling or cracking.

Previous studies at 3000 psig have demonstrated that both single- and two-phase mixtures exhibit effective cleaning of photoresist and etch residues, although single phase mixtures appear to be more efficient[1]. In the previous investigations, fluid composition data were fit to thermodynamic equations of state to establish a model for the fluid mixtures[3]. The model incorporated experimental data at 70°C; those data were extrapolated to 90°C to estimate fluid compositions in the current experiments. At 90°C, compositions in the range of 100 psig to 2500 psig corresponded to 1 mol% to 53 mol% CO_2, respectively. As noted above, although initial addition of CO_2 reduces cleaning ability through a reduction in $TMAHCO_3$ concentration, increasing concentrations of CO_2 appear to assist the cleaning process by swelling the polymer film. The swollen film permits the lower density GXL to diffuse through the film thereby releasing the film and residue by a lift-off mechanism[7, 10]. In all studies a minimum initial amount of liquid (400mL) in the mixing chamber was necessary to ensure that the sample was completely

immersed in the GXL and that all the gas originally in the reactor chamber was displaced by the entering GXL.

The etch residue samples were also treated to cleaning mixtures at various temperatures. Due to kinetic limitations, as well as the difference in composition, lower temperatures of 50°C and 70°C resulted in incomplete cleaning as depicted in Figure 4.6.

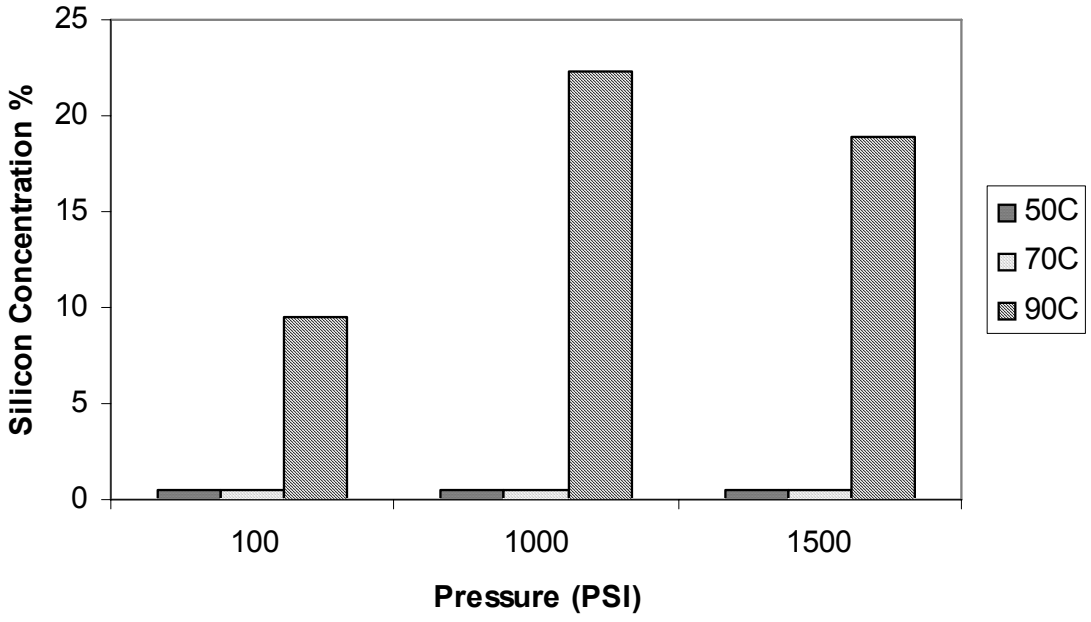

Figure 4.6: Silicon concentration is around 20% only at 1000 psig or higher and 90°C. At the lower temperature conditions, no silicon is present at the surface due to the unremoved etch residue. Samples processed were plasma etch residue samples subjected to CO_2 expanded $TMAHCO_3/CH_3OH$ with a molar ratio of 0.020.

Post Plasma Etch Residue Removal Using C_2H_6

The post plasma etch residue removal experiments were repeated with C_2H_6 instead of CO_2. Although the CO_2 expanded TMAB was not able to remove the residue at 50°C, the C_2H_6 expanded TMAB was able to remove the film at this lower temperature. Furthermore, the C_2H_6 GXL was also effective at the higher temperature of 90°C. XPS results are shown in Figures 4.7 and 4.8 for the 50°C and 90°C experiments.

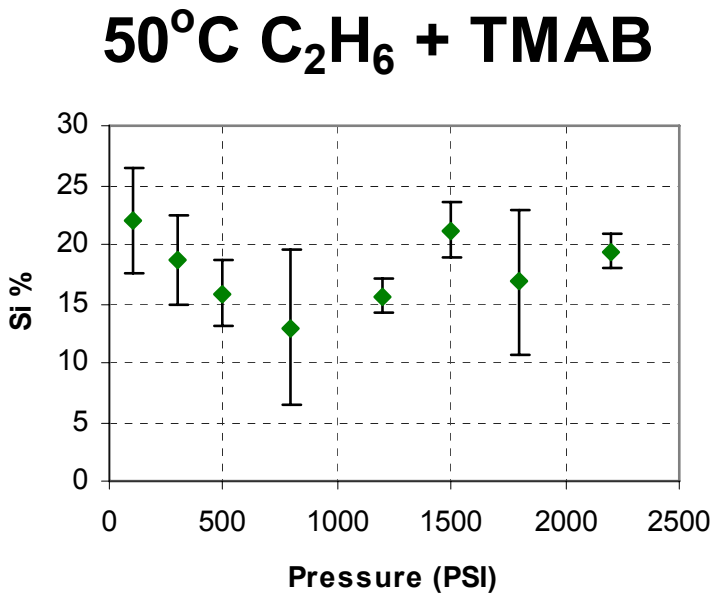

Figure 4.7: Si% at different pressures of C_2H_6 dissolved TMAB at 50°C.

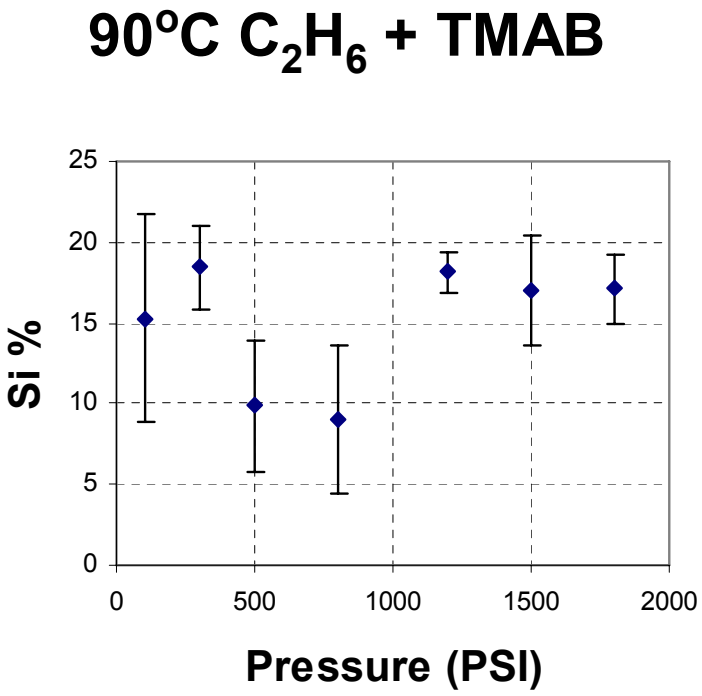

Figure 4.8: Si% at different pressures of C_2H_6 dissolved TMAB at 90°C.

The improved effectiveness of photoresist/residue removal observed with liquid expansion using C_2H_6 gas is likely due to the fact that C_2H_6 does not react with the

TMAH basic solution whereas CO_2 reacts to form TMAB. This reaction is important because the low hydroxide ion concentration etches the underlying SiO_2 to lift off the photoresist and residue. Under high pressure the CO_2 reacts with the TMAH solution so that essentially only the bicarbonate ions remain whereas for C_2H_6 hydroxide ion concentration will be higher due to nonreactivity of C_2H_6. The reactions that occur in TMAH solutions are shown below.

$(CH_3)_4NOH + CO_2 \rightarrow (CH_3)_4NHCO_3$

$(CH_3)_4NOH + (CH_3)_4NHCO_3 \rightarrow [(CH_3)_4N]_2CO_3 + H_2O$

Excess CO_2:

$[(CH_3)_4N]_2CO_3 + CO_2 + H_2O \rightarrow 2(CH_3)_4NHCO_3$

During the preparation of the TMAB solution, CO_2 is bubbled into the TMAH solution at room temperature and atmospheric conditions which gives a hydroxide concentration of $5.65x10^{-5}$M. However, when TMAB is expanded using CO_2 in a high pressure environment, the TMAB solution remains in excess CO_2 due to the over pressure CO_2 which may decrease the hydroxide concentration further. In the case of C_2H_6 the CO_2 is not in excess and hence most of the hydroxide ions will not have been converted to bicarbonate ions.

Conclusions

Due to their unique physical properties, gas-expanded liquids display improved transport properties relative to liquids, but are superior solvents in comparison to supercritical fluids. Therefore, GXLs may prove useful as alternatives to conventional liquids for cleaning processes, and preliminary cost estimates suggest feasibility[11]. Models for physical property estimation have been applied in order to predict properties

of GXLs as functions of CO_2 concentration. Equipment capable of forming and delivering GXLs has been designed and assembled[11]. With this equipment, GXLs of varying composition can be studied. Gas-expansion of organic solvents corresponds well with pressure-composition data previously reported.

Conceptual demonstration of the use of CO_2-expanded solvents for photoresist and post-plasma etch residue removal has been achieved. Of specific interest are the effects of CO_2 and gas-expanded liquids on films such as polyhydroxystyrene (PHOST). These experiments illustrate the tunability of GXLs through the removal of PHOST-based films using CO_2-expanded solvents. CO_2-expanded ethanol and NMP containing up to approximately 75 mol% CO_2 maintains the removal ability/solvent strength of the pure solvent. These fluids can therefore be modified to obtain optimal physical properties and reduce environmental safety and health (ES&H) concerns of toxic, flammable solvents. In addition, experiments performed on post plasma etch residue samples indicate that removal is possible at moderate pressure conditions of 1000 psig and 90^{o}C for CO_2. Experiments using C_2H_6 gas confirmed this expansion gas that does not react with TMAH can remove photoresist/etch residue films at lower temperature conditions (50^{o}C), apparently due to the existence of increased hydroxide ions in the etch solution. However, the quadrupole versus nonpolar natures of the gases and their effects on photoresist removal were not investigated in this study but are examined in Chapter 6.

References

1. Levitin, G.; Myneni, S.; Hess, D., Post Plasma Etch Residue Removal Using CO2-TMAHCO3 Mixtures: Comparison of Single-Phase and Two-Phase Mixtures. *Journal of the Electrochemical Society* **2004,** 151, (6), G380-G386.

2. Spuller, M. T.; Perchuk, R. S.; Hess, D. W., Evaluating Photoresist Dissolution, Swelling, and Removal with an In Situ Film Refractive Index and Thickness Monitor. *Journal of The Electrochemical Society* **2005,** 152, (1), G40-G44.

3. Levitin, G.; Bush, D.; Eckert, C. A.; Hess, D. W., Phase Behavior and Modeling of CO2/Methanol/Tetramethylammonium Bicarbonate and CO2/Methanol/Tetramethylammonium Bicarbonate/Water Mixtures at High Pressures. *J. Chem. Eng. Data* **2004,** 49, (3), 599-606.

4. Myneni, S.; Hess, D. W., Post-Plasma-Etch-Residue Removal Using CO_2-Based Fluids. *Journal of The Electrochemical Society* **2003,** 150, (12), G744-G750.

5. Levitin, G.; Myneni, S.; Hess, D. W., Reactions Between CO2 and Tetramethylammonium Hydroxide in Cleaning Solutions. *Electrochemical and Solid State Letters* **2003,** 6, (8), G101-G104.

6. Tucker, S. A.; Acree, W. E., A Student Designed Analytical Laboratory Method: Titrations and Indicator Ranges in Mixed Aqueous-Organic Solvents. *Journal of Chemical Education* **1994,** 71, (1), 71-74.

7. Myneni, S.; Hess, D. W., Post Plasma Etch Residue Removal Using CO_2-Based Mixtures: Mechanistic Considerations. *Journal of The Electrochemical Society* **2005,** 152, (10), G757-G765.

8. Zubchenko, Y. P.; Shskova, S. F.; Ladygina, O. P., Solubility of carbon dioxide in N-methylpyrrolidinone under pressure. *Khimicheskaya Promyshlennost* **1985,** 9, 535-536.

9. Brunner, E.; Hultenschmidt, W.; Schlichtharle, G., Fluid mixtures at high pressures IV. Isothermal phase equilibria in binary mixtures consisting of (methanol+hydrogen or nitrogen or methane or carbon monoxide or carbon dioxide. *J. Chem. Thermodynamics* **1987,** 19, 273-291.

10. Sawan, S. P.; Shieh, Y.-T.; Su, J.-H.; Manivannan, G.; Spall, W. D., Evaluation of Supercritical Fluid Interactions with Polymeric Materials. In *Supercritical Fluid Cleaning Fundamentals, Technology, and Applications*, McHardy, J., Ed. Noyes Publications: Westwood, NJ, 1998.

11. Spuller, M. Resist and Residue Removal Using Gas Expanded Liquids. PhD, Georgia Institute of Technology, Atlanta, 2003.

CHAPTER 5

COMPATIBILITY OF LOW K MATERIALS WITH GXLS

Introduction

GXLs incorporating high pressure CO_2 expanded methanol with tetramethyl ammonium bicarbonate ($TMAHCO_3$) successfully removed photoresist and etch residue at an elevated temperature of 90°C and pressures above 1000psi[1]. However, the cleaned multilayer film stack shown in Figure 5.1 only exposed the sidewalls of the low k material (e.g., Coral™) to the cleaning solution.

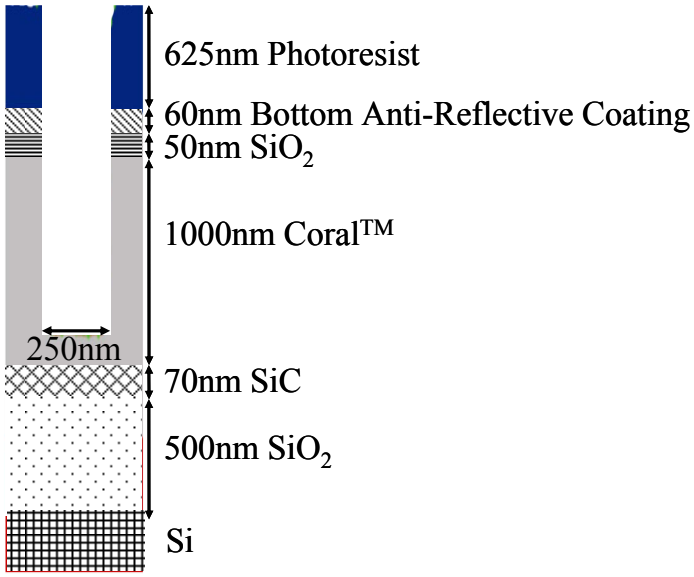

Figure 5.1: Cross section of silicon wafer sample supplied by Sematech.

A SiO_2 layer covering the underlying Coral™ low k material partially protects the Coral™ (except at the sidewall) against the GXL but at the expense of increasing the effective dielectric constant of the interlevel dielectric material consisting of the combined Coral™ and SiO_2. Processing the film stack without the capping SiO_2 layer is important in order to achieve the lowest possible dielectric constant for the dielectric stack. This will be explained in more detail in subsequent sections.

Low k materials are included in current state of the art semiconductor devices as interlevel dielectric layers and must be compatible with the cleaning solutions used. In order to assess whether GXLs offer a possible alternative for photoresist and etch residue removal to supercritical and standard liquid processes wherein porous low k materials are present, MSQ films were exposed to the previously described GXL solutions and the physical and electrical properties of the films characterized.

Low k or low dielectric constant materials insulate the metal lines that interconnect transistors and other circuit components, and must reduce cross talk, current leakage, and parasitic capacitance between metal layers [2]. Such reductions result from both the low permittivity and low polarizability that establish effective insulation between metal layers. Low k materials such as methylsilsesquioxane (MSQ) have dielectric constants of 2.6-2.8 where a lower value for the dielectric constant is more desirable. A dielectric constant is defined as the ratio of charge stored in the film with respect to that of a vacuum when an electric field is applied as shown in Equation 5.1[3].

$$k = \frac{C_x}{C_0} \tag{5.1}$$

where k = dielectric constant

C_x = capacitance of film

C_0 = capacitance of vacuum

A film with a lower dielectric constant is advantageous because the lower value reduces the capacitance between metal layers. Because the lower dielectric film stores less charge, the time to charge the capacitor is reduced, thereby reducing the circuit delay time for signal transfer. Indeed, this is the capacitance part of the resistive-capacitive

(RC) time delay where capacitance can be reduced by using low k films and resistance is reduced by employing copper instead of aluminum as an interconnect material.

For comparison, silicon dioxide which had been the primary interlayer dielectric material since the inception of the IC industry has a dielectric constant of ~4. The larger dielectric constant results in more parasitic capacitance. Capacitance and dielectric constant are related as indicated by Equation 5.2.

$$k = \frac{cd}{A\varepsilon} \tag{5.2}$$

where k = dielectric constant

c = capacitance (F)

d = film thickness (m)

A = area of electrode (m^2)

ε = permittivity in a vacuum (8.854×10^{-12} F/m)

Therefore SiO_2 with a dielectric constant of ~4 would have a capacitance 1.5x that of a low k film with a dielectric constant of 2.7. Current intermetal dielectrics use silicon dioxide doped with carbon in order to reduce the dielectric constant to ~3. To put these values into perspective, air has a dielectric constant of 1 whereas water has a value of ~80 at room temperature [4]. Therefore, in order to reduce the dielectric constant below ~2.5, nanopores and elimination of polarizable groups or chemical moieties are needed to further reduce the dielectric constant. Inclusion of nanopores incorporates air into the film to decrease the dielectric constant. Furthermore, imparting hydrophobic character to film inhibits water adsorption that increases the dielectric constant. MSQ creates nanopores as a result of its structure; MSQ has a silicon oxygen structure that is cubic as shown in Figure 5.2A or hexagonal as shown in Figure 5.2B.

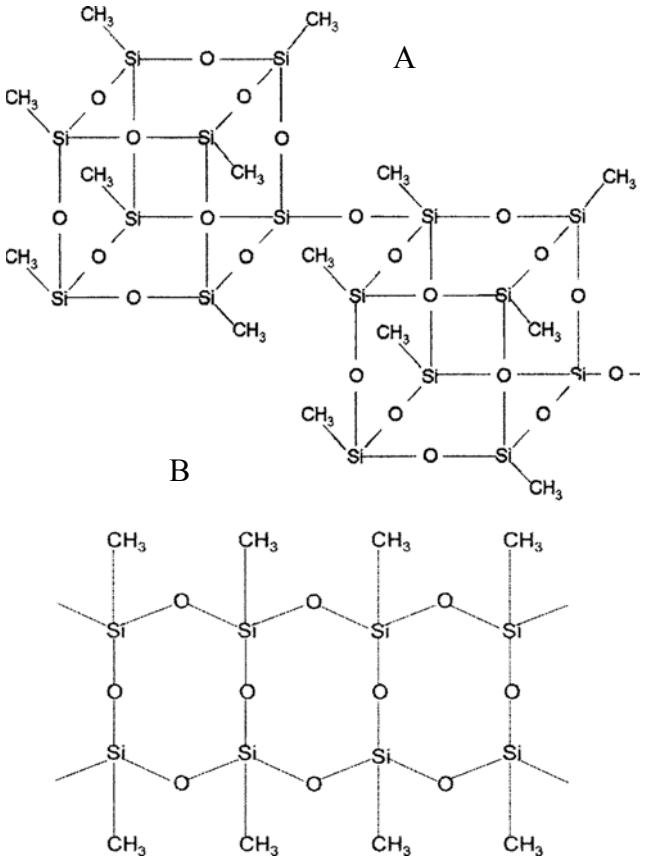

Figure 5.2: Chemical structure of MSQ A) cage structure B) ladder structure[5].

In addition, the presence of methyl groups on the silicon enhance the hydrophobicity of the material relative to amorphous SiO_2 where hydrogen is attached to oxygen or to silicon. In both cases a more hydrophilic material results compared to MSQ.

Increasing porosity and hydrophobocity both decrease the dielectric constant of low k films but in different ways. As noted previously, porosity is important because the inclusion of pores introduces void spaces with a dielectric constant of 1. For MSQ the void space is created by the silicon-oxygen bonding structure. The cage structure in Figure 5.2A creates 3-dimensional void spaces while the ladder structure in Figure 5.2B creates 2-dimensional voids. The presence of methyl groups also creates space between adjacent silicon atoms and thereby decreases the density and packing of the SiO_2 units. The ladder structure offers more void space but the structure itself is less robust

compared to the cage structure. The greater percentage of porosity decreases the dielectric constant but also decreases the modulus and hardness of the film[6]. In addition to the inclusion of porosity through molecular structure means, other techniques include the use of porogens that are UV sensitive. Upon UV exposure these porogens degrade and leave behind a void space[7]. Another method uses high curing temperatures at 425^{o}C that also degrade porogens such as trimethoxysilyl norbornene and triethoxysilyl norbornene in MSQ[8]. MSQ has a porosity of 10% whereas the use of porogens can increase the porosity to 34% with pore size increasing from 0.6nm to 2.7nm[9]. The inclusion of porosity can reduce the dielectric constant to below 2[10].

While the inclusion of pores decreases the dielectric constant, the inclusion of water significantly increases the dielectric constant. MSQ can become hydrophilic if hydrogen instead of silicon with a methyl group caps the oxygen at the interface. The hydrogen bonded to oxygen forms a hydroxyl group which is polar and which through hydrogen bonding attracts water. The adsorption of water with a k value of ~80 increases the k value of the film. In addition to the higher k value the leakage current increases and the breakdown voltage decreases[11].

Experimental Methods

The MSQ precursor solution was purchased from Filmtronics under the trade name FG65; the resulting film has a dielectric constant in the range 2.6-2.8. The solution was stored at 5^{o}C and was equilibrated at room temperature for 5 hours before processing. In order to reduce the viscosity of the MSQ solution, the MSQ was diluted four times with ethyl acetate 99.98% purity purchased from EMD. The film was spincast onto 4" silicon wafers at 1000rpm with a ramp rate of 750r/s for 45s on a Cost Effective

Equipment 100CB spincoater. The 4" silicon test wafers from Nova Electronic Materials were p-type <100> with a boron concentration of 10^{16} to $5.5x10^{14}$ atoms/cm^3 corresponding to resistivities between 1 and 25 ohm-cm. After spin casting, the film was baked at 200°C in air for 5min. Although curing initiates at 200°C, some previous investigators have cured the films at 400°C under a N_2 ambient[12]. The silicon wafer was cut into 1cm^2 sized pieces and placed in the GXL reactor chamber. The system required 30min to heat to the desired 90°C. Then the GXL formulated as described in chapter 4 was introduced into the reactor at pressures of 1050psi, 1500psi, or 2200psi. The GXL contained a liquid solution of 25wt% tetramethyl ammonium hydroxide (TMAH) in methanol that was diluted with four parts of methanol. The solution was bubbled with CO_2 to form a mostly tetramethyl ammonium bicarbonate (TMAB) solution with some OH^- ions in equilibrium. Pressures from 1050psi to 2200psi were chosen because these pressures were effective in removing photoresist and etch residue according to previous studies[1]. After processing for 40min, the system was depressurized using a Hoke 1300 series metering valve in 1min, and the sample rinsed with methanol and dried with a N_2 gun. In order to ensure complete removal of methanol, the sample was baked again by temperature ramping for 30min and holding at 90°C for 40min.

In addition to the high pressure studies, three other treatments were invoked and MSQ samples characterized for comparison. In the first treatment, a standard unprocessed MSQ sample that was exposed only to the baking steps served as a control. A second MSQ sample was exposed to liquid TMAH wherein CO_2 had been introduced to form $TMAHCO_3$; of course, hydroxide ions were present in this solution due to the equilibrium established[13]. The liquid solution was heated to only 50°C to avoid excessive

methanol evaporation; the sample was immersed in this solution for 40min. The third sample was processed at 2200psi but following the TMAH treatment, was rinsed with a CO_2 / CH_3OH rinse at 2200psi and room temperature with a flow rate of 200mL/hr for 30min. Liquid CO_2 is miscible in CH_3OH and the composition of the rinsing solution was 0.548 CO_2[14]. Thus a total six samples were analyzed as shown in Table 5.1.

Table 5.1: Abbreviations for sample types.

Abbreviation	Sample Type
A	Unprocessed standard
B	Liquid TMAB, 14.7psi at 50°C
C	1050psi CO_2 expanded TMAB in methanol at 90°C
D	1500psi CO_2 expanded TMAB in methanol at 90°C
E	2200psi CO_2 expanded TMAB in methanol at 90°C
F	2200psi CO_2 expanded TMAB in methanol at 90°C, CO_2/methanol rinse at 23°C

Finally, the GXLs experiments were repeated using C_2H_6 as the expansion gas. C_2H_6 does not react with TMAH. Although Chapter 4 indicated that C_2H_6 was able to remove the residues at more favorable conditions (lower temperature of 50°C), the increased hydroxide ion concentration may adversely affect low k films. The C_2H_6 GXLs were applied to the MSQ films at 1000psi and 90°C. The TMAH had been pre-bubbled with CO_2 before the C_2H_6 addition. Beaker tests were performed at 50°C with TMAH diluted by four parts of methanol and also TMAH bubbled with CO_2 and then diluted by four parts of methanol. The samples were exposed for 40min.

Experimental Analysis Techniques

Films were characterized using ellipsometry, video contact angle, FTIR, and XPS. In addition, MIS (metal insulator semiconductor) capacitors fabricated from the films treated as described above were characterized by capacitance-voltage (CV) and current-voltage (IV) methods. In particular, CV curves were used to determine the dielectric constants. All analyses were performed before and after fluid processing in order to effectively compare results.

Ellipsometry measurements were performed with a variable angle spectroscopic ellipsometer (VASE) M-2000VI from J.A. Woollam with WVASE32 version 3.632 program for analysis. The angles chosen for measurements were 65^{o}, 70^{o}, and 75^{o}. Cauchy parameters were fitted to calculate the MSQ thickness. The first Cauchy parameter A also known as the refractive index was set to 1.38 because this value is known from prior Filmtronics studies. In addition to the Cauchy parameters, a roughening parameter was added to compensate for the uneven surface.

Goniometry or video contact angle measurements were performed using water as the liquid in contact with the film. An AST Products Video Contact Angle System 2500XE recorded the pictures and calculated the corresponding contact angles using five set points. A nitrogen rinse before testing was important to ensure a clean surface because small particles could increase the contact angle.

A Bruker IFS 66v/S FTIR system with a KBr beam splitter ran 128 scans with a resolution of $4cm^{-1}$ in absorbance mode. A blank silicon wafer was used as the background which was subtracted from the final spectra results. The measurements were performed under vacuum.

In order to measure the CV and IV curves, an MIS (metal-insulator-semiconductor) structure was fabricated. The metal used as the top electrode was gold. The insulation layer was the MSQ film and the semiconductor was boron-doped silicon. A shadow mask with 2mm diameter holes was used to pattern the top electrodes. Using a CVC e-beam evaporator, 300A of Ti was deposited at 3A/s as an adhesion layer between the MSQ and the subsequent 3000A of Au deposited at 3A/s. A bottom electrode deposition was not necessary because of the doped silicon substrate. Metal depositions were performed in a class 1000 cleanroom at the MIRC (Microelectronics Research Center) at Georgia Tech.

Using a Keithley 590 CV Analyzer, CV plots of capacitance versus voltage were measured from -20V to 20V. The frequency used was 100kHz with a voltage step size of 0.1V. For IV curves, the voltage was varied from -20V to 20V with a step size of 0.1V using a HP 4156A Precision Semiconductor Parameter Analyzer.

Results and Discussion

Ellipsometry was performed to determine if the MSQ film thickness had changed due to OH^- etching of the film during treatment. As shown in Table 5.2, film thicknesses remained nearly constant, indicating little to no film etching.

Table 5.2: MSQ film thickness before and after various processing steps.

	Process	Thickness Before (nm)	Thickness After (nm)	Difference %
A	Unprocessed	701.2	700.4	-0.1%
B	Liquid	599.1	597.8	-0.2%
C	1050psi GXL	697.5	700.2	0.4%
D	1500psi GXL	677.5	676.6	-0.1%
E	2200psi GXL	626.9	634.5	1.2%
F	2200psi GXL + Rinse	646.2	645.8	-0.1%

Although spincasting is an effective method to create uniform films, variations in film thickness normally appear at sample edges; thus, the same measurement locations were used to assess accurately the thickness changes. The GXL solutions investigated did not etch or alter the film thicknesses unless the etching and subsequent film growth rates were essentially equal; however, this possibility is unlikely based on other characterization measurements that will be discussed in the next sections.

Analagous to the ellipsometry measurements, contact angle values did not change as shown in Table 5.3.

Table 5.3: Contact angles as a function of processing conditions.

	Process	Contact Angle Before (^{o})	Contact Angle After (^{o})	difference %
A	Unprocessed	94.5	94.5	0.0%
B	Liquid	94.5	94.8	0.3%
C	1050psi GXL	94.5	94.6	0.1%
D	1500psi GXL	94.5	95.5	1.0%
E	2200psi GXL	94.5	94.3	-0.2%
F	2200psi GXL + Rinse	94.5	95.3	0.8%

The contact angle measurements suggest that from the standpoint of the surface, the film chemistry and roughness have not changed. If the methyl groups on silicon had been

replaced by hydrogen, the contact angle would have been much lower and the surface hydrophilic[15]. Likewise, if film roughness was altered, contact angles should have changed[16]. Because the film is not hydrophilic, the dielectric constant has likely not changed. That is, since a hydrophilic film can absorb water, the film dielectric constant should increase as a result of the high k value (~80) of water.

Although the contact angle measurements support that no surface changes have occurred, FTIR was also used to assess possible changes in bulk chemical structure of the films in Figures 5.3, 5.4, and 5.5.

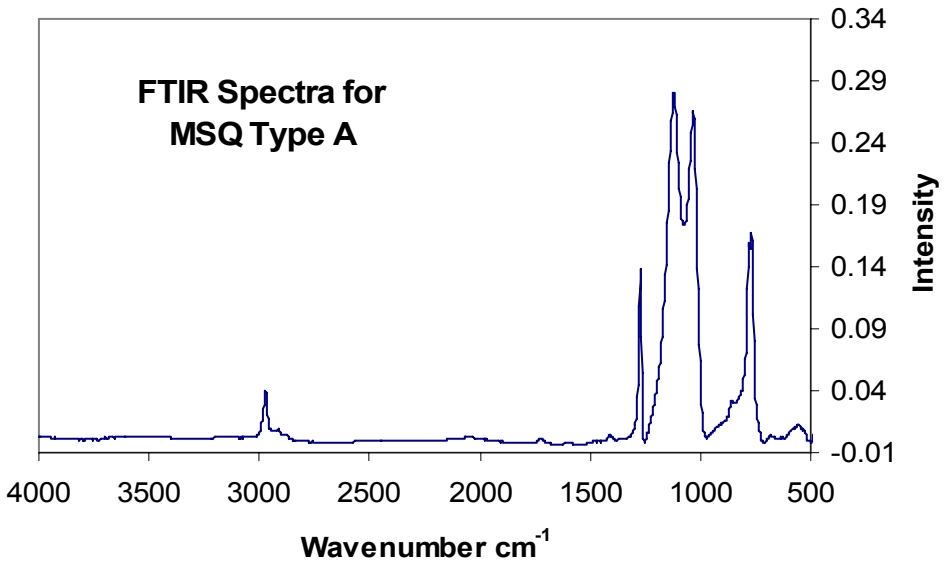

Figure 5.3: FTIR spectra for unprocessed MSQ. See Table 5.4 for details.

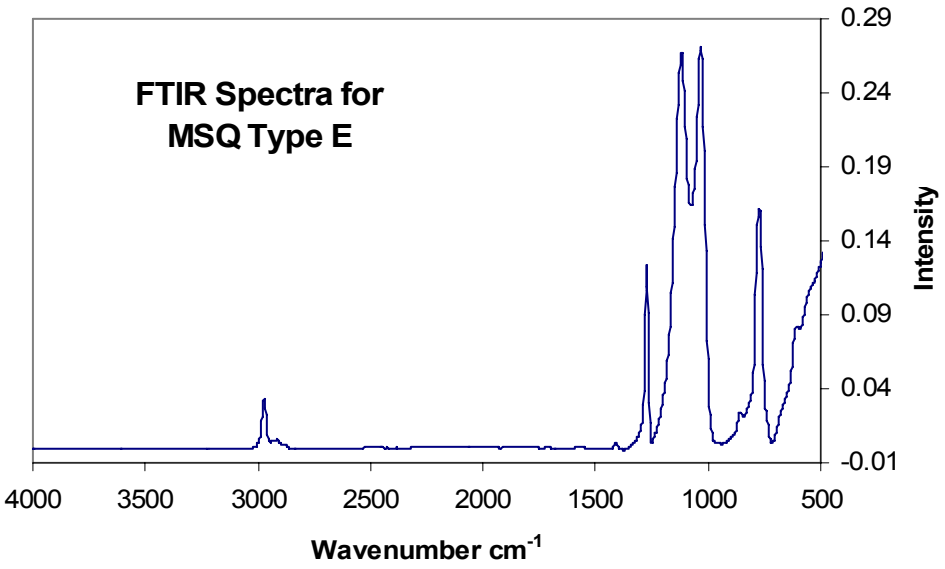

Figure 5.4: FTIR spectra for MSQ processed using a 2200psi GXL. See Table 5.4 for details.

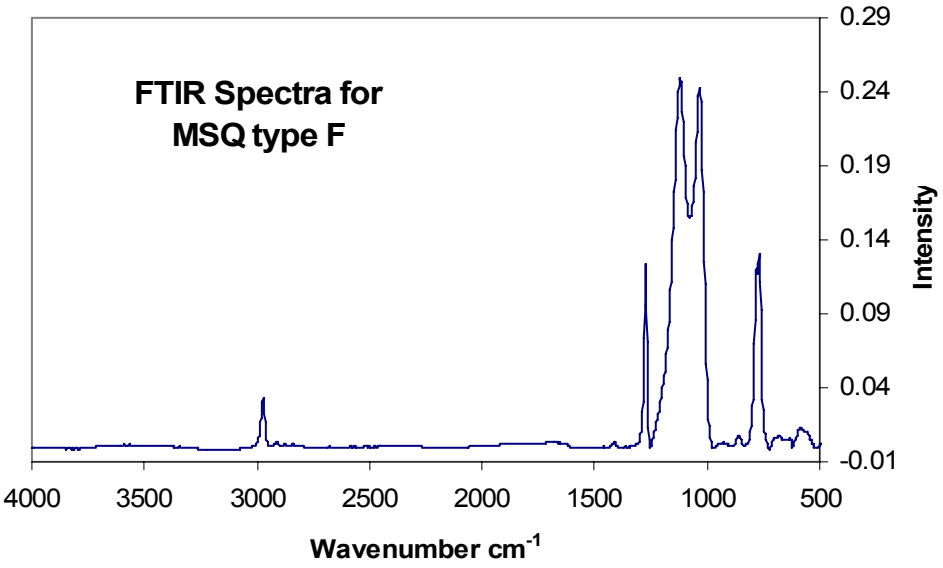

Figure 5.5: FTIR spectra for MSQ processed using a 2200psi GXL with CO_2/CH_3OH rinse. See Table 4 for details.

These spectra demonstrate that the primary absorption peaks have not changed in intensity or shape. Peak positions of the absorptions observed are listed in Table 5.4.

Table 5.4: Bonding structure and corresponding wave numbers.

Bonding Structure	Peak Wavenumber (cm^{-1})	Literature Values[15, 17, 18, 19]
CH_3 (stretch, asymmetric)	2964	2977
Si-CH_3 (deformation)	1271	1279
Si-O-Si (cage)	1115	1118
Si-O-Si (network)	1030	1062
Si-CH_3 (stretch)	757	779

In addition, the unprocessed MSQ film was exposed only to the high pressure CO_2/CH_3OH rinse to confirm that this rinse had no effect on the bonding structures; indeed, no changes are observed as indicated by the FTIR spectra in Figures 5.6 and 5.7.

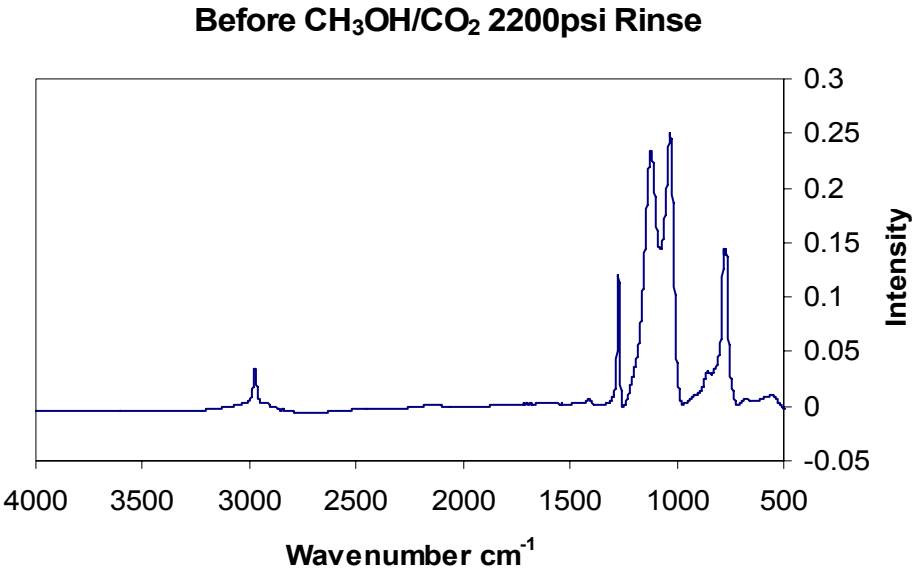

Figure 5.6: FTIR spectra of MSQ film before 2200psi CO_2/CH_3OH rinse.

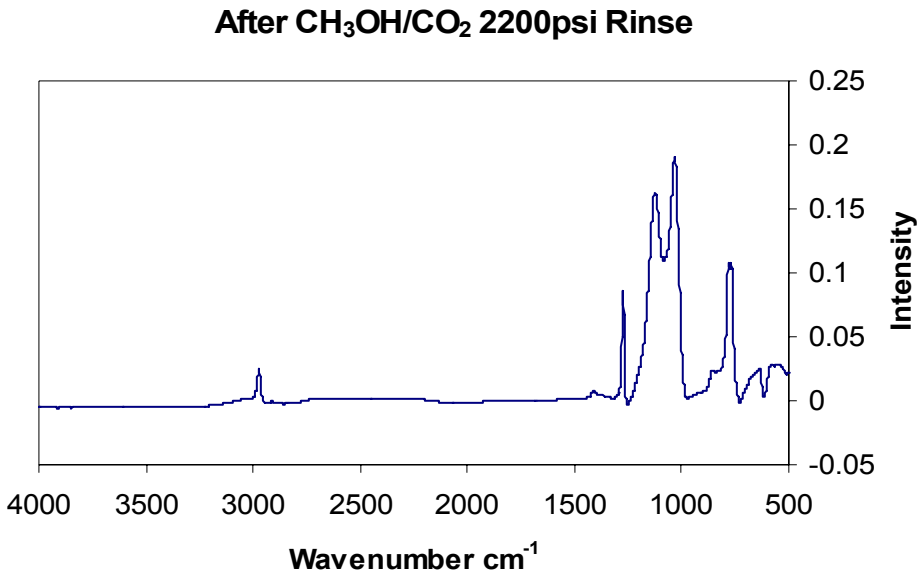

Figure 5.7: FTIR spectra of MSQ film after 2200psi CO_2/CH_3OH rinse.

Although FTIR evaluates the bonding structures present in the bulk film, if the chemical composition change is small, detection of such changes is unlikely. FTIR spectra have detection limits on the order of ppb but the sensitivity also depends on the specific chemical bond. In the case of Si-O, the detection limit is 10^{13}bonds/cc[20].

Since no apparent chemical changes were observed in the processed MSQ films, electrical characterization, which is more sensitive to film property changes, were performed. Small changes in the incorporation of ions or polar moieties can be detected by examining capacitance-voltage and current-voltage plots. MIS (metal insulator semiconductor) structures were created to measure the capacitance and current across the MSQ film as a function of voltage.

Because the wafers were p-type, accumulation of majority carriers (holes) occurred at negative voltages while depletion occurred at around zero voltage and inversion at positive voltages. The maximum capacitance at accumulation was used to calculate the dielectric constant of the MSQ film according to Equation 5.2:

$$k = \frac{cd}{A\varepsilon} \tag{5.2}$$

where k = dielectric constant

c = capacitance (F)

d = film thickness (m)

A = area of electrode (m^2)

ε = permittivity in a vacuum (8.854×10^{-12} F/m)

From Equation 2, a dielectric constant of 2.64 was calculated which lies within the 2.6-2.8 range that Filmtronics reported. Table 5.5 gives values of MSQ films processed under different conditions.

Table 5.5: Dielectric constant values for MSQ films.

	Process	Dielectric Constant
A	Unprocessed	2.64+/-0.05
B	Liquid	13.50 +/- 0.68
C	1050psi GXL	26.80 +/- 0.39
D	1500psi GXL	26.18 +/- 0.64
E	2200psi GXL	27.01 +/- 0.14
F	2200psi GXL + Rinse	2.73 +/- 0.08

Sample A which was the unprocessed MSQ film and sample F which was processed at 2200psi and then underwent a 2200psi CO_2/CH_3OH rinse, had dielectric constants within the specified range. All but one other sample displayed an increase in dielectric constant by one order of magnitude. Sample B which had been exposed to a 50°C liquid solution of TMAH bubbled with CO_2 diluted four times with CH_3OH had a lower dielectric constant compared to those processed under higher pressures. Although the samples before and after processing had similar thicknesses (Table 5.1), contact angles (Table 5.2), and FTIR spectra (Figure 5.3-5.5), the change in dielectric constant indicated that

other effects were involved. Specifically, all the MSQ films exposed to the TMAH solution bubbled with CO_2 had higher than normal dielectric constant values. That is, treatment in the TMAH solution resulted in higher dielectric constants, which suggests the incorporation of polar moieties into MSQ. These moieties likely include tetramethyl ammonium (TMA^+), hydroxide (OH^-), or bicarbonate (HCO_3^-) ions from the TMAH solution. During TMAH exposure, these ions may have diffused into the MSQ film due to the concentration gradient at the surface.

In the liquid solution, fewer ions appear to have diffused into the film as indicated by the lower dielectric constant of 13.5 (Table 5.5). Since the high pressure solutions yielded higher dielectric constants of ~26, the presence of high pressure CO_2 may have swelled the MSQ film and allowed the incorporation of a higher concentration of ions into the film. High pressure CO_2 is a common plasticizer and typically swells polymers[21]. However, swelling only occurs if the gas is soluble in the film whereas pressurization of the film occurs with a gas that is not soluble in the film[22]. Although no reports have appeared describing the absorption and swelling of MSQ films by CO_2, Xie has investigated the interaction of supercritical CO_2 with additives on MSQ that had been exposed to an oxygen plasma[23]. A study examining the swelling absorption of CO_2 into MSQ would be useful in clarifying this hypothesis. The possibility of MSQ swelling seems plausible because the ladder or cage like structure of MSQ may allow the inclusion of other moieties such as CO_2. Kim has investigated the absorption of solvents such as acetone, methyl isobutyl ketone, 1-methoxy-2-propanol acetate, and water in liquid or vapor phases into MSQ films using QCM. In addition neutron reflectivity measurements confirmed swelling[24].

The increased dielectric constants observed may have been caused by surface inclusion of polar moieties rather than incorporation of polar species by diffusion into the bulk film. In order to investigate this possibility, a CH_3OH rinse from a squirt bottle was used to rinse off any TMAH solution that remained after depressurization and removal of the sample from the reactor. In addition, the surface was dried with a N_2 gun to remove any remaining CH_3OH. Although rinsing steps were incorporated after the GXL processing, the dielectric constant remained high. These studies suggest that ions have been incorporated into the bulk of the MSQ film rather, and are not merely present at the surface.

CV curves were used to calculate the dielectric constant under semiconductor accumulation conditions and to investigate shifts in the flat-band voltage that relate to charges present in the dielectric (MSQ). Flat-band voltage is the voltage at which the semiconductor has zero induced charge. That is, flat-band voltage is the applied voltage necessary to establish a uniform flat electron energy potential for the conduction, valence, and intrinsic Fermi energy bands; this is distinct from the normal situation where the energies either increase or decrease near the interface between the silicon and MSQ due to differences in the work function between the silicon and the metal and to charges present in the dielectric or at the dielectric-silicon interface[25]. Because the silicon wafer is doped, the condition of zero charge will occur near the inflection point of the depletion part of the CV curve where the transition from accumulation to inversion takes place[25]. As described above, a shift in the flat-band voltage position also indicates the introduction or removal of charge in the dielectric, which includes charge due to incorporated ions[26]. Figure 5.9 indicates that the CV curve and thus the flat-band has

shifted to more negative voltages compared to that in Figure 5.8 because a more negative voltage is necessary to compensate the silicon surface potential for the positive charges trapped in the MSQ film[27].

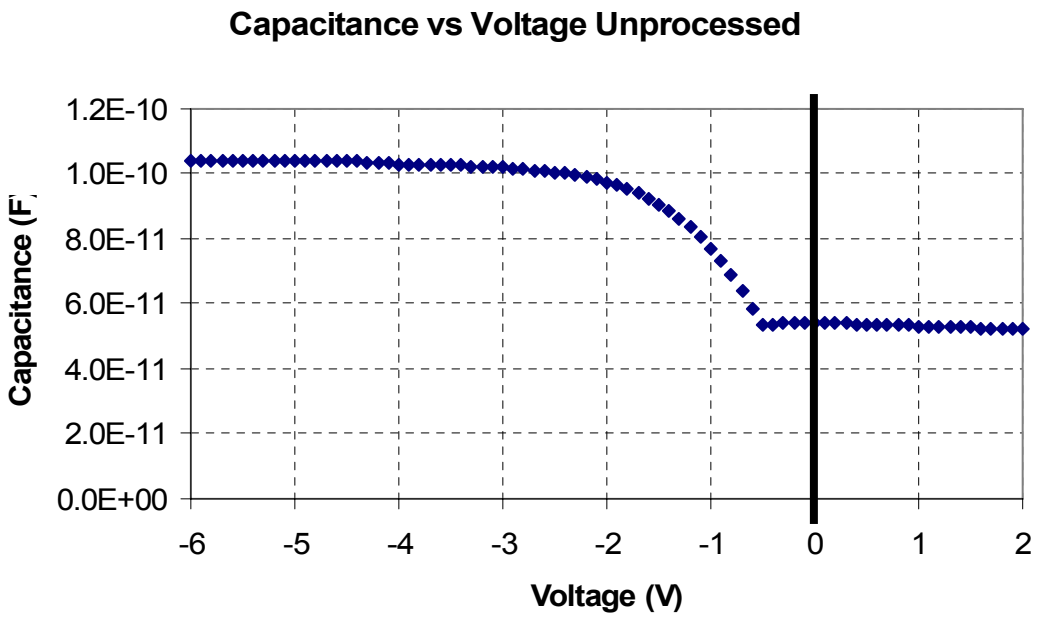

Figure 5.8: CV curve for unprocessed MSQ film.

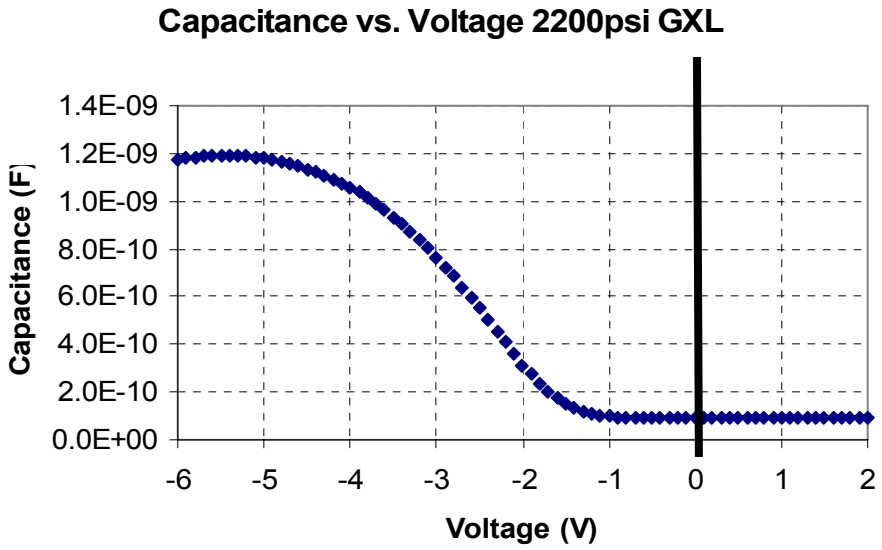

Figure 5.9: CV curve for MSQ film exposed to 2200psi GXL solution.

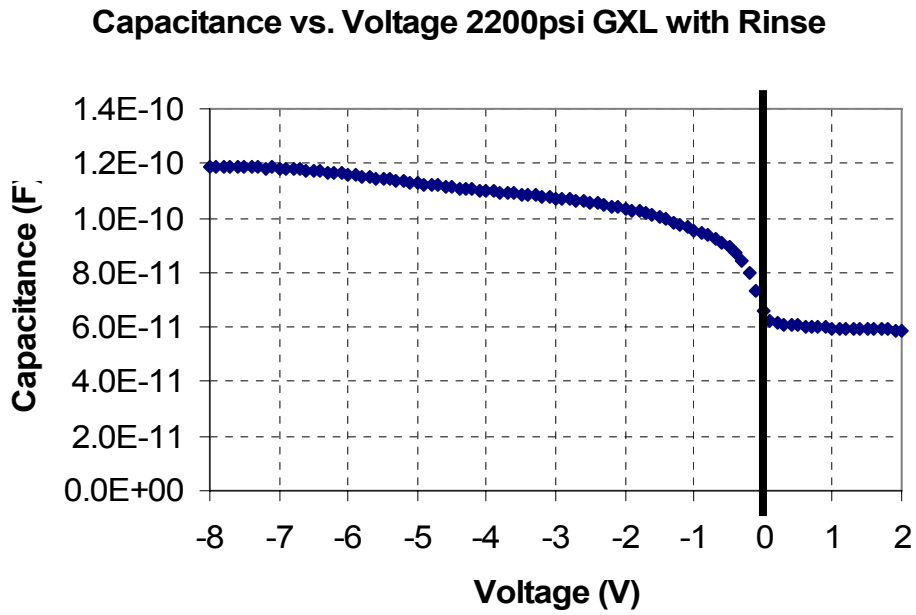

Figure 5.10: CV curve for MSQ film exposed to 2200psi GXL solution and subsequent 2200psi CO_2/CH_3OH rinse.

The CV curve shifts back to its original position after the CO_2/CH_3OH 2200psi rinse as shown in Figure 5.10. The voltage shift may be caused by the diffusion of TMA^+, OH^-, or HCO_3^- ions in the MSQ due to a concentration gradient. Because the voltage shift is negative, positive ions may have been incorporated. A larger negative flat-band voltage may have resulted in order to compensate for the inclusion of the positive ions. Of course, the shift may also be due to the combination of an electric field as supplied by a constant applied voltage and an increased temperature above 100^oC[25]. Since no applied voltage was used in the GXL experiments, the shift in the CV curve is probably due to a concentration gradient that drives ions into the MSQ film.

In addition to CV measurements, IV measurements can be obtained from MIS capacitor structures. The IV results can also lend support to the possible incorporation of polar moieties into MSQ by the detection of increased currents at lower voltages due to lower MSQ resistance. It is well-known that the inclusion of ions in a dielectric can

increase the conductivity of a film. One example is the incorporation of tetrabutyl ammonium picrate in PVC (polyvinyl chloride) layers[28].

Current vs. voltage measurements show the magnitude of current leakage through an MSQ film. Figure 5.11 shows IV results for an unprocessed MSQ film in an MIS structure. The slope of the current vs. voltage plot in Figure 5.12 significantly increases after the film has been exposed to a 2200psi GXL treatment. However, after a 2200psi CO_2/CH_3OH rinse, the slope returns to essentially that of an unprocessed MSQ sample as shown in Figure 5.13.

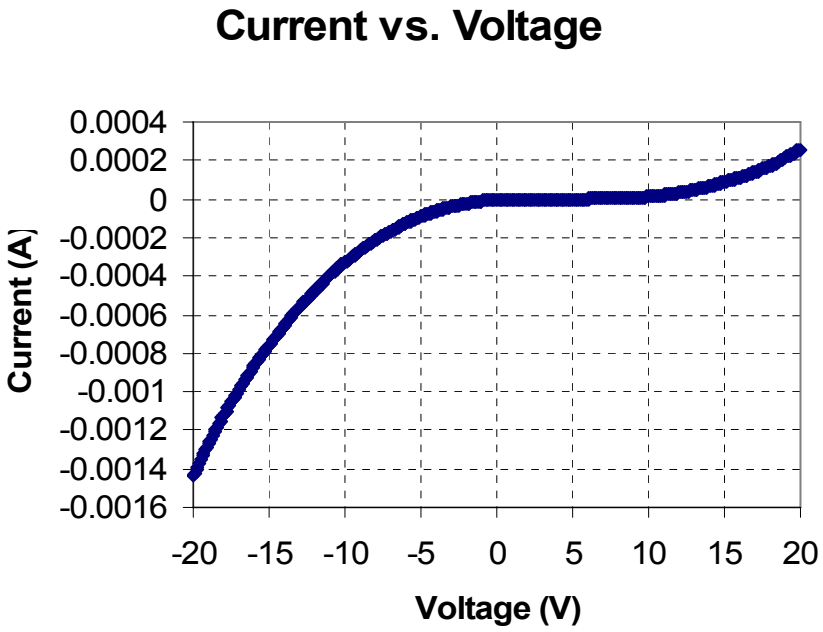

Figure 5.11: IV curve for unprocessed MSQ.

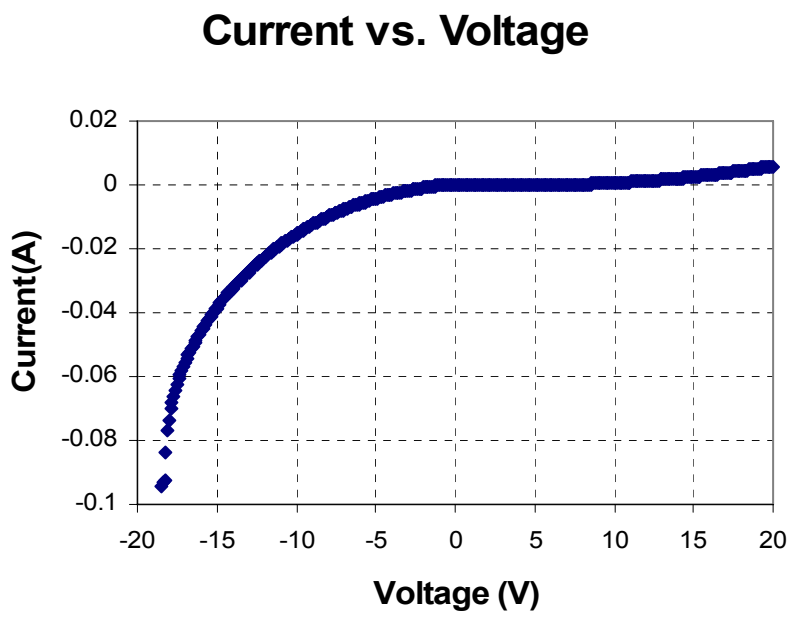

Figure 5.12: IV curve for MSQ processed in 2200psi GXL.

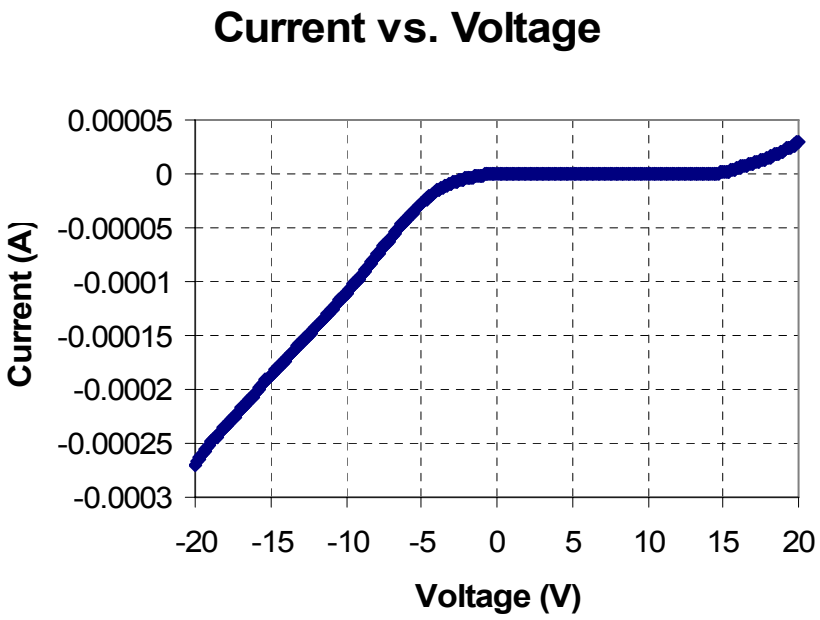

Figure 5.13: IV curve for MSQ processed in 2200psi GXL and 2200psi CO_2/CH3OH rinse.

Different samples were compared directly by noting the current flowing at a voltage of 10V. A more negative current at the same voltage indicates that the MSQ film is passing

more current and behaving less like a capacitor. Table 5.6 below compares the currents measured for samples exposed to different processing conditions.

Table 5.6: The current (A) at 10V for different MSQ films.

	I (A) at -10v	A/cm^2
Unprocessed	-3.34E-04	-1.06E-02
Liquid	-4.67E-04	-1.49E-02
1050psi GXL	-1.23E-03	-3.90E-02
1500psi GXL	-2.88E-03	-9.17E-02
2200psi GXL	-1.50E-02	-4.77E-01
2200psi GXL + Rinse	-1.11E-04	-3.53E-03

Although the dielectric constants for the high pressure treated samples C, D, and E are similar (within ~10% according to Table 5.5), the currents measured for each are significantly different. It should be noted that the currents observed are relatively high compared to an industry standard value of 10^{-7} A/cm^2. However, these higher currents may result from pinholes in the film; Fukuda has shown that an increased pinhole density contributes to a significantly higher leakage current[29].

At increasing pressures, the current increases indicating that the capacitor is more leaky, probably due to ions that have diffused into the films. During GXL exposure, the high pressure CO_2 component of the GXL may swell the MSQ and allow the ions to penetrate into the film. Swelling may be possible because Kim has shown that MSQ can absorb various organic solvents in both liquid and gas phases and then swell the MSQ film[24, 30]. Neutron reflectivity was used to measure the swelling. Irrelevant of the solvent phase, the solvent surface tension had to be less than 38dyn/cm[24]. Methanol at room temperature has a surface tension of 22dyn/cm and with the inclusion of CO_2 the surface tension would have decreased. Although not a direct comparison, ethanol with CO_2 at 1050psi, 1500psi, and 2200psi and 90^{o}C has surface tensions of 4.9dyne/cm, 2.2 dyne/cm, and 0.8 dyne/cm, respectively[31]. Methanol should have the same order of

magnitude for the surface tensions because methanol and ethanol are structural very similar and have similar properties. The CO_2/CH_3OH 2200psi rinse may have swelled the MSQ film. After rinsing with CH_3OH and drying with N_2, the negative OH^- and HCO_3^- ions may have been removed while the positive TMA^+ ion remained.

The concentration of TMA^+ and HCO_3^- ions incorporated into the MSQ film should be similar because of their equal concentrations in the GXL. Although there is some OH^-, this amount is very small in comparison to TMA^+ and HCO_3^- ions[13]. The molecular weights of TMA^+ and HCO_3^- ions are 74g/mol and 61g/mol respectively. Their similar sizes, concentrations and concentration gradients should yield similar diffusion rates if no other differences are present. Although both ions may have diffused in the MSQ film, the TMA^+ positive ion may be more stable within the film structure due to attraction to electronegative oxygen moieties in MSQ. Negative HCO_3^- ions may not interact effectively with the MSQ due to repulsion. The negative ions may interact with the silicon; however, this seems unlikely because silicon is not strongly positive whereas oxygen is strongly electronegative as indicated by oxygen's large electronegativity of 3.44. Because the positive ions interact more strongly with the film structures, they would be more difficult to remove by rinsing. The high pressure CO_2/CH_3OH rinse should remove the TMA^+ ions because CH_3OH interacts with the positive ions while the CO_2 would cause the MSQ film to swell. In addition, the concentration gradient supplies a driving force for the positive ions to diffuse out of the MSQ film.

Aw has observed similar results with incorporated positive Al ions diffusing through MSQ films to cause a shift in the CV curve towards more negative voltage values[32]. In addition Myneni through ATR-FTIR spectra demonstrated that high pressure

CO_2 aids in the diffusion of CH_3OH and $TMAHCO_3$ into a fluorocarbon film[33]. Although the fluorocarbon film is a polymer and not an inorganic material like MSQ, CO_2 can aid in transport and may serve that same role for MSQ which can be a network or polymer[30]. The current level and dielectric constant value return to the unprocessed conditions after a 2200psi CO_2/CH_3OH rinse. A related diffusion investigation has also been performed using fluorescence methods by Cao where the diffusion coefficients of pyrene out of polystyrene increased with higher CO_2 pressures[34]. Although pyrene is not a polar molecule as indicated by its low solubility of 2-3μM in water, the large 202g/mol MW of pyrene shows that large molecules can diffuse out of polymers at high pressures[35].

Samples of Coral™ (from Novellus) and Black Diamond™ (from Applied Materials) were exposed to the same high pressure GXL treatment conditions as those invoked in the MSQ experiments; details of these experiments are described in Appendix A. For those samples, a surface chemical change did occur as indicated by a lower post treatment contact angle, whereas the current MSQ GXL processed films did not display a change in contact angles. Due to the surface changes observed, surface repair techniques would be invoked to recover the low k value. The approaches used (see below) only affect the surface in contrast to the CO_2/CH_3OH high pressure rinse used in the MSQ GXL processing which affects the bulk film.

In order to repair the surface modification, previous investigators have used a variety of different methods to re-establish the low k value and hydrophobic character. Xie and Muscat have recovered low dielectric constants after plasma processing of low k materials by using supercritical CO_2 with additives such as HMDS

(hexamethyldisalizane), TMDS (tetramethyldisalizane) or TMCS (trimethylchlorosilane)[36]; chemical structures of these molecules are shown in Figures 5.14, 5.15, and 5.16.

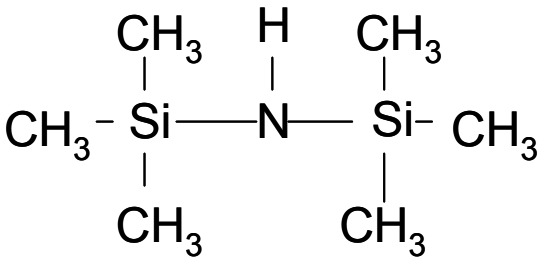

Figure 5. 14: Chemical structure of HMDS.

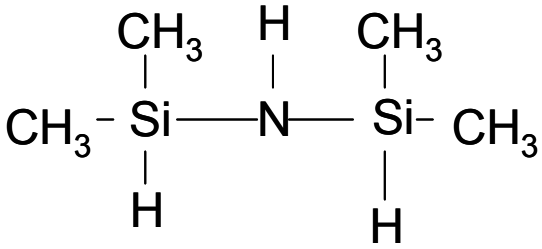

Figure 5.15: Chemical structure of TMDS.

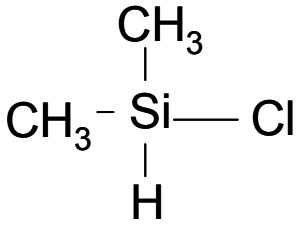

Figure 5.16: Chemical structure of TMCS.

These three additives cap the dangling oxygen atom attached to the silicon with methyl groups. Silicon with its surrounding methyl groups replace the hydrogen atom that was formerly attached to oxygen. The methyl groups render the surface more hydrophobic and prevent the absorption of water that increases the dielectric constant. However, this

process is a surface sensitive process and may not be effective with GXL processed MSQ. Although GXL processed MSQ shows an increase in dielectric constant, this is probably caused by diffusion of ions into the bulk film. Because treatments with supercritical CO_2 containing HMDS, TMDS, or TMCS would merely incorporate these additives into the film surface, no reduction in dielectric constant is anticipated due to the trapped ions in the bulk below the reacted surface.

Another method to reduce the hydrophilicity of the MSQ film is to use a NH_3 plasma in order to create a thin protective layer to seal the hydrophilic surface[37]. Liu has used a plasma treatment with NH_3 to inhibit the hydrophilicity caused by TMAH. TMAH exposure causes an increase in dielectric constant and leakage current density that was reversed with the NH_3 plasma. Analogous to the process used by Xie, this procedure only modifies the surface but does not remove trapped ions.

The C_2H_6 experiments demonstrated that although C_2H_6 can remove photoresist and etch residue at reduced temperatures, the increased hydroxide ion concentration relative to that of the CO_2-expanded GXL, poses a problem because the higher OH- concentration results in substantial etching of silicon dioxide-based low k dielectrics such as MSQ. Table 5.7 show significant etching of MSQ after C_2H_6 GXL exposure at 1000psi, TMAH bubbled with CO_2 to form TMAB, and finally TMAH alone.

Table 5.7: Before and after exposure to C_2H_6 GXL, TMAB, and TMAH.

	Before (nm)	After (nm)	% Change
C2H6 GXL	640.9	497.8	22.3%
TMAB Beaker	640.9	532.0	17.0%
TMAH Beaker	669.4	2.4	99.6%

The C_2H_6 in the C_2H_6 GXL may have shifted the chemical equilibrium towards a higher hydroxide concentration even after bubbling the initial TMAH with CO_2. As a result, the

MSQ film was etched. The beaker studies with TMAH bubbled with CO_2 showed that the MSQ was etched more extensively than it had when C_2H_6 was used as the expansion gas because the CO_2 remained in solution and was not displaced by C_2H_6; therefore, the hydroxide ion concentration did not increase. MSQ was completely removed by the TMAH solution, since only a native silicon dioxide film resulting from air exposure of the silicon surface, was detected.

Conclusions

The various analytical and electrical characterization techniques used to assess the effect of GXL treatments on MSQ assisted in the formulation of a model to explain the changes of MSQ properties observed. Thickness measurements confirmed that the film had not been etched while contact angle measurements indicated that no detectable hydrophobicity changes had occurred. In addition, FTIR spectra verified that the bulk film had not changed. However, none of these analytical methods took into consideration the effect of small concentrations ions that were clearly detected by the CV and IV studies.

The GXL solutions contained HCO_3^-, OH^-, and TMA^+ in the CH_3OH, CO_2, and water solvent. Ellipsometry and contact angle studies determined that the MSQ film had not been etched by the small OH^- presence in the GXL. If the film had been etched then the film thickness would have changed and the film would have had a lower contact angle indicating a hydrophilic surface.

Although no etching occurred, ions could have diffused into the MSQ film. The presence of these ions could have been detected by FTIR and XPS spectra if they were present at sufficiently high concentrations. However, no changes were observed in the

spectra, which suggests that the ion concentrations were below detection or that ions were not present.

The CV curves indicated that ions had penetrated into the film although at extremely low concentrations. Dielectric constants increased from 2.64 to ~26 after exposure to the GXL solution without the 2200psi CO_2/CH_3OH rinse. In addition, CV curves shifted to more negative voltage values as well. This shift could be caused by trapped positive TMA^+ ions. Trapping of positive ions rather than negative ions is likely because of possible interactions of positive ions with the electronegative oxygen in MSQ.

Current-voltage (IV) measurements showed that the current significantly increased at lower voltages indicating greater current flow, possibly due to the inclusion of positive ions. Because of the positive ions, more negative voltage is necessary to initiate accumulation in the CV curve.

A high pressure 2200psi CO_2/CH_3OH rinse was successful in recovering the electrical properties observed for the untreated MSQ films. It is expected that this treatment removes TMA^+ ions from the MSQ films. The CH_3OH serves as a medium for the ions to diffuse through to exit the film and the CO_2 would help swell the MSQ films. Finally, the concentration gradient would promote the diffusion of these ions out of the MSQ film. After the rinse, the CV and IV curves were the same as those observed for the untreated films. These studies indicate that processing of low k MSQ films with GXLs is possible without degradation of film properties, although a high pressure CO_2 with CH_3OH rinse will be required in order to fully recover the low k film properties. In addition because C_2H_6 increases the hydroxide ion concentration in GXLs that subsequently etches the MSQ, CO_2 is a more suited gas for these applications. Although

CO_2 reacts with the TMAH, this reaction allows the maintenance of a low controllable hydroxide ion concentration that is sufficient for photoresist removal and compatible with low k dielectric materials.

References

1. Song, I.; Spuller, M.; Levitin, G.; Hess, D. W., Photoresist and Etch Residue Removal using Gas-Expanded Liquids. *Journal of The Electrochemical Society* **2006,** 153, (4), G314-G318.

2. Association, S. I., International Technology Roadmap for Semiconductors 2006 update. **2006**.

3. Dean, J. A., *Lange's Handbook of Chemistry*. 15th ed.; McGraw-Hill: New York City, NY, 1999; p 5.105.

4. Knovel, Knovel Critical Tables. In 2003.

5. Maex, K.; Baklanov, M. R.; Shamiryan, D.; Iacopi, F.; Brongersma, S. H.; Yanovitskaya, Z. S., Low dielectric constant materials for microelectronics. *Journal of Applied Physics* **2003,** 93, (11), 8793-8841.

6. Choi, K.-K.; Cho, I. H.; Park, S. J.; Lim, J. E.; Jung, O. J.; Park, J. H.; Min, B. S.; Hwang, S. B.; Ko, M. J.; Lee, J. G., Characterization and integration of new porous low-k dielectric (k <2.3) for 65 nm technology and beyond. *Thin Solid Films* **2007,** 515, (12), 5025-5030.

7. Hosali, S.; Smith, G.; Smith, L.; Das, S.; Arkalgud, S., Process response of UV curable CVD porous Ultra-Low K dielectric. *Advanced Metallization Conference 2006, Proceedings, Tokyo, Japan, Sept. 26-27, and San Diego, CA, United States, Oct. 17-19, 2006* **2007**, 375-381.

8. Padovani, A. M.; Rhodes, L.; Bidstrup Allen, S. A.; Kohl, P. A., Chemically bonded porogens in methylsilsesquioxane. *Journal of the Electrochemical Society* **2002,** 149, (12), F161-F170.

9. Lee, H.-J.; Soles, C. L.; Liu, D.-W.; Bauer, B. J.; Lin, E. K.; Wu, W.-L.; Gallagher, M., Structural characteristics of methylsilsesquioxane based porous low-k thin films fabricated with increasing cross-linked particle porogen loading. *Journal of Applied Physics* **2006,** 100, (6), 064104/1-064104/8.

10. Xu, J.; Moxom, J.; Yang, S.; Suzuki, R.; Ohdaira, T., Porosity in porous methyl-silsesquioxane (MSQ) films. *Applied Surface Science* **2002,** 194, (1-4), 189-194.

11. Michelon, J.; Hoofman, R. J. O. M., Impact of moisture on porous low-k reliability. *IEEE International Integrated Reliability Workshop Final Report, S. Lake Tahoe, CA, United States, Oct. 17-20, 2005* **2005**, 35-38.

12. Kim, K.-H.; Lee, D. J.; Rhee, H.-W.; Char, K.; Yoon, D. Y.; Choi, J.-S., Preparation and Characterization of Low Dielectric Methyl Silsesquioxane (MSSQ) Thin Films. *Journal of the Korean Physical Society* **2001,** 39, (1), 119-122.

13. Levitin, G.; Myneni, S.; Hess, D. W., Reactions Between CO2 and Tetramethylammonium Hydroxide in Cleaning Solutions. *Electrochemical and Solid State Letters* **2003,** 6, (8), G101-G104.

14. Panza, J. L.; Beckman, E. J., Chemistry and Materials Design for CO2 Processing. In *Supercritical Fluid Technology for Drug Product Development*, York, P.; Kompella, U. B.; Shekunov, B. Y., Eds. Marcel Dekker: New York City, NY, 2004; p 4.

15. Xie, B.; Muscat, A. J., Silylation of porous methylsilsesquioxane films in supercritical carbon dioxide. *Microelectronic Engineering* **2004,** 76, (1-4), 52-59.

16. Nosonovsky, M.; Bharat, B., Hierarchical roughness makes superhydrophobic states stable. *Microelectronic Engineering* **2007,** 84, (3), 382-386.

17. Grill, A.; Neumayer, D. A., *J. Appl. Phys* **2003,** 94, 6697-6707.

18. Wang, C. Y.; Shen, Z. X.; Zheng, J. Z., *Appl. Spectrosc* **2000,** 54, 209-213.

19. Wang, C. Y.; Shen, Z. X.; Zheng, Z., *Appl. Spectrosc* **2001,** 55, 1347-1351.

20. Cox, J. N., FTIR: Fourier Transform Infrared Spectroscopy. In *Encyclopedia of Materials Characterization*, Brundle, C. R.; Jr., C. A. E.; Wilson, S., Eds. Butterworth-Heinemann: Boston, MA, 1992; pp 416-421.

21. Wissinger, R. G.; Paulaitis, M. E., Swelling and sorption in polymer-carbon dioxide mixtures at elevated pressures. *Journal of Polymer Science, Part B: Polymer Physics* **1987,** 25, (12), 2497-510.

22. Assink, R., Plasticization of Poly((dimethyl Siloxane) by High-pressure Gases as Studied by NMR Relaxation. *Journal of Polymer Science: Polymer Physics Edition* **1974,** 12, 2281-2290.

23. Xie, B.; Muscat, A. J., Condensation of Silanol Groups in Porous Methylsilsesquioxane Films Using Supercritical CO2 and Alcohol Cosolvents. *IEEE Transactions on Semiconductor Manufacturing* **2004,** 17, (4), 544-553.

24. Kim, H.-C.; Volksen, W.; Miller, R. D.; Huang, E.; Yang, G.; Briber, R. M.; Shin, K.; Satija, S. K., Neutron Reflectivity on Nanoporous Poly(methylsilsesquioxane) Thin Films. *Chemistry of Materials Communications* **2003,** 15, (3), 609-611.

25. Grove, A. S., *Physics and Technology of Semiconductor Devices*. John Wiley and Sons: New York City, NY, 1967; p 265.

26. Wieder, H. H., Insulator/Semiconductor Contacts. In *Contacts to Semiconductors - Fundamentals and Technology*, Brillson, L. J., Ed. William Andrew Publishing/Noyes: New York City, NY, 1993; p 299.

27. Sze, S. M.; Ng, K. K., *Physics of Semiconductor Devices*. 3rd ed.; John Wiley and Sons: Hoboken, NJ, 2007; p 199-200.

28. Sears, J. K.; Darby, J. R., *Technology of Plasticizers*. John Wiley and Sons: New York City, NY, 1982; p 374.

29. Fukuda, T.; Nishino, H.; YAnazawa, H., Analysis of Leakage Current of Low-k Materials for Use as Interlayer Dielectric. *Japanese Journal of Applied Physics* **2004,** 43, (1), 86-90.

30. Kim, H.-C.; Wilds, J. B.; Hinsberg, W. D.; Johnson, L. R.; Volksen, W.; Magbitang, T.; Lee, V. Y.; Hedrick, J. L.; Hawker, C. J.; Miller, R. D., Selective Sorption of Nanoporous Poly(methyl silsesquioxane). *Chem. Mater.* **2002,** 14, 4628-4632.

31. Sun, Y.; Shekunov, B. Y., Surface tension of ethanol in supercritical CO2. *J. of Supercritical Fluids* **2003,** 27, 73-83.

32. Aw, K. C. In *Reliability of MSQ spin-on glass as low-k interlayer dielectric in VLSI device*, Kuala Lumpur, Malaysia, 2004; IEEE: Kuala Lumpur, Malaysia, 2004; pp 1-4.

33. Myneni, S.; Hess, D. W., Post Plasma Etch Residue Removal Using CO_2-Based Mixtures: Mechanistic Considerations. *Journal of The Electrochemical Society* **2005,** 152, (10), G757-G765.

34. Cao, T.; Johnston, K. P.; Webber, S. E., CO2-Enhanced Transport of Small Molecules in Thin Films: A Fluorescence Study. *Macromolecules* **2004,** 37, (5), 1897 - 1902.

35. Tedeschi, C.; Moehwald, H.; Kirstein, S., Polarity of Layer-by-Layer Deposited Polyelectrolyte Films As Determined by Pyrene Fluorescence. *Journal of the American Chemical Society* **2001,** 123, (5), 954-960.

36. Xie, B.; Muscat, A. J., Water removal and repair of porous ultra low-k films using supercritical CO2. *Proceedings - Electrochemical Society* **2004,** 2003-26, (Cleaning Technology in Semiconductor Device Manufacturing VIII), 279-288.

37. Liu, P.-T.; Chang, T.-C.; Huang, M.-C.; Tsai, M. S.; Sze, S. M., Highly reliable chemical–mechanical polishing process for organic low-k methylsilsesquioxane. *J. Vac. Sci. Technol. B* **2001,** 19, (4), 1212-1218.

CHAPTER 6

CHARACTERIZING ABSORPTION OF CO_2 AND C_2H_6 INTO PHOTORESIST FILMS USING A QUARTZ CRYSTAL MICROBALANCE (QCM)

Introduction

Photoresist and etch residue removal is a key step in semiconductor device manufacturing because this step ensures a clean foundation for the many deposited and etched layers required to make an integrated circuit (IC) chip. The increased awareness of using toxic cleaning solvents has called for more environmentally benign solutions such as supercritical fluids and gas expanded liquids. Gas expanded liquids reduce liquid solvent usage by the inclusion of a high pressure gas such as CO_2. Gas expanded liquids composed of CO_2[1] or C_2H_6 that expand a methanol-based liquid containing an tetramethylammonium bicarbonate (TMAB) additive effectively removed photoresist films. In this study we compare CO_2 with C_2H_6 as the gas in gas expanded liquids by characterizing the absorption of the gases into two films, polystyrene (PS) and polyhydroxystyrene (PHOST). PHOST is a resin used in photoresists while PS lacks the hydroxyl group of PHOST; Figure 6.1 shows the structures of PS and PHOST.

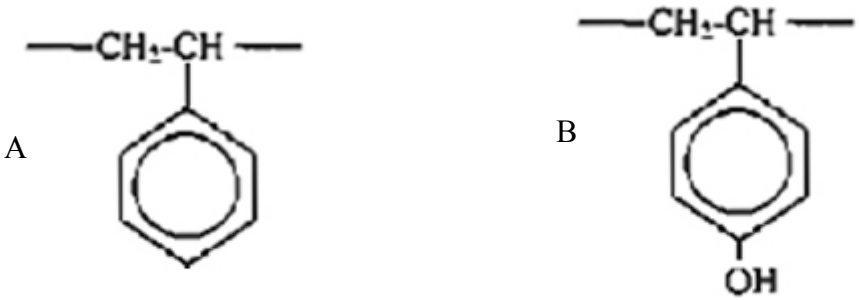

Figure 6.1: Molecular structure of A) PS and B) PHOST.

Contact angle measurements using water as the probe liquid are performed to determine the hydrophilicity of the films which is expected to affect the gas absorption.

C_2H_6 has similar molecular weight (30g/mole vs. 44g/mole), critical temperature (32.3°C vs. 31.1°C), and critical pressure (707.8psi vs. 1073psi) to CO_2 but lacks the quadrupole moment of CO_2 which may cause enhanced interaction with the hydroxyl group in PHOST. Although C_2H_6 is nonpolar, it has a small quadrupole moment as indicated in Table 6.1.

Table 6.1: Quadrupole moments for different gases where esu is electrostatic unit of charge[2].

	Quadrupole Moment (esu) 10^{26}
Carbon Dioxide	-4.3 +/- 0.2
Ethane	-0.8 +/- 0.1
Nitrogen	-1.4 +/ -0.1
Oxygen	-0.4 +/- 0.1

Due to the quadrupole moment in CO_2, the electron density is higher at the oxygen atom and lower at the carbon atom. Therefore, CO_2 can behave as both a Lewis acid and Lewis base[3]. For instance, it behaves as a Lewis acid when the electron depleted carbon in CO_2 interacts with an electron rich oxygen in a carbonyl group[4] and behaves as a Lewis base when the electron rich oxygen in CO_2 interacts with a hydrogen in an acid[5].

PHOST and PS films were exposed to CO_2 and C_2H_6 at increased pressures to investigate the absorption of the gases into the films. Specifically, the gases may swell the films and thereby allow improved penetration of the liquid component of the GXLs to enhance film removal. Prior studies using the CO_2-expanded TMAB mixture indicated that the mechanism for photoresist removal on silicon wafers was film liftoff wherein the small hydroxide concentration in equilibrium with bicarbonate in TMAB etched the underlying silicon dioxide to lift off the photoresist and etch residue film[6]. The CO_2 gas

swells the photoresist film and allows the liquid to penetrate through the photoresist film to reach the underlying silicon dioxide.

The existence of a hydroxyl group in PHOST but not in PS may be important in establishing the effect of the quadrupole moment in CO_2. The quadrupolar CO_2 may interact more with PHOST as a result of hydroxyl group. Increased interaction may be interpreted as a larger mass uptake of the gas. Understanding the gas absorption assist in selection of the most appropriate gas to use for photoresist/etch residue removal in GXLs.

Experimental

Polyhydroxystyrene 11,800 MW was obtained from Dupont Electronic Technologies and polystyrene 13,200 MW was obtained from Scientific Polymer. The powder forms of the polymers were dissolved in 99% propylene glycolmethylether acetate (PGMEA) from Sigma Aldrich in a 15wt% solution. The solutions were spincast onto 6MHz AT cut 0.55" polished gold quartz crystals from Colorado Crystal. The crystals had gold electrodes for contacts. A Cost Effective Equipment 100CB spin coater was used to spin the films at 2500rpm for 30s and then the films were baked at 110^{o}C for 1min to remove the PGMEA solvent. Films thicknesses were measured with a J.A. Woollam M-2000VI ellipsometer. Incident angles of 65^{o}, 70^{o}, and 75^{o} were used and a Cauchy model was used to fit the film thicknesses.

The crystals were mounted on a Maxtek BSH-150/151 QCM sensor head. A Maxtek RQCM and Q-Sense QCMD were used to measure the frequencies of the crystals. Frequency measurements were taken before and after film deposition to obtain the film mass. Measurements were recorded after the frequency stabilized which was ~30min. CO_2 gas (SFC grade with eductor tube, 99.9995%) and C_2H_6 gas (CP grade

with eductor tube, 99%) from Airgas were injected into the reaction chamber where the frequency change of the two crystals with either PHOST or PS was measured by the QCMD and RQCM, respectively. A diagram of the experimental configuration is shown in Figure 6.2.

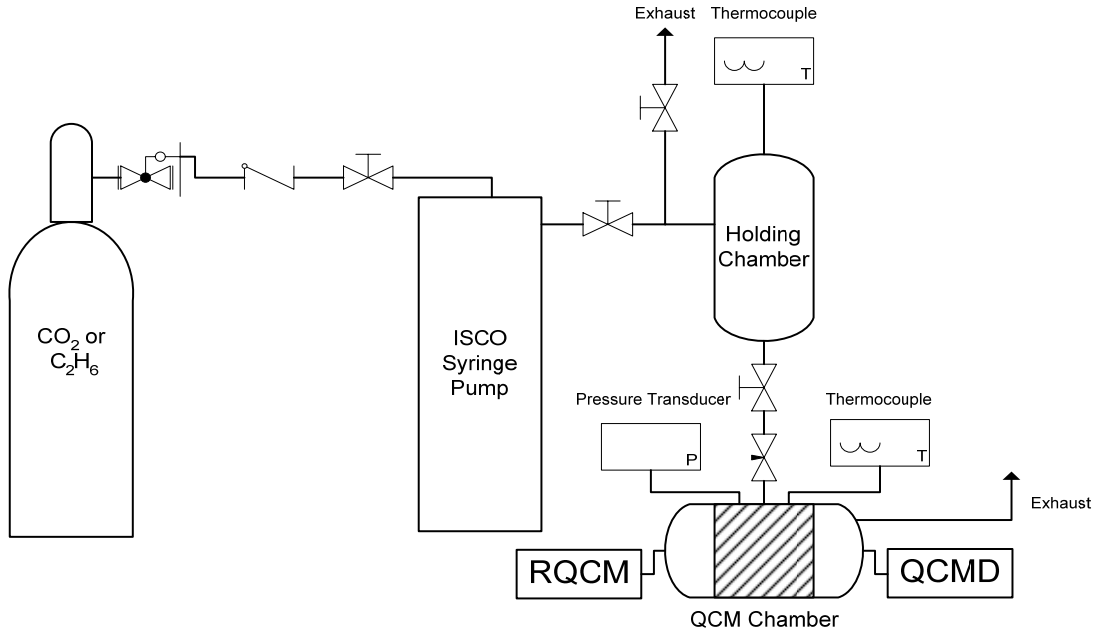

Figure 6.2: Experimental setup for QCM studies.

An Isco 1000D syringe pump regulated the gas pressurization from atmosphere to 1500psi. HiP valves controlled gas flow and a Hoke microneedle valve was used to slowly leak gas into the QCM chamber. Pressure measurements were performed using an Omega pressure transducer connected to Labview 7 software. RQCM data was recorded using RQCM Data Logging Software and QCMD data was recorded using QSoft 301. In addition to the fundamental frequency at 6MHz, the QCMD recorded the 3rd and 5th overtones at 18MHz and 30MHz and recorded the dissipation factor. Excluding the gas cylinder and Isco pump, the entire system was enclosed in a polycarbonate shield with exits leading to a snorkel and the building exhaust system.

Contact angle measurements of the PHOST and PS coated crystals were performed on an AST Products Video Contact Angle System 2500XE using water.

Results and Discussion

The mass uptake of CO_2 and C_2H_6 by PHOST and PS were measured by converting the frequency changes of the gold plated piezoelectric crystal to a mass[7, 8] using Equation 6.1:

$$\Delta F = F - F_o = \Delta F_m + \Delta F_p + \Delta F_n \qquad (6.1)$$

$\Delta F_p = F_o \alpha P$ $\quad F_o\alpha = 0.43 Hz/psi$[9] (frequency change due to pressure)

$\Delta F_n = -0.5 C_m (\pi F_o)^{-1/2} (\rho_f \eta_f)^{1/2}$ (frequency change due to viscosity)

$C_m = -2F_o^2/(\mu_q \rho_q)^{1/2}$

$\mu_q = 2.947 \times 10^{11}$ g/cm-s^2

$\rho_q = 2.648$ g/cm^3

$\Delta F_m = -2F_o^2 \Delta m/(\mu_q \rho_q)^{1/2} = -C_m \Delta m/A$ (frequency change due to mass)

$A = 1.53$ cm^2

where F = current frequency (Hz)

F_o = original frequency (Hz)

ΔF_m = frequency change due to mass (Hz)

ΔF_p = frequency change due to pressure (Hz)

ΔF_n = frequency change due to viscosity (Hz)

α = pressure correction factor

C_m = mass sensitivity constant $\left(\frac{Hz^2}{g/cm^2 s} \right)$

ρ_f = density of fluid (g/cm^3)

n_f = viscosity of fluid (g/cm-s)

μ_q = shear modulus of crystal (g/cm-s^2)

ρ_q = density of crystal (g/cm^3)

A = area of crystal (cm^2)

Between 750 and 1500 psi, and at room temperature, both PS and PHOST absorbed more CO_2 than did PS as indicated in Figures 6.3 and 6.4.

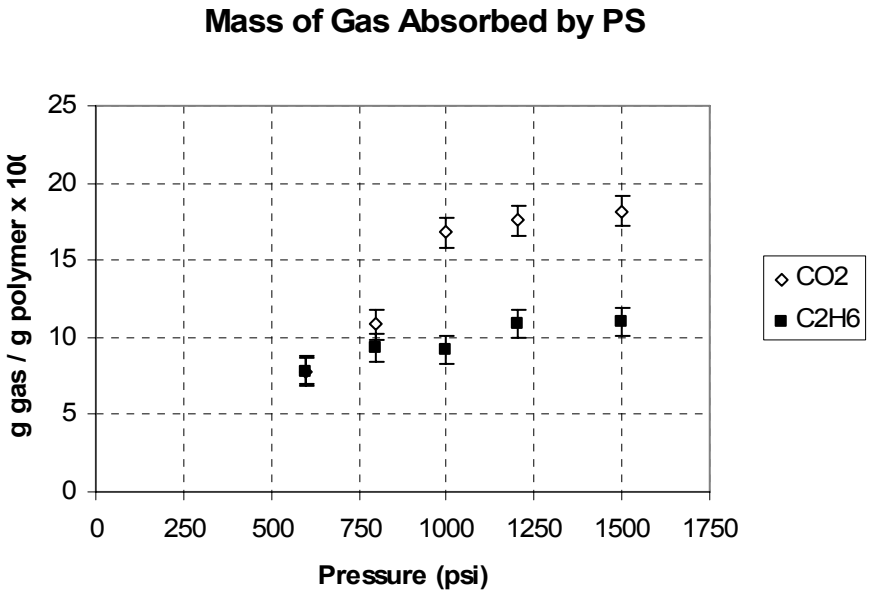

Figure 6.3: Mass of CO_2 and C_2H_6 absorbed by PS.

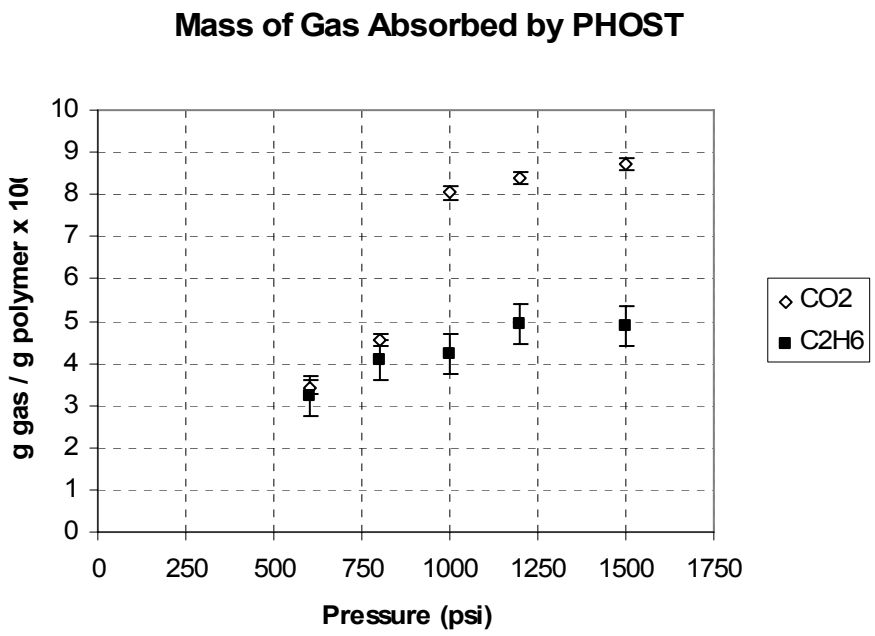

Figure 6.4: Mass of CO_2 and C_2H_6 absorbed by PHOST.

CO_2 is absorbed to a greater extent by both polymers because CO_2 has a higher critical pressure of 1070psi compared to 706psi for C_2H_6[10, 11]. In addition, PS absorbed more CO_2 and C_2H_6 because the PS film has a lower density[12]; PS has a density of 1.05g/cm^3 compared to 1.17g/cm^3 for PHOST[13]. Sorption increases with larger molecular weight (MW) polymers and consequently the polymers chosen had fairly similar molecular weights[14]. However, the MW of PS is 13,200 compared to 11,800 for PHOST. This may also contribute to PS ability to absorb more gas.

PS absorbed a higher mass of both CO_2 and C_2H_6 compared to PHOST. However, the ratio of CO_2/C_2H_6 absorbed by PHOST is greater than that of PS. Comparing the mass absorbed ratios CO_2/C_2H_6 demonstrates that PHOST preferentially absorbs relatively more CO_2 compared to PS. This is shown in Table 6.2.

Table 6.2: Ratio of CO_2/C_2H_6 absorbed by PHOST and PS.

	Ratio of CO2/C2H6 Mass Absorbed	
Pressure (psi)	PHOST	PS
600	1.07	1.00
800	1.12	1.16
1000	1.90	1.83
1200	1.70	1.61
1500	1.78	1.65

For example, at 1000psi PHOST would absorb 1.9 times more CO_2 than C_2H_6 whereas PS would absorb 1.83 times more CO_2 than C_2H_6. Therefore, although PS absorbs more gas overall by comparing Figure 6.3 and 6.4, PHOST absorbs more CO_2 relative to C_2H_6. In addition, at higher pressures the ratio of CO_2/C_2H_6 becomes larger for both polymers.

As mentioned before, more CO_2 is absorbed compared to C_2H_6 for both polymers; however, the relative amount of mass absorbed is larger for PHOST. This observation may be due to the hydroxyl group present in PHOST. That is, the hydrogen in the hydroxyl group in PHOST behaves as a Lewis acid and the oxygen in CO_2 behaves as a Lewis base[15, 16]. Thus, the hydroxyl group may interact with the quadrupolar CO_2. Indeed, other investigators have observed similar trends for carbonyl groups as well; however, in those experiments different nonpolar gases such as C_2H_6 were not used[12, 17]. Rather, CO_2 gas was absorbed into polymers that contained different chemical moieties such as carbonyl groups.

The hydroxyl group in PHOST also caused the PHOST film to be more hydrophilic as shown in Table 6.3.

Table 6.3: Contact angles for PS and PHOST coated crystals.

	Contant Angle	
	PS	PHOST
Immediately	104.4	94.3
After 1min	98.2	84.0
After 5min	86.5	51.3

Although the experiments were not performed in a dry box, the hydrophilic nature of PHOST did not measureably affect gas absorption because during stability trials, the frequency of the PHOST coated crystal was constant. That is, the QCM frequency would have continuously decreased if moisture from the air had been absorbed.

Although the studies only measured mass uptake, film swelling also occurred as evidenced by the increase in the dissipation factor with increasing pressure. Dissipation factor is defined as the ratio between energy lost and energy stored[18]. Using the QCMD, the applied voltage is intermittently turned on and off and the oscillation decay is measured. A larger dissipation indicates that the film has become more viscoelastic and less rigid; polymers become more viscoelastic upon absorption of gases. The viscosity of the polymers decrease with mass absorption[19]. If the films had been compressed due to applied hydrostatic pressure, then the dissipation would have remained the same or decreased at higher pressures indicating a more rigid film. The dissipation changes with increased pressure areshown in Figures 6.5 and 6.6.

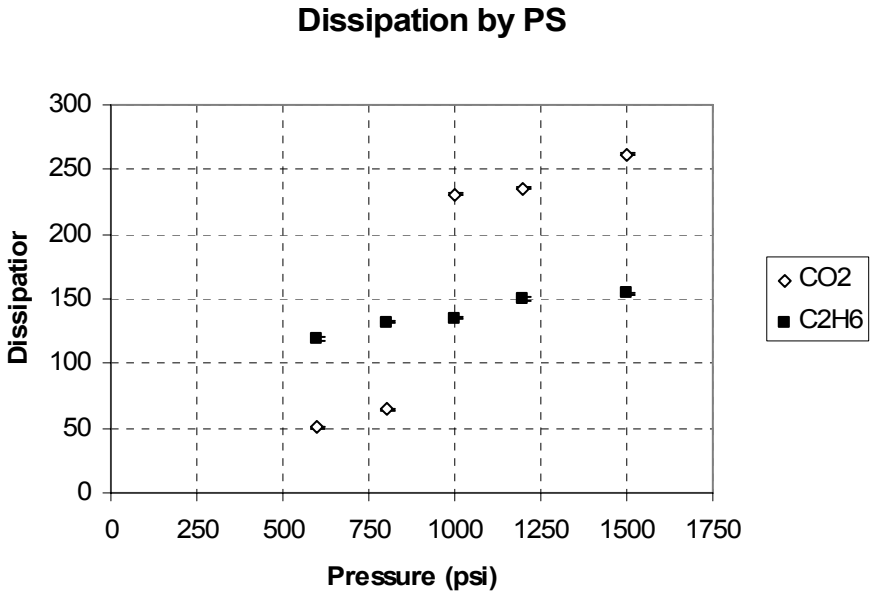

Figure 6.5: Dissipation by PS as a function of pressure.

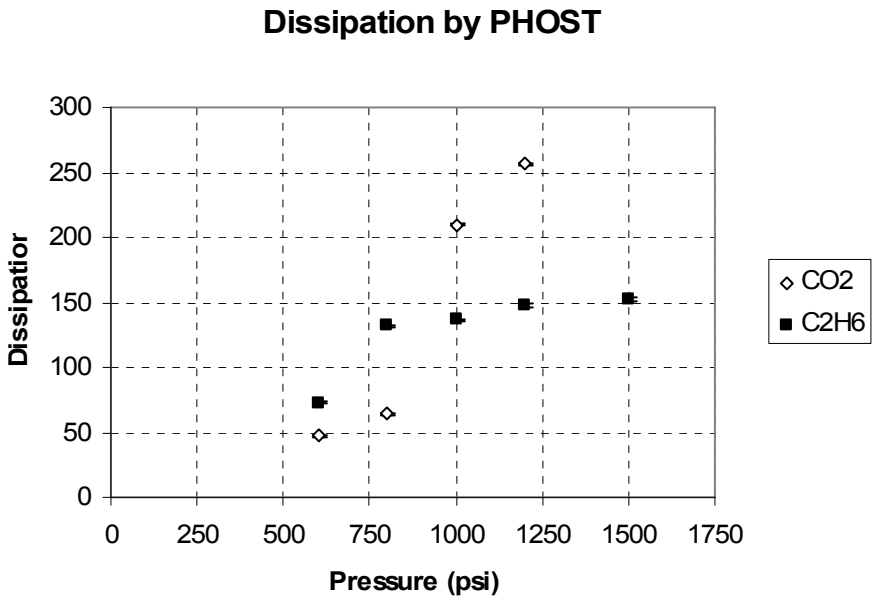

Figure 6.6: Dissipation by PHOST as a function of pressure.

Conclusions

QCM studies indicate that CO_2 plays a unique role as an expansion gas in GXLs because CO_2 has a quadrupole moment, relatively high critical pressure, and swells polymer films. Due to the quadrupole moment, CO_2 may possibly display greater interaction with hydroxyl groups in PHOST compared to PS through a Lewis acid-base interaction. Although PS absorbs more CO_2 by comparing Figure 6.3 to 6.4, PHOST had mostly higher ratios of CO_2/C_2H_6 absorbed according to Table 6.1 from 600 to 1500psi. The relatively high critical pressure of CO_2 compared to C_2H_6 results in higher CO_2 solubility in the polymer films. Film dissipation measurements indicated that film swelling occurred and the swelling was more evident with CO_2 gas. Although CO_2 has benefits of being relatively environmentally friendly, abundant, well characterized, and inexpensive, CO_2 also has unique physical and chemical properties that make it an excellent choice as the expansion gas in GXLs.

References

1. Song, I.; Spuller, M.; Levitin, G.; Hess, D. W., Photoresist and Etch Residue Removal using Gas-Expanded Liquids. *Journal of The Electrochemical Society* **2006,** 153, (4), G314-G318.

2. Buckingham, A. D.; Disch, R. L.; Dunmur, D. A., Quadrupole moments of some simple molecules. *Journal of the American Chemical Society* **1968,** 90, (12), 3104-7.

3. Blatchford, M. A.; Raveendran, P.; Wallen, S. L., Spectroscopic Studies of Model Carbonyl Compounds in CO2: Evidence for Cooperative C-H.O Interactions. *Journal of Physical Chemistry A* **2003,** 107, (48), 10311-10323.

4. Meredith, J. C.; Johnston, K. P.; Seminario, J. M.; Kazarian, S. G.; Eckert, C. A., Quantitative Equilibrium Constants between CO2 and Lewis Bases from FTIR Spectroscopy. *J. Phys. Chem.* **1996,** 100, 10837-10848.

5. Bell, P. W.; Thote, A. J.; Park, Y.; Gupta, R. B.; Roberts, C. B., Strong Lewis Acid-Lewis Base Interactions between Supercritical Carbon Dioxide and Carboxylic Acids: Effects on Self-association. *Industrial & Engineering Chemistry Research* **2003,** 42, (25), 6280-6289.

6. Myneni, S.; Hess, D. W., Post Plasma Etch Residue Removal Using CO_2-Based Mixtures: Mechanistic Considerations. *Journal of The Electrochemical Society* **2005,** 152, (10), G757-G765.

7. Zweber, A. E.; Carbonell, R. G., Monitoring photoresist dissolution in supercritical carbon dioxide using a quartz crystal microbalance. *Proceedings of SPIE-The International Society for Optical Engineering* **2006,** 6153, (Pt. 2, Advances in Resist Technology and Processing XXIII), 61534C/1-61534C/9.

8. Sauerbrey, G., The use of quartz oscillators for weighing thin layers and for microweighing. *Zeitschrift fuer Physik* **1959,** 155, 206.

9. Stockbridge, C. D., Effect of hydrostatic pressure on rotated Y - cut quartz crystal resonators. *Vacuum Microbalance Techniques* **1966,** 5, 179-191.

10. Ismail, A. F.; Lorna, W., Penetrant-induced plasticization phenomenon in glassy polymers for gas separation membrane. *Separation and Purification Technology* **2002,** 27, (3), 173-194.

11. Chiou, J. S.; Barlow, J. W.; Paul, D. R., Plasticization of Glassy Polymers by COz. *Journal of Applied Polymer Science* **1985,** 30, 2633-2642.

12. Aubert, J. H., Solubility of carbon dioxide in polymers by the quartz crystal microbalance technique. *Journal of Supercritical Fluids* **1998,** 11, (3), 163-172.

13. Puleo, A. C.; Muruganandam, N.; Paul, D. R., Gas sorption and transport in substituted polystyrenes. *Journal of Polymer Science, Part B: Polymer Physics* **1989,** 27, (11), 2385-406.

14. Toi, K.; Paul, D. R., Effect of polystyrene molecular weight on the carbon dioxide sorption isotherm. *Macromolecules* **1982,** 15, (4), 1104-7.

15. Gugliuzza, A.; Fabiano, R.; Garavaglia, M. G.; Spisso, A.; Drioli, E., Study of the surface character as responsible for controlling interfacial forces at membrane-feed interface. *Journal of Colloid and Interface Science* **2006,** 303, (2), 388-403.

16. Kachi, Y.; Tsukahara, T.; Kayaki, Y.; Ikariya, T.; Sato, J.; Ikeda, Y., Raman spectral shifts of CO2 as measure of CO2-philicity of solutes in supercritical carbon dioxide. *Journal of Supercritical Fluids* **2007,** 40, (1), 20-26.

17. Bos, A.; Punt, I. G. M.; Wessling, M.; Strathmann, H., CO2-induced plasticization phenomena in glassy polymers. *Journal Of Membrane Science* **1999,** 155, (1), 67-78.

18. http://www.q-sense.com/ (09/2007).

19. Bae, Y. C., Gas plasticization effect of carbon dioxide for polymeric liquid. *Polymer* **1996,** 37, (14), 3011-3017.

CHAPTER 7

CONCLUSIONS

The role of CO_2 in GXLs as applied to photoresist and etch residue removal was investigated. Previous studies[1] modeled the wetting of small features using GXLs. The current investigation concentrated on the removal of commercial etch residues on patterned wafers, the effects of GXLs on the chemical, electrical, and physical properties of low k dielectrics, and the effect of expansion gas on the properties and cleaning ability of GXLs.

CO_2 expanded tetramethyl ammonium bicarbonate (TMAB) in methanol GXLs removed photoresist and etch residue from commercially patterned samples at temperatures >90^oC and pressures >1000psi. At lower pressures (0-100psi), the film was removed by the solvent power of the concentrated solution. At intermediate pressures (100-1000psi), the CO_2 addition simply diluted the fluid which prevented film and residue removal. At higher pressures (>1000psi) CO_2 penetrated into the photoresist, swelled the film, and allowed TMAH to diffuse through the polymer and etch the underlying SiO_2, thereby resulting in a lift-off removal process.

In addition, low k materials which are being incorporated into the IC industry as the next generation of interlayer dielectric materials, were exposed to the GXL process used to remove photoresist and etch residue. Upon GXL exposure, HCO_3^-, OH^-, and TMA^+ ions penetrated into the low k MSQ film. Although no etching was detected by ellipsometry, electrical measurements (capacitance-voltage and current-voltage) indicated that ions had been trapped in the dielectric film. The most likely scenario was that positive ions have been trapped due to attraction to the highly electronegative oxygen in

MSQ. This was also supported by current-voltage (IV) measurements which showed that the current significantly decreased at negative voltages indicating greater current flow, consistent with the introduction of positive ions. In addition, incorporation of positive ions required a more negative voltage to initiate accumulation in the capacitance (CV) curve; indeed this result was also observed. From the CV curves, a dielectric constant was calculated, the value of which increased from 2.7 to ~26, again consistent with ion inclusion. However, a CH_3OH/CO_2 high pressure rinse at 2200psi enabled out diffusion of the ions from the MSQ and thereby returned the dielectric constant to its original value of 2.7.

GXL treatments of industrially-generated patterned samples and low k dielectric materials demonstrated the feasibility of GXL for photoresist and etch residue applications. In order to better understand and ultimately extend the possible use of GXLs, CO_2 was compared to C_2H_6 in order to take advantage of the unique characteristics of CO_2 such as the quadrupole moment that may be responsible for the specific properties of CO_2. CO_2 is an acidic gas and reacts with basic TMAH, but C_2H_6 does not. When C_2H_6 was used as the expansion gas in a GXL, the process temperature required for photoresist and etch residue removal dropped to 50^oC as compared to 90^oC for CO_2. A lower temperature was possible because C_2H_6 did not react with the TMAH to form tetramethyl ammonium bicarbonate and hence a higher hydroxide concentration was available as the photoresist and etch residue removal agent. However, this increased hydroxide concentration was detrimental to low k dielectrics. Upon exposure to C_2H_6 expanded TMAH, the increased hydroxide concentration etched the low k material more

rapidly than was observed with CO_2-based GXLs, thereby limiting the applications possible.

The mass absorption of CO_2 and C_2H_6 into polystyrene (PS) and polyhydroxystyrene (PHOST) were compared using QCM. More CO_2 was absorbed by both polymers compared to C_2H_6 due to the relatively higher critical temperature of CO_2 compared to C_2H_6. The quadrupolar nature of CO_2 may possibly have allowed increased interaction with the hydroxyl group in PHOST via a Lewis acid-base interaction as indicated by the larger ratio of CO_2/C_2H_6 absorbed by PHOST compared to PS. Although swelling was not directly measured, the increased dissipation determined by QCMD indicated that the films had become less rigid which suggests film swelling because if the film had been compressed by the high pressure gas, a constant dissipation would have resulted.

Although CO_2 was initially investigated as the gas for GXLs due to its low cost, well studied characteristics, relatively benign nature, and low critical temperature and pressure, CO_2 possesses several other advantageous properties. CO_2's quadrupolar nature, a high critical pressure that allows increased solubility, and ability to swell polymer films such as photoresists reveals CO_2 multifaceted benefits for photoresist and etch residue removal in the microelectronics fabrication process. Although many of these characteristics were well known, this study confirmed them with specific experiments and provided new insight described in the next section.

Despite the fact that wet cleaning methods have been the industry standard, high pressure methods such as GXLs and SCFs are creating interest due to their use of gases that reduce solvent use, reduce viscosities, and lower surface tensions. GXLs possess

several advantages compared to SCFs. Namely, GXLs are a liquid based solution therefore the solvent strength is greater due to the higher concentration of the solutes that perform the cleaning. In addition, the properties of GXLs such as viscosity and surface tension can be tuned by adjusting the gas pressure dissolved in the liquid.

GXLs have been used previously for separation processes[2-4] but have not yet been applied to microelectronics fabrication processes until recently[1]. Furthermore, this study shows for the first time that GXLs can be used to remove photoresist and etch residue from commercially patterned samples. Past GXL studies had only removed model films such as polyhydroxystyrene (PHOST)[1]. In addition, studies have reported the effects of supercritical fluids (SCFs) on low k materials, but those studies focused on the effects of SCFs on pore size[5] and on the repair of low k materials using cosolvents dissolved in SCFs[6]. Because GXLs are liquid based solutions, liquid can be trapped in the pores of porous low k dielectrics. The low k GXL studies demonstrated that with a high pressure 2200psi CO_2/CH_3OH rinse the low dielectric constant value could be recovered. This is important because in order for GXLs to be used in IC manufacturing processes, they must be compatible with the low k materials that are being implemented.

Many studies have been performed on the effect of CO_2[7-11] and C_2H_6[12, 13] on polystyrene (PS) properties. Those studies focused on the mass sorption of these gases into PS. But the gases were not compared to each other with respect to quadrupolar moment discussion. Instead, polymer with different groups such as carbonyl groups were compared using only CO_2. The results in relation to carbonyl group were inconclusive[7, 11]. Our QCM studies showed that CO_2 was more extensively absorbed by both polymers. PS absorbed more CO_2 and C_2H_6 compared to PHOST; however, PHOST absorbed a

high ratio of CO_2/C_2H_6 compared to PS which may possibly mean that the hydroxyl group interacted more with the quadrupole in CO_2.

The studies described in this thesis that investigate commercially patterned samples and low k samples with CO_2 and C_2H_6 has added new information and insight into understanding GXLs for photoresist and etch residue removal in IC fabrication.

References

1. Spuller, M. T. Ph.D. Dissertation, Georgia Institute of Technology, Atlanta, GA, 2003.

2. Lee, S. T.; Olesik, S. V.; Fields, S. M., *Journal of Microcolumn Separations* **1995,** 7, 477-483.

3. Chang, C. J.; Randolph, A. D., *Biotechnology Progress* **1991,** 7, 275-278.

4. Eckert, C. A.; Bush, D.; Brown, J. S.; Liotta, C. L., *Ind. Eng. Chem. Res.* **2000,** 39, 4615-4621.

5. Myneni, S.; Peng, H.-G.; Gidley, D. W.; Hess, D., Compatibility of high pressure cleaning mixtures with a porous low dielectric constant film: A positronium annihilation lifetime spectroscopic study. *J. Vac. Sci. Technol. B* **2005,** 23, (4), 1463-1469.

6. Xie, B.; Choate, L.; Muscat, A. J., Repair and capping of porous MSQ films using chlorosilanes and supercritical CO2. *Microelectronic Engineering* **2005,** 80, 349-352.

7. Aubert, J. H., Solubility of carbon dioxide in polymers by the quartz crystal microbalance technique. *Journal of Supercritical Fluids* **1998,** 11, (3), 163-172.

8. Kumar, S. K.; Chhabria, S. P.; Reid, R. C.; Suter, U. W., Solubility of polystyrene in supercritical fluids. *Macromolecules* **1987,** 20, (10), 2550-7.

9. Toi, K.; Paul, D. R., Effect of polystyrene molecular weight on the carbon dioxide sorption isotherm. *Macromolecules* **1982,** 15, (4), 1104-7.

10. Miura, K.-i.; Otake, K.; Kurosawa, S.; Sako, T.; Sugeta, T.; Nakane, T.; Sato, M.; Tsuji, T.; Hiaki, T.; Hongo, M., Solubility and adsorption of high pressure carbon dioxide to polystyrene. *Fluid Phase Equilibria* **1998,** 144, (1-2), 181-190.

11. Bos, A.; Punt, I. G. M.; Wessling, M.; Strathmann, H., CO2-induced plasticization phenomena in glassy polymers. *Journal Of Membrane Science* **1999,** 155, (1), 67-78.

12. Rothstein, D. P.; Wu, B. G.; Lee, T. V.; Madey, R.; Huang, J. C., Adsorption isotherms and isosteric heats of adsorption for ethane, propane, and n-butane on polystyrene. *Journal of Colloid and Interface Science* **1985,** 106, (2), 399-409.

13. Pradhan, D.; Chen, C.-k.; Radosz, M., Fractionation of Polystyrene with Supercritical Propane and Ethane: Characterization, Semibatch Solubility Experiments, and SAFT Simulations. *Ind. Eng. Chem. Res.* **1994,** 33, 1984-1988.

CHAPTER 8

FUTURE WORK

The work in this thesis demonstrated the feasibility of applying GXLs to patterned dielectric films on silicon wafers and isolated low k dielectric films. In addition, fundamental characteristics of CO_2 such as its quadrupolar nature were investigated but not completely proven. The future work will focus on expanding these two areas, namely applications to IC manufacture and additional fundamental studies. In particular, the specific gas and liquid used in GXLs will be examined.

Although the tetramethylammonium hydroxide (TMAH) bubbled with CO_2 is an effective solution for the removal of photoresist and etch residue, etching of SiO_2 base materials poses a problem. Future IC nodes will require SiO_2 gate oxide layers thinner than 1.2nm where the sensitivity to etching will be important[1]. Other possible solutions such as GXLs with NH_4F may be interesting to explore[2]. Although the fluoride solution will etch as well, the solution can be more dilute which may supply a larger processing window. A patent has been filed for NH_4F applications with supercritical CO_2 and methanol[2]. Other gases can be used in GXLs because they will not react with the NH_4F chemistry. Acidic gases such as CO_2 react with basic TMAH; thus, comparison of gases is difficult if some gases react with the liquid. Therefore, a possible non-reactive solution such as NH_4F in methanol may be useful for comparing certain gases such as C_2H_6 to CO_2.

Gases with higher critical pressures may not be advantageous for supercritical applications because of the higher pressures necessary, but such gases with higher critical pressures will allow increased mass absorption into polymers[3]. Examples of these gases

include NH_3 or SO_2 which have critical pressures of 1639psi and 1140psi. In addition, NH_3 is a polar gas and SO_2 contains a quadrupole like CO_2. QCM experiments with these gases may further support that gases with high critical pressure and either dipolar or quadrupolar nature would be the best gases for GXLs. In addition to the properties of the gas, another important issue will be the interaction of the gas with the liquid solvent which is currently methanol. A gas that is more soluble in the liquid would be advantageous in order to expand the gas more and reduce the liquid solvent usage. NH_3 and SO_2 are both more soluble in methanol compared to CO_2[4-6]. The absorption of water may be a problem for NH_3 and SO_2 but the high pressure applications may render the water sorption minor.

Rather than assuming that the films had swelled based on dissipation data, another method would be to use in situ high pressure ellipsometry in order to determine exact swelling. Other groups have performed such experiments[7, 8] but they did not focus on the interaction of polar groups. A diagram of their setup is shown in Figure 8.1

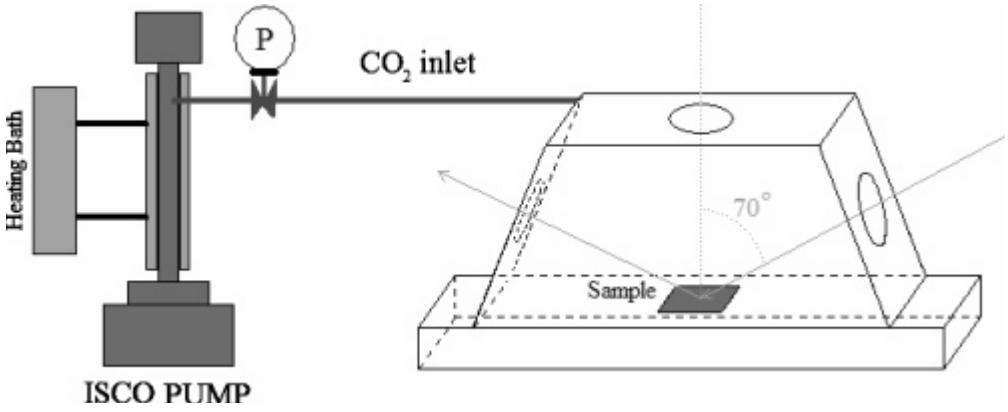

Figure 8.1: Setup for high pressure in situ ellipsometry[7].

The system could be modified to work with GXLs. Although measuring film removal may be difficult due to light scattering if the film is removed non-uniformly, experiments using GXLs with a non reactive liquid and gas would be interesting. The swelling may

differ between high pressure gases and actual GXLs. These experiments would quantitatively show whether or not swelling occurred. Swelling behavior may be different for GXLs compared to SCFs and gases due to the higher inclusion of liquids.

The current method for photoresist and etch residue removal according to this study is film swelling that allows the removal agent to penetrate through the film to etch the underlying SiO_2 for lift-off. However, the swelling may cause problems if the film swells too much. Again, in-situ ellipsometry experiments will help determine how much swelling has occurred. Using the electron beam lithography, small structures could be created and tested to determine whether those structures would be damaged by the increased photoresist swelling. SEM images could be used to assess the results.

Along with photoresist swelling, low k dielectric materials such as methylsilsesquioxane (MSQ) may swell as well. Using neutron reflectivity, toluene has been shown to swell MSQ[9]. Due to the nanoporous nature of MSQ, swelling would probably occur upon exposure to gases and GXLs; however, whether the pores remain dilated after depressurization is unknown. It is important that the film returns to its prior state after processing. QCM and in situ ellipsometry would help determine the mass sorption, swelling, and subsequent desorption.

Previously, 3M had provided HFE (hydrofluoroether) to our group as a liquid solvent to expand in GXLs. Figure 8.2 shows the molecular structure of HFE.

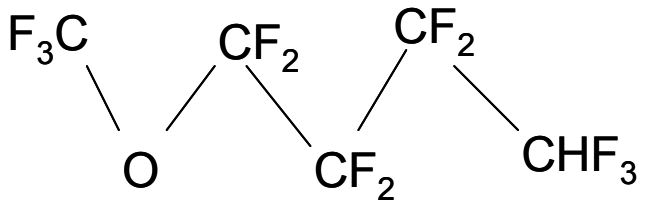

Figure 8.2: Hydrofluoroether, 1,1,1,2,2,3,3,4,4 nonafluoro-4-methoxybutane.

HFE has a surface tension of 14 dyne/cm compared to 72 dynes/cm for water[10]. HFE in combination with HF is able to remove photoresist according to studies performed by Clark at 3M[10]. CO_2 may be more soluble in HFE due to the presence of fluorine, since fluorinated polymers have increased CO_2 solubility compared to their alkyl counterparts[11].

The above future experiments would provide additional directions to the current research by investigating photoresist swelling and if this will damage small feature sizes. The different gases and liquids suggested would provide insight into the formulation of improved GXLs where a more effective GXL would have increased solubility of gases dissolved in the liquid to reduce liquid solvent usage.

References

1. Thompson, S., *IEDM Technical Digest* **2002**, 61.

2. Korzenski, M. B.; Ghenciu, E. G.; Xu, C.; Baum, T. H. Removal of particle contamination on patterned silicon/silicon dioxide using supercritical carbon dioxide/chemical formulations. US Patent Number 6,943,139, 2002.

3. Ismail, A. F.; Lorna, W., Penetrant-induced plasticization phenomenon in glassy polymers for gas separation membrane. *Separation and Purification Technology* **2002,** 27, (3), 173-194.

4. Schaefer, D.; Xia, J.; Vogt, M.; Perez-Salado Kamps, A.; Maurer, G., Experimental Investigation of the Solubility of Ammonia in Methanol. *Journal of Chemical & Engineering Data* **2007,** 52, (5), 1653-1659.

5. Hayduk, W.; Pahlevanzadeh, H., The solubility of sulfur dioxide and hydrogen sulfide in associating solvents. *Canadian Journal of Chemical Engineering* **1987,** 65, (2), 299-307.

6. Young, C. L., Solubility data. Sulfur dioxide-methanol system. *Solubility Data Series* **1983,** 12, (Sulfur Dioxide, Chlorine, Fluorine Chlorine Oxides), 174-80.

7. Carla, V.; Wang, K.; Hussain, Y.; Efimenko, K.; Genzer, J.; Grant, C.; Sarti, G. C.; Carbonell, R. G.; Doghieri, F., Nonequilibrium Model for Sorption and

Swelling of Bulk Glassy Polymer Films with Supercritical Carbon Dioxide. *Macromolecules* **2005,** 38, (24), 10299-10313.

8. Sirard, S. M.; Green, P. F.; Johnston, K. P., Spectroscopic Ellipsometry Investigation of the Swelling of Poly(Dimethylsiloxane) Thin Films with High Pressure Carbon Dioxide. *Journal of Physical Chemistry B* **2001,** 105, (4), 766-772.

9. Kim, H.-C.; Volksen, W.; Miller, R. D.; Huang, E.; Yang, G.; Briber, R. M.; Shin, K.; Satija, S. K., Neutron reflectivity on nanoporous poly(methylsilsesquioxane) thin films. *Chemistry of Materials* **2003,** 15, (3), 609-611.

10. Clark, P. G.; Zazzera, L. A., Use of Segregated Hydrofluoroethers in Semiconductor Wafer Processing. *IEEE/SEMI Advanced Semiconductor Manufacturing Conference* **2006**, 296-300.

11. Aubert, J. H., Solubility of carbon dioxide in polymers by the quartz crystal microbalance technique. *Journal of Supercritical Fluids* **1998,** 11, (3), 163-172.

APPENDIX A

EFFECT OF GXL EXPOSURE ON LOW K DIELECTRIC FILMS

Introduction

In addition to decreasing the gate length between the source and drain regions, transistor speed can be enhanced by the implementation of low k dielectrics. Low k dielectrics serve as insulators between the different metal layers in order to reduce parasitic capacitance between those layers[1]. Current low k materials include Coral™ developed by Novellus and Black Diamond™ developed by Applied Materials both of which are carbon doped silicon dioxide films. An alternative low k material is MSQ (methylsilsesquioxane) which is silicon dioxide with methyl groups attached as shown in Figure 5.2; MSQ is dissolved in a solvent and spin-cast onto a substrate. In the current study, the compatibility of low k films with GXLs (gas expanded liquids) will be investigated.

Although current processes for the incorporation of low k dielectrics include deposition of a silicon nitride layer (or other film) on top of the low k film to chemically and mechanically protect it, this additional film increases the overall dielectric constant of the stack[2]. Therefore, in our study, low k films will be directly exposed to the cleaning chemistries without the protective silicon nitride layer. In a prior paper, GXLs such CO_2 expanded methanol with the cosolvent tetramethyl ammonium bicarbonate (TMAB) were used to remove photoresist and etch residues at 1500psi and 90^{o}C[3]. This solution was exposed to three low k films, Coral™, Black Diamond™, and MSQ investigated at 50^{o}C and 90^{o}C[3]. This solution was comprised of tetramethyl ammonium hydroxide 25wt% in methanol that had been bubbled with CO_2 to form tetramethyl ammonium bicarbonate.

The reacted solution was diluted by four parts of methanol and then pressurized with CO_2. Various measurements such as contact angle, ellipsometry, XPS, and FTIR were used to chemically and physically characterize the films, and dielectric constant measurements were performed before and after GXL exposure to assess electrical property changes. Experiments involving liquid solutions of NH_4HCO_3, NH_4OH, and NaOH in CH_3OH and H_2O were performed in order to gain insight into chemical changes that could result in alteration of the dielectric constant.

Experimental

The experimental configuration and procedure for the GXL experiments can be found in chapters 4 and 5. The low k dielectric films on silicon substrates were obtained from Sematech; unfortunately, specific deposition methods are unknown. Samples were cut into small $1cm^2$ pieces and placed in the GXL chamber for processing with CO_2 expanded tetramethyl ammonium bicarbonate solution at 90^oC and 50^oC at 1500psi. In addition to the GXL treatments, solutions of ammonium bicarbonate, ammonium hydroxide and sodium hydroxide were also investigated. A solution of 0.02 molar ratio solution of ammonium bicarbonate in methanol was further diluted in methanol to obtain a 0.081M solution; this corresponds to the same molar ratio for tetramethylammonium bicarbonate solution in methanol used in prior investigations[3]. To allow direct comparion to these previous studies, the temperature and time used were 50^oC and 45min, respectively[4]. Samples employed were from Novellus (obtained via Sematech), which were the same sample type used in GXL experiments[3]. Finally, an MSQ sample was also tested to investigate whether bicarbonate or hydroxide ions were the cause of an observed decreased contact angle after treatment.

Results and Discussion

The mechanism for photoresist removal according to Myneni involves etching of the silicon dioxide beneath the photoresist by hydroxides that are in equilibrium in the TMAB solution to allow lift off the photoresist layer[5]. Consequently, the low k silicon dioxide based-films will decrease in thickness. TMAH attacks and breaks Si-O bonds[6]. In order to assess this possibility, the films were analyzed using ellipsometry to measure whether the film had been etched significantly. Initial experiments were performed with GXLs at 90°C and 1500psi to emulate the previous GXL photoresist and etch residue studies described in Chapter 4; subsequently, the experiments were repeated at the lower temperature of 50°C.

Experiments at 90°C and 1500psi

All three low k films were exposed to CO_2 expanded TMAB at 90°C and 1500psi.; see Chapter 4 for details of the solution composition. According to Table A.1 the thicknesses of the films do not change significantly after exposure to the GXL.

Table A.1: Film thicknesses before and after GXL exposure.

	Before (nm)	After (nm)	% difference
Coral™	467.7 +/-1.5	467.4 +/- 0.3	-0.07
Black Diamond™	452.3 +/-1.6	448.2 +/-0.1	-0.91
MSQ	392.7 +/-1.8	390.4 +/-0.4	-0.56

In fact, the difference is within the estimated range of error (+/- 2.5). Although ellipsometry indicates that the bulk thickness has not changed, contact angle measurements revealed that the surface chemistry has changed significantly.

Table A.2: Contact angles before and after GXL exposure.

	Before(°)	After(°)	% difference
Coral™	97	56	-42.64
Black Diamond™	88	53	-40.55
MSQ	106	57	-45.76

The films were originally hydrophobic as shown in Table A.2; this property is beneficial because a hydrophilic surface would attract water which, upon absorption increases the k value of the films. After GXL exposure, the contact angle decreased in each case, demonstrating the hydrophilic nature of the film. However, contact angle measurements only tell if the film is less or more hydrophobic; no information on the specific changes can be obtained. Consequently XPS and FTIR were used to measure chemical bonding structure changes on the surface and in the bulk film, respectively.

XPS results are shown in Table A.3, which lists the atomic percentages of C, O, and Si for each sample before and after GXL exposure.

Table A.3: Atomic concentrations in film before and after GXL exposure.

	Coral™		Black Diamond™		MSQ	
	Before(%)	After(%)	Before(%)	After(%)	Before(%)	After(%)
C1s	28.25	35.21	23.04	23.17	19.02	21.03
O1s	46.78	44.07	51.93	52.07	54.78	53.91
Si2p	24.97	20.72	25.03	24.75	26.20	25.06

The values indicated are averages of three points take on each sample. Apparently, the atomic concentrations on the surface of Black Diamond™ and MSQ changed very little, whereas for Coral™, the silicon concentration decreased and the carbon content increased. These results are surprising, since we expect that Black Diamond™ and Coral™ are both carbon-doped plasma-deposited silicon dioxide layers, and thus should be chemically and physically more similar to each other than to MSQ. Nevertheless,

such results may be due to the different conditions (and perhaps methods) of deposition or processing conditions which are unfortunately unknown.

In addition, XPS curve fitting was performed in order to investigate bonding changes that may be reflected in the shifting of the binding energies. Three points were taken on each sample and during curve fitting one to two curves were fitted to the peaks in order to reduce the chi squared value where a smaller chi value indicates a better fit. The curves were fitted to two peaks. The primary peak corresponds to C-C which is located at 248.8eV whereas the smaller secondary peak which if apparent is Si-C which is located at 283.4eV. The peaks were shifted from the raw data so that the primary C-C peak was aligned to the theoretical binding energy of 284.8 eV. These results are shown in Tables A.4 and A.5.

Table A.4: Before GXL exposure

	peak 1	peak 2	chi squared
Coral 1	284.8		3.779
Coral 2	284.8		3.123
Coral 3	284.8	282.73	2.136
BD 1	284.8	282.75	1.375
BD 2	284.8	282.86	1.731
BD 3	284.8	283.20	3.931
MSQ 1	284.8	283.09	1.275
MSQ 2	284.8	283.94	2.697
MSQ 3	284.8	283.18	1.706

Table A.5: After GXL exposure

	peak 1	peak 2	chi squared
Coral 1	284.80	287.67	1.468
Coral 2	284.80		1.862
Coral 3	284.80	286.54	3.083
BD 1	284.80	285.55	2.480
BD 2	284.80	282.46	1.666
BD 3	284.80		2.625
MSQ 1	284.80		1.733
MSQ 2	284.80		1.951
MSQ 3	284.80		3.107

No clear generalization can be made for Coral™ and Black Diamond ™ but for MSQ the unexposed samples have two peaks for carbon (i.e., Si-C and C-C as described below) whereas the exposed samples have only one peak. The before and after XPS carbon spectra are shown in Figure A.1 and A.2, respectively.

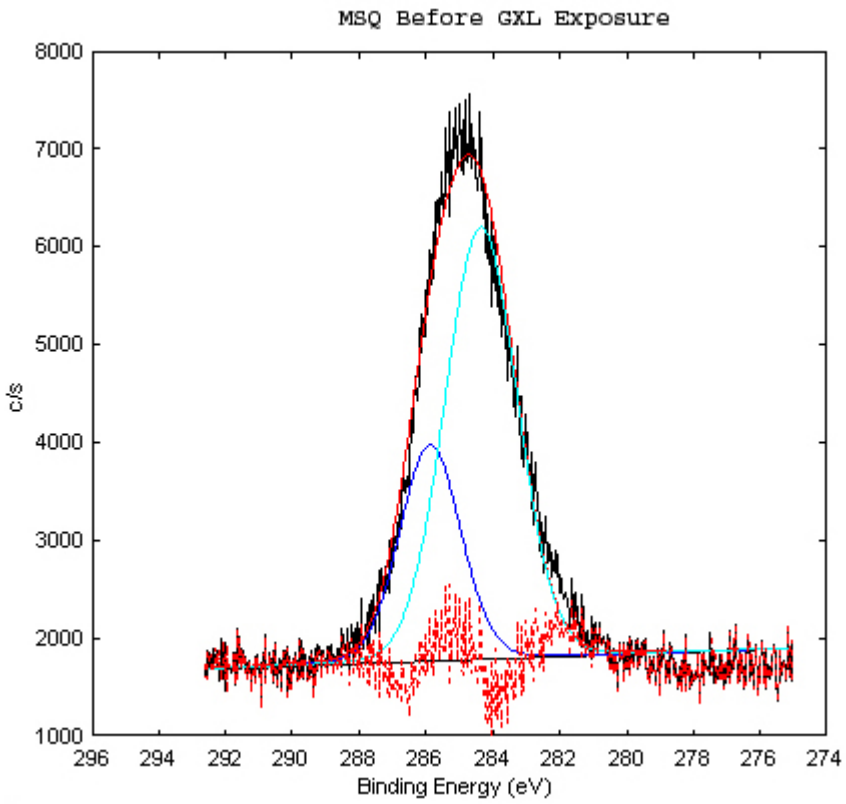

Figure A.1: XPS spectra of carbon in MSQ before GXL exposure.

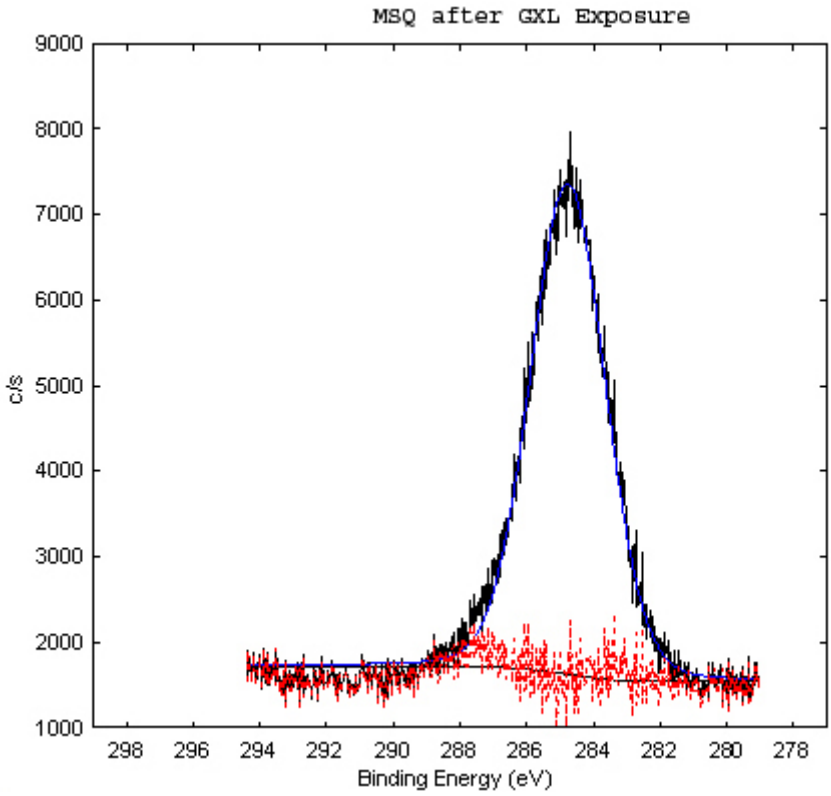

Figure A.2: XPS spectra of carbon in MSQ after GXL exposure.

The unexposed MSQ sample has two carbon peaks whereas the exposed sample has only one carbon peak. These peaks correspond to Si-C and C-C which are located at 284.8 eV and 283.4 eV. The Si-C peak is due to the MSQ and the C-C is due to adventitious carbon from the atmosphere[7]. The exposed MSQ only has the C-C peak from adventitious carbon because the hydroxide ions may have cleaved the Si-C bond[8].

Curve fitting was performed for silicon as well in the case of Coral™. The silicon curve fittings for Black Diamond™ and MSQ were inconsistent but both had little change in silicon concentration after the GXL exposure. Curve fittings were inconsistent because for some peaks only one Gaussian curve was fitted whereas for other peaks two Gaussian curves were fitted. The inconsistencies lie in the number of curves fitted to the peaks for the before and after GXL exposures. In the case of MSQ,clearly the before GXL exposure peak had two curve fits and after GXL exposure peak had only one curve fit. Figure A.3 and A.4 show the silicon curve fittings before and after GXL exposures, respectively.

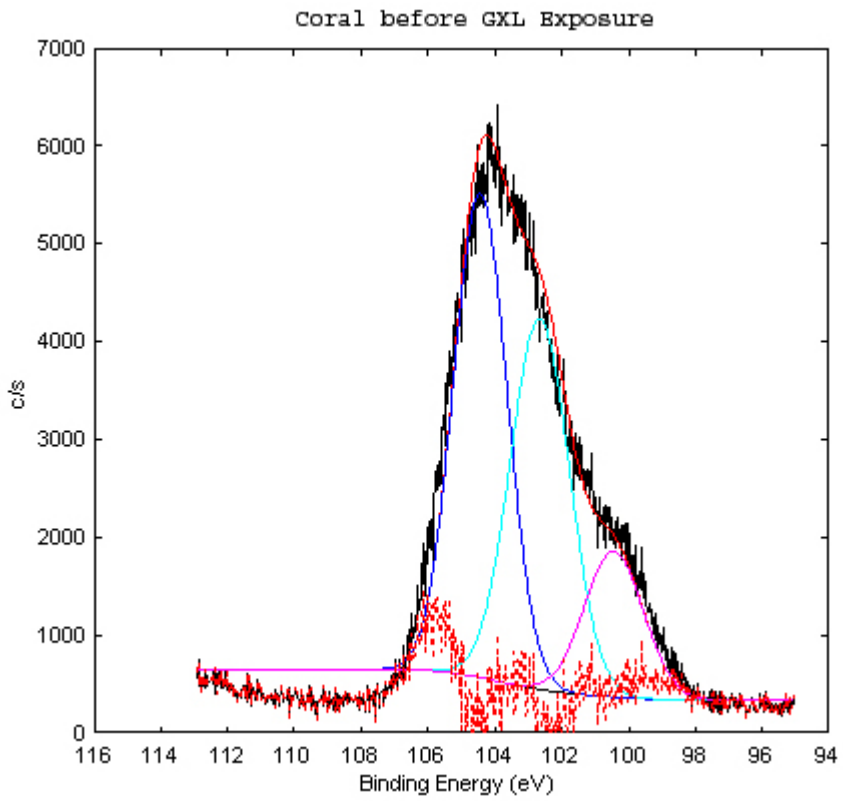

Figure A.3: XPS spectra of silicon in Coral before GXL Exposure

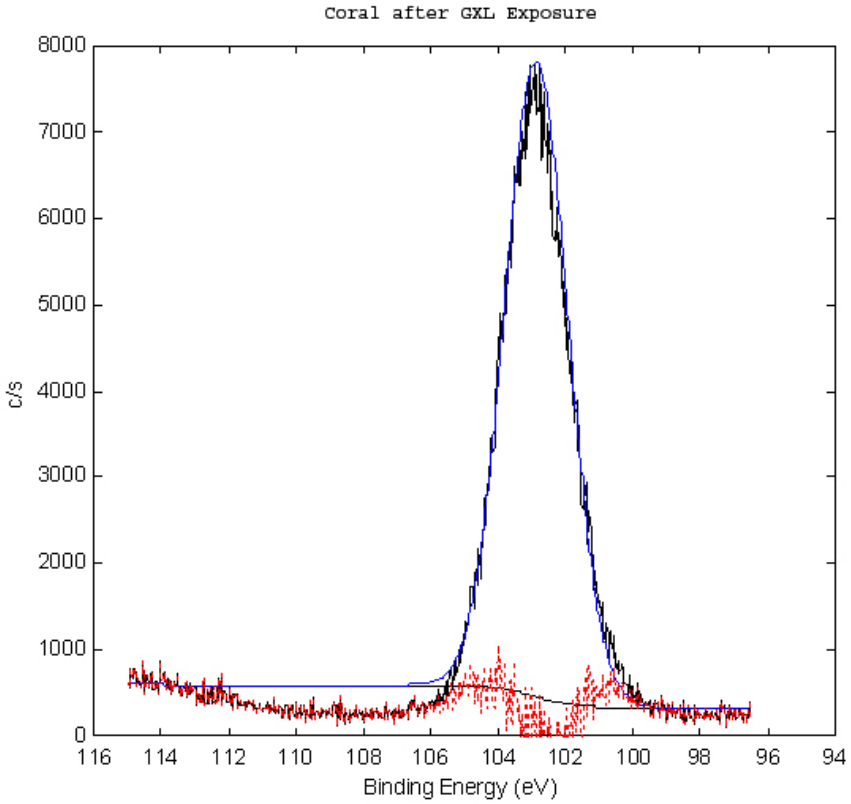

Figure A.4: XPS spectra of silicon in Coral after GXL exposure.

The Si peak before GXL exposure indicates three types of bonding Si-C (100.4eV), Si-O (103eV), and Si-O_2 (104.1eV) whereas the spectrum after exposure shows only Si-O bonding. This seems reasonable because after GXL exposure the contact angle decreased indicating a hydrophilic surface, likely caused by Si-OH on the surface rather than Si-C.

Gold electrodes were deposited on the low k films and aluminum was deposited on the silicon wafer backside. From the accumulation capacitance of the C-V plots, dielectric constant values were calculated for Coral™ and MSQ to be 20.2 and 25.3. Since the accumulation regime for Black Diamond™ was not stable, accurate dielectric constant values could not be obtained. Because Black Diamond™ and Coral™ represent specific trade names for carbon-doped SiO_2, they have similar structures and contact angle values although the proprietary deposition processes are probably somewhat different. Nevertheless, we expect that the dielectric values should be similar. Before exposure, the dielectric constant values for Coral™, Black Diamond™, and MSQ were 2.72, 2.86, and 2.7 respectively. These results indicate that exposure to the GXL TMAB solution is not compatible with this cleaning approach due to the increased dielectric constant. However, as described below, other experiments were run at lower temperatures such as 50^{o}C with more promising results.

Experiments at 50^{o}C

The exposures to GXLs were repeated albeit at the lower temperature of 50^{o}C. In addition, FTIR was implemented to assess bonding strurctures. Contact angle measurements were performed on the samples to the 50^{o}C GXL. Unlike the samples exposed at 90^{o}C, the contact angles were much higher but not as high as the unexposed

samples as shown in Table A.6. In addition, the wafers were softbaked at 120°C for 5min to ensure that all the cleaning solution had been removed.

Table A.6: Contact angles before and after GXL exposure.

	before	after	% difference
Coral	98	77	-21.90
BD	91	61	-33.08
MSQ	108	83	-23.15

CV measurements were taken again in order to determine the dielectric constant, but the results were inconclusive because the accumulation capacitance was not stable. However, based on the higher contact angles, it is assumed that the dielectric constants are lower than those samples exposed at 90°C because the higher contact angles result from higher concentrations of Si-OH on the surface and possibly throughout the bulk film. The OH^- containing solution should diffuse readily into the bulk film at higher temperatures and will therefore cause the generation of a more hydrophilic surface containing Si-OH bonds.

Instead of XPS, FTIR measurements were performed to investigate chemical structure. As discussed in the earlier Experiments at 90°C section, XPS measurements were inconsistent and hence were not performed. Some data indicated multiple curve fittings while others did not. The FTIR measurements supported the expectation from contact angle studies that the $-CH_3$ peak at 2977cm^{-1} and Si-O-Si peak at 1062cm^{-1} peaks were unchanged after GXL exposure at 50°C and 1500psi as indicated in Fig A.5[9].

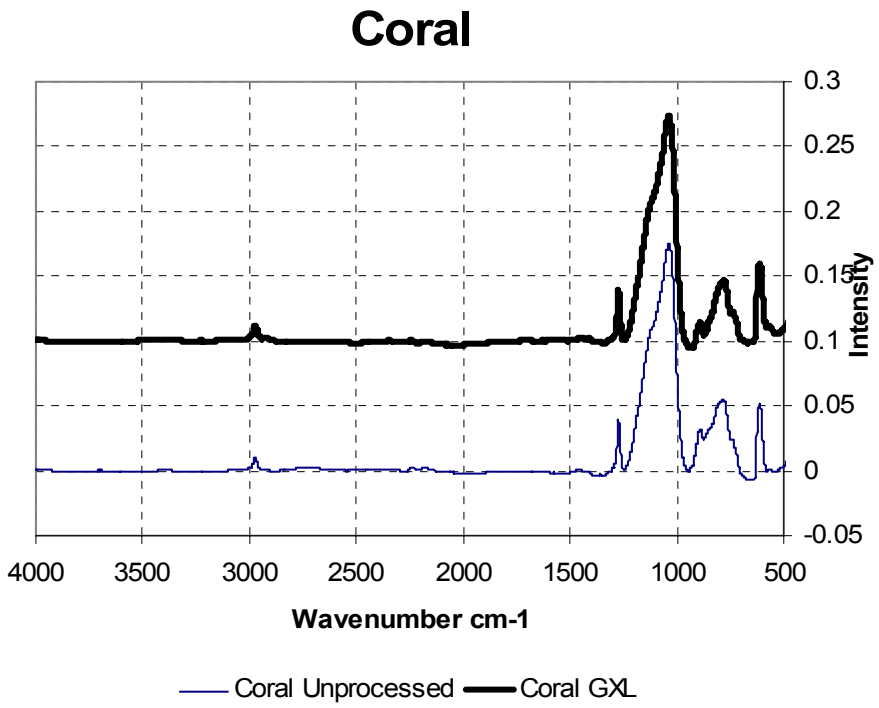

Figure A.5: FTIR spectra of Coral.

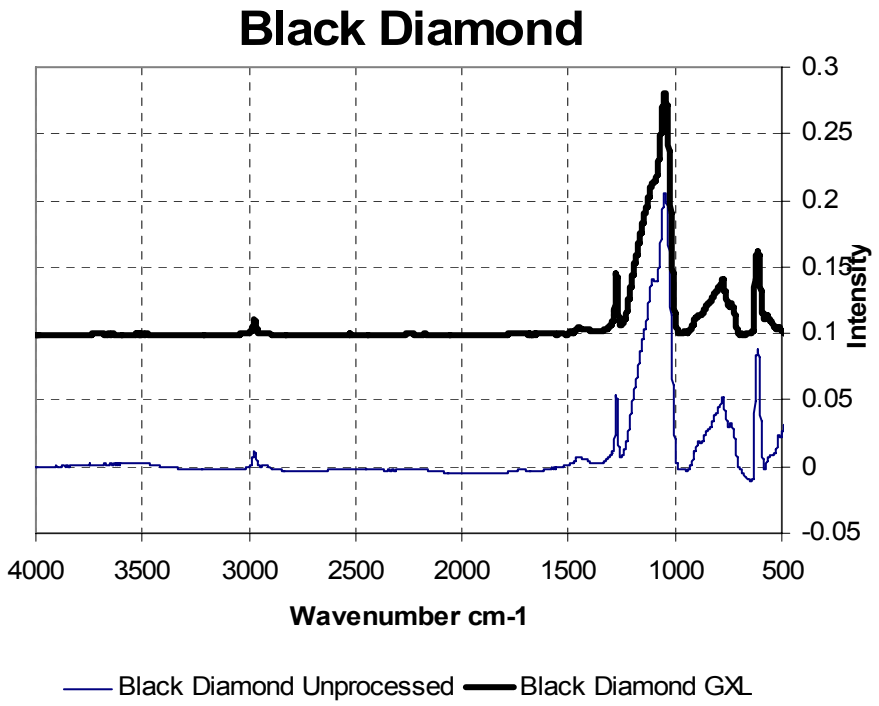

Figure A.6: FTIR spectra of Black Diamond.

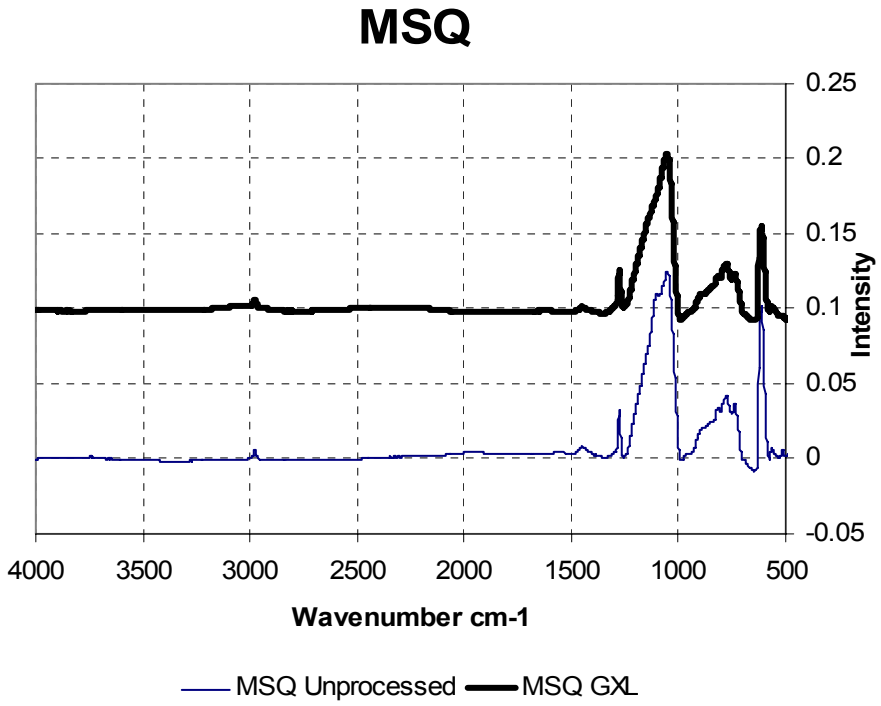

Figure A.7: FTIR spectra of MSQ.

A Si-OH peak at 3740cm^{-1} or 942cm^{-1} was expected for the GXL exposed samples because Si-OH bonds are the likely cause of the increased hydrophilicity but this peak did not appear in the GXL-exposed samples. Interestingly, for Black Diamond™ and MSQ, the peak at 611cm^{-1} decreased significantly after the GXL exposure. The 611cm^{-1} peak is associated with Si-Si[10]. According to the FTIR spectra, fewer Si-Si and Si-O-Si bonds exist, indicating that the film may have become less structured because local bonding structures have been altered.

The lower temperature used allows more CO_2 to be dissolved in the liquid, thereby generating a more dilute solution. At 90^{o}C, ~22mL of liquid was collected; however, at 50^{o}C, ~11mL of liquid was collected from the reactor. The mole fraction of CO_2 that dissolves in methanol at 90^{o}C and 1500psi is 0.3[3] while for CO_2 at 50^{o}C and 1500psi the mole fraction is 0.55[5]. Because the GXL is more dilute due to the higher

fraction of CO_2, a lower concentration of reactive chemical moieties are present and the contact angle remains moderately high. In Myneni's studies, which were performed at 3000psi and 70^{o}C, a considerably higher concentration of CO_2 exists; thus, the low k dielectric may not be affected, although electrical measurements were not performed in this study[11]. In the current GXL experiments, the bicarbonate solution through OH^- ions appears to attack the low k film and render it hydrophilic, thereby increasing the dielectric constant. In comparison, a more dilute (in reactive chemical) solution will display lower reactivity.

Experiments with Bicarbonates and Hydroxide Solutions

The liquid cleaning studies using ammonium bicarbonate, ammonium hydroxide, and sodium hydroxide were carried out in order to investigate the cleaning capabilities of bicarbonate and hydroxide ions. Previous studies used a tetramethylammonium bicarbonate solution where it was postulated that OH^- ions from the tetramethylammonium hydroxide was responsible for the cleaning observed as a result of etching of the underlying silicon oxide layer, thereby promoting a lift off mechanism[5]. The GXL used in the current study contains both bicarbonate and hydroxide ions. Distinct bicarbonate or hydroxide solutions were examined to determine which of the two ions were involved in the cleaning. In addition two different solvents water and methanol were studied because water is a source of hydroxide ions whereas methanol does not dissociate to give hydroxide ions.

After processing the patterned and MSQ film samples in methanol or water with different bicarbonate or hydroxide solutions, the MSQ appears the same visually, but the commercially patterned sample showed either incomplete or complete removal of the

photoresist depending upon the specific cleaning solution. Incomplete removal may be due to low concentrations of OH^- in equilibrium with bicarbonate due to the presence of water or may be due to the bicarbonate itself. The complete removal was most likely due to the presence of OH^-. From the equilibrium shown below and a bicarbonate pKa of 10.3 the OH^- concentration in water was $7.1x10^{-7}M$[12].

$$HCO_3^- + H_2O \Leftrightarrow H_2CO_3 + OH^- \qquad (A.1)$$

Because water can provide an OH^- source, the hydroxide and bicarbonate solutions were dissolved in methanol as well. These experiments permit an investigation of the effects of ammonium bicarbonate on cleaning. Table A.7 summarize the results. The fluid used for contact angle measurements was water but the solvent in which NH_4HCO_3, NH_4OH, and NaOH were dissolved in was either water or methanol.

Table A.7: Summary of contact angle results for MSQ and removal evaluation for commercial samples.

	Molarity (M)		Contact Angle (°) MSQ		PR Removal Patterned Sample	
	CH_3OH solvent	H_2O solvent	CH_3OH solvent	H_2O solvent	CH_3OH solvent	H_2O solvent
NH_4HCO_3	0.081	0.01	105.6	70	not clean	not clean
NH_4OH	n/a	7.7	n/a	39.4	n/a	clean
NaOH	0.01	0.01	98.3	32.1	not clean	clean

Only the solutions containing OH^- ions that could dissociate in water were able to fully remove the photoresist films but at the expense of decreasing the MSQ contact angle and hence increasing the dielectric constant. Moreoever, the hydroxide solutions or strong bases were unable to remove the photoresist films if they were dissolved in methanol because in methanol the salts cannot fully dissociate. The NH_4HCO_3 salt in water was not able to completely remove the photoresist film but was somewhat successful. This

result is plausible because the equilibria suggest that HCO_3^- can interact with water to create OH^- that etched the underlying silicon dioxide film and also caused a lowering of the contact angle for the MSQ sample.

A molarity of 0.01M corresponds to a pH of 12 for complete dissociation of the strong base NaOH in water whereas a molarity of 7.7M for NH_4OH also corresponds to a pH of 12. A pH of 12 was chosen because the $TMAHCO_3$ solution has a pH of ~12 in water where the 5% water in the $TMAHCO_3$ solution is sufficient to generate the OH^- concentration needed for the observed pH[13].

Comparing the results of the GXL experiments at 50°C and NH_4HCO_3 in water at 50°C, the contact angles for MSQ are 83° and 70°, respectively. The GXL experiments may have given higher contact angle because the solution in contact is more diluted due to the inclusion of CO_2, leading to a lower concentration of hydroxide ions for surface etching

Conclusions

Coral™, Black Diamond™, and MSQ low k dielectric films were exposed to CO_2 expanded TMAB in methanol GXLs. Although the resulting film thicknesses were unchanged, the contact angles demonstrated significant hydrophilicity after GXL processing. XPS and FTIR demonstrated bond changes from Si-C to Si-O that supports the transition to hydrophilicity. GXLs may be compatible with low k dielectric materials if other cosolvents besides those that use hydroxide ions are used. The fully dissociated hydroxide ions are able to remove the photoresist films but at the expense of increasing the dielectric constant of the low k material by increasing the hydrophilicity of the film. The strong bases NaOH and NH_4OH in methanol that are apparently not fully dissociated

were unable to remove the photoresist film but did not affect the hydrophobic nature of the MSQ film. GXLs that are more diluted with CO_2 or that possess no hydroxide ions may be necessary to allow GXLs to be fully compatible with low k materials. Similar studies to those described in this appendix on spin cast MSQ films provided by Sematech have been described in Chapter 5. However, due to different processing conditions for the MSQ films, the results were significantly different. It is likely that the low k dielectric films from Sematech had not been completely post baked or were prepared under processing conditions that resulted in enhanced susceptibility to reaction with hydroxide ions.

References

1. Association, S. I., International Technology Roadmap for Semiconductors 2006 update. **2006**.

2. Hu, C. K.; Gignac, L.; Rosenberg, R., Electromigration of Cu/low dielectric constant interconnects. *Microelectronics Reliability* **2005,** 46, (2-4), 213-231.

3. Song, I.; Spuller, M.; Levitin, G.; Hess, D. W., Photoresist and Etch Residue Removal using Gas-Expanded Liquids. *Journal of The Electrochemical Society* **2006,** 153, (4), G314-G318.

4. Levitin, G.; Myneni, S.; Hess, D., Post Plasma Etch Residue Removal Using CO2-TMAHCO3 Mixtures: Comparison of Single-Phase and Two-Phase Mixtures. *Journal of the Electrochemical Society* **2004,** 151, (6), G380-G386.

5. Myneni, S.; Hess, D. W., Post Plasma Etch Residue Removal Using CO_2-Based Mixtures: Mechanistic Considerations. *Journal of The Electrochemical Society* **2005,** 152, (10), G757-G765.

6. Liu, P.-T.; Chang, T.-C.; Huang, M.-C.; Tsai, M. S.; Sze, S. M., Highly reliable chemical–mechanical polishing process for organic low-k methylsilsesquioxane. *J. Vac. Sci. Technol. B* **2001,** 19, (4), 1212-1218.

7. Barr, T. L.; Seal, S., Nature of the use of adventitious carbon as a binding energy standard. *Journal of Vacuum Science & Technology, A: Vacuum, Surfaces, and Films* **1995,** 13, (3, Pt. 2), 1239-1246.

8. Yoshida, J.; Itami, K.; Kajimoto, O. Silicon-carbon bond cleavage using supercritical water. Patent Number 2003-121750, 2004323436, 20030425, 2004.

9. Alayo, M.; Pereyra, I., On the nitrogen and oxygen incorporation in plasma-enhanced chemical vapor deposition (PECVD) SiOxNy films. *Thin Solid Films* **2002,** 402, 154-161.

10. Morioka, T.; Kimura, S.; Tsuda, N.; Taito, C.; Saito, Y.; Koike, C., Study of the structure of silica film by infrared spectroscopy and electron diffraction analyses. *Mon. Not. R. Astron. Soc.* **1998,** 299, 78-82.

11. Myneni, S.; Peng, H.-G.; Gidley, D. W.; Hess, D., Compatibility of high pressure cleaning mixtures with a porous low dielectric constant film: A positronium annihilation lifetime spectroscopic study. *J. Vac. Sci. Technol. B* **2005,** 23, (4), 1463-1469.

12. Serjeant, E. P.; Dempsey, B., *Ionization Constants of Organic Acids in Solution*. Pergamon Press: Oxford, UK, 1979.

13. Myneni, S.; Hess, D. W., Post-Plasma-Etch-Residue Removal Using CO_2-Based Fluids. *Journal of The Electrochemical Society* **2003,** 150, (12), G744-G750.

APPENDIX B

COMPATIBILITY OF CO_2 WITH COMMERCIAL SOLVENTS FROM EKC TECHNOLOGY

Introduction

Dupont-EKC Technology partnered with Georgia Tech in order to investigate the compatibility of CO_2 with EKC Technology's solvent solutions for photoresist and etch residue removal. In addition, possible new chemistries were explored. EKC Technology is an industry leader in photoresist and etch residue removal products. Their portfolio of removal solutions includes products that are compatible with Al, Cu, and various low k materials. Their most successful products rely on amine basic chemistry to remove photoresist and etch residue. All of their current solutions are liquid based and through the partnership with Georgia Tech possible gas-expanded liquids were explored using EKC Technology solvents expanded with CO_2. Key relationships, interactions and modifications that were examined included pressure, precipitation, and dilution. The molecular structure of the chemical components in various EKC solvents based on hydroxylamine and diglycolamine chemistries were correlated with photoresist removal efficiency and solution behavior. In addition, the solvents monoethanolamine, choline hydroxide, and propylene glycol were proposed as possible alternatives or additions to the current EKC products. In order to examine branching effects, diethanolamine and triethanolamine which have more branching compared to monoethanolamine were tested. Based on the experimental results, 2-methoxyethylamine and 2-(2-aminoethylamino) ethanol were investigated as possible CO_2 compatible amines. The following sections describe the studies performed with a number of different bases and solvents to evaluate

the feasibility of using CO_2 gas expansion to promote photoresist removal using commercial solvents from EKC.

The primary mechanisms for removal of photoresist are oxidation, dissolution, and reduction[1]. Specifically, dissolution studies are the most interesting because they relate to current EKC products. The solvent/amine stripper penetrates the photoresist, swells the film, and then dissolves it. The base reacts with acidic photoresist. Specifically, the amine group in hydroxylamine attacks the carbonyl in the photoresist Studies at Georgia Tech have noted similar results but the photoresist film swells due to the addition of high pressure CO_2 (>1000PSI) and the film does not dissolve but rather lifts off due to the etching of underlying silicon oxide by hydroxide ions[2]. The most commonly incorporated compound type in the EKC removal agents is an amine. EKC265 which uses hydroxylamine, removes the photoresist even in post metal processes by a combination of reduction, chelation, and nucleophilic attack on the carbonyl group in the photoresist[1]. In contrast, the chemistry used at Georgia Tech for photoresist film removal is not amine based but rather hydroxide based. The two chemical structures are shown in Figure B.1.

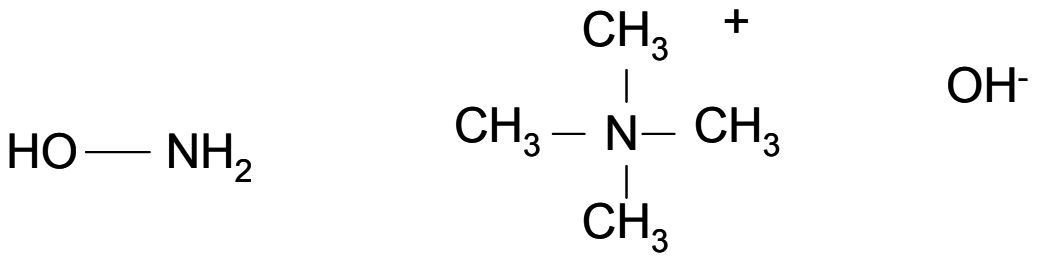

Figure B.1: A) hydroxylamine and B) tetramethyl ammonium hydroxide.

The base tetramethyl ammonium hydroxide (TMAH) is used in the IC industry to develop positive photoresist[3]. However, at Georgia Tech, CO_2 has been added to this base to create tetramethyl ammonium bicarbonate in equilibrium with hydroxide ions, which is effective in removing photoresist and post plasma etch residue that exists on a Coral® low-k dielectric sample[2, 4-6].

Experimental Method

Positive photoresist (Shipley SPR3012) coated silicon wafers were used as test wafers. The film thickness was 1.8μm according to factory specifications. The wafer was baked for 15min at 180°C to toughen the film and ensure removal of all casting solvent. A solution of potassium hydroxide 1M was used to remove the film in order to create a removal standard. Film removal was confirmed via visual observation of the silicon surface.

The wafer was cut into small $1cm^2$ pieces and then immersed in the solutions. The photoresist samples were exposed to monoethanolamine (MEA), propylene glycol (PPG), choline hydroxide (COH) (see Figure B3 for chemical structures), and combinations of these chemicals at 65°C for 30 minutes each in beaker studies. MEA was semiconductor grade, PPG was semiconductor grade, and COH was semiconductor grade with 55% water from Sigma Aldrich. Samples were subsequently rinsed with isopropyl alcohol using a squirt bottle. For the combination studies, the solutions were mixed in equal volume amounts. In a dilution study, MEA was diluted with nine parts of ethanol, methanol, or choline hydroxide. After the liquid studies, CO_2 was added to the various solutions to determine their interactions with CO_2. The CO_2 was SFC grade from Air Liquide. For the experiments using CO_2 and MEA, CO_2 was added

continuously for 15 minutes until the temperature of the MEA solution began to decrease indicating completion of the reaction between the acidic gas CO_2 and the basic MEA. The CO_2 added MEA was heated to 65^oC and the Shipley hard baked sample was placed into the solution. After 30 minutes, the Shipley sample was removed and rinsed with isopropyl alcohol.

In addition to MEA, other amines such as diethanolamine and triethanolamine were tested in order to examine the branching effects on photoresist removal and interaction with CO_2. The photoresist film was exposed to these fluids at 65^oC for 30min and rinsed with isopropyl alcohol.

EKC solvents are based on amine chemistries such as hydroxylamine and diglycolamine. EKC265 which contains hydroxylamine and EKC830 which contains diglycolamine were heated to 65^oC and the samples were submerged in the solution for 30min. CO_2 was added to EKC265 and EKC830 in order to assess the effects of CO_2 on these solvents. High pressure studies at 1000psi for 30min were performed for EKC830.

Similar chemicals to diglycolamine such as 2-(2-aminoethylamino) ethanol and 2-methoxyethylamine (Figure B.7) that result in photoresist removal despite the addition of CO_2 were also tested. Although the MSDS specifically stated that CO_2 was not to be added to 2-methoxyethylamine, this warning was not heeded; the warning was given because in all cases, adding CO_2 to amines will cause a highly exothermic reaction that can release NO_x fumes. These fumes are hazardous, but all experiments were performed in a fume hood. 2-methoxyethylamine was pressurized with CO_2 at pressures of 500psi, 775psi, 1000psi, and 1800psi at 65^oC for 30min for all studies. Figure B.2 shows a schematic diagram of the high pressure reactor configuration.

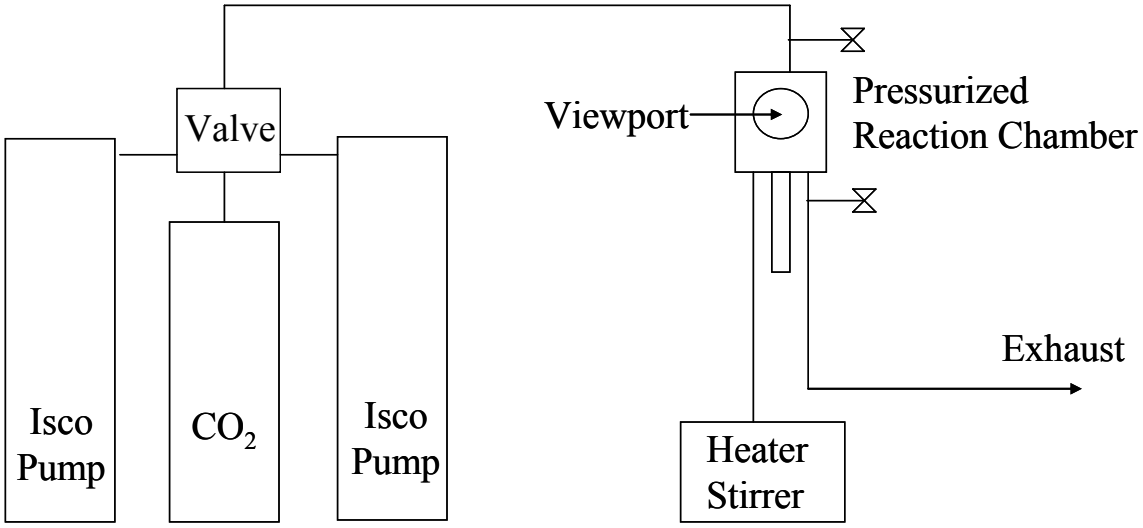

Figure B.2: Diagram of high pressure GXL system.

Two 1000D Isco pumps were used to maintain the desired pressure. A Parr reactor 4566 with a magnetic stir system and heating jacket was used as the reaction chamber. The waste was exhausted into a high pressure compatible container.

Results and Discussion

Monoethanolamine, Choline Hydroxide, and Propylene Glycol

MEA is a primary amine and base that can function as the removal agent for a photoresist film. COH is possibly the OH^- source that may aid in removal because of its ability to etch silicon dioxide[7]. PPG is used as the solvent, although a smaller molecule such as methanol may also serve as the solvent. Figure B.3 displays the chemical structures of these reactants.

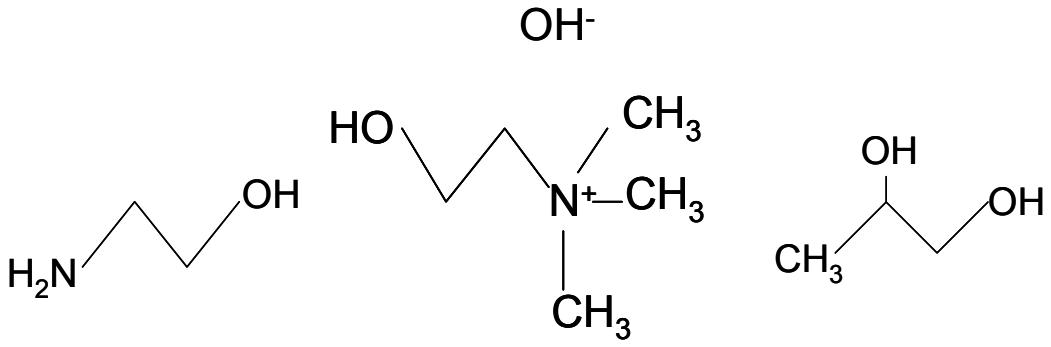

Figure B.3: A) monoethanolamine, B) choline hydroxide, and C) propylene glycol

MEA appears to be the key agent in removal of photoresist. MEA, MEA plus COH, and MEA plus COH plus PPG were all able to remove the film at 65^{o}C within 30 minutes, when the solutions were prepared in equal volume ratios. The photoresist film was removed in one piece or in fragments rather than dissolved into the solution as was the case for removal using the strong base KOH. MEA was further investigated at room temperature and with other diluents such as ethanol and methanol. No removal occurred at room temperature for 30 min using MEA. MEA is fairly viscous; therefore, diluting this material would reduce the viscosity. MEA was diluted with ethanol, methanol, or COH with a 1:9 ratio each. However, none of the three diluted mixtures MEA+ethanol, MEA+methanol, or MEA+ COH were able to remove the film at 65^{o}C and 30 minutes.

Carbon dioxide was bubbled into the solutions to investigate possible reactions. Visually, COH and PPG seemed unreactive to carbon dioxide whereas MEA reacted strongly with the CO_2 in a highly exothermic reaction where the temperature increased to ~ 80^{o}C. In contrast, tetramethylammonium hydroxide (TMAH) which has been investigated previously at Georgia Tech increased to 50^{o}C with the addition of CO_2.

CO_2 reacts more rapidly with MEA than with TMAH, possibly due to the fact that the MEA is more concentrated whereas the TMAH solution was diluted in methanol (3 parts methanol to 1 part TMAH). In addition, MEA is a primary amine whereas TMAH is a quaternary amine. CO_2 probably attacks MEA to form a carbamate whereas CO_2 attack on TMAH forms a bicarbonate[8, 9]. The carbamate formation is a two step process as shown below in Figure B.4.

Zwitterion Formation

$$R_1R_2NH + CO_2 \xleftrightarrow{k_1,k_2} R_1R_2NH^+COO^-$$

Carbamate Formation

$$R_1R_2NH^+COO^- + B \xrightarrow{k_B} BH^+ + R_1R_2NCOO^-$$

B = any base

Figure B.4: Formation of a carbamate from an amine and CO_2[10].

After CO_2 reaction with MEA, the solution was unable to remove the photoresist film indicating that the CO_2 chemically modified the MEA to render it less potent. In addition, the viscosity significantly increased.

MEA has been used in to absorb CO_2 from flue streams; after subsequent heating, the absorbed CO_2 is released[11, 12]. However, even after the MEA was heated to 100^oC, the viscosity remained the same, which suggests that the CO_2 had in fact not been desorbed. Interestingly, CO_2 added to MEA and 5% DI water at 65^oC and 30 minutes partially removed the film indicating that the CO_2 preferentially reacted with the water instead of the amine, forming carbonic acid.

Diethanol Amine and Triethanol Amine

In addition to the primary amine MEA, secondary and tertiary amines diethanol amine (DEA) and triethanol amine (TEA), respectively, were evaluated. Due to the

increased branching structure compared to MEA (Figure B.5), the larger ethanol amines are inherently more viscous even before CO_2 addition.

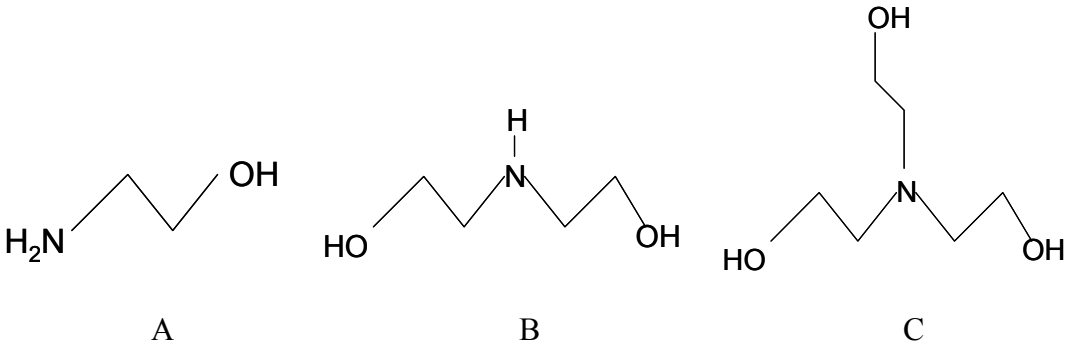

Figure B.5: A) monoethanolamine, B) diethanolamine and C) triethanolamine.

The increased branching may limit the ability of CO_2 molecules to react with DEA and TEA and thus inhibit the creation of carbamate. The carbamate formed may be the reason for the increased viscosity after CO_2 addition and this could account for incomplete removal of the photoresist film. Pure (liquid) DEA and TEA were expected to remove the photoresist films because of the fundamentally similar chemical structure to that of MEA. However, even pure liquid DEA and TEA were ineffective in removing photoresist films at 65^{o}C for 30 minutes. When CO_2 was added to DEA, the temperature rose slightly (on the order of 1-2^{o}C) whereas the TEA solution decreased in temperature by 1-2^{o}C possibly due to the cooling of CO_2 gas from the Joule-Thomson effect[13]. Due to the increased branching, the CO_2 was not absorbed readily by the fluids and was not effective in promoting removal of the photoresist film.

Hydroxylamine and Diglycolamine

The two industrial solvents of interest based on preliminary results at Georgia Tech were EKC265 which contains hydroxylamine (HDA) and EKC830 which contains diglycolamine (DGA). The chemical structures are show in Figure B.6.

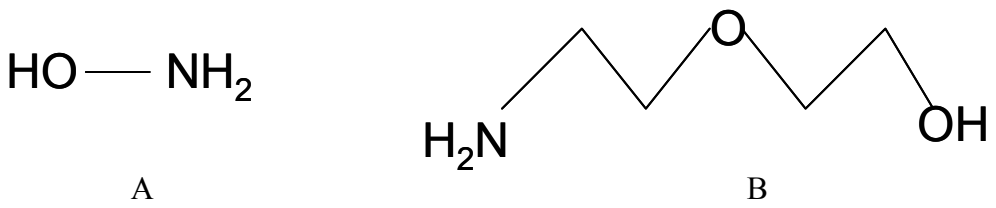

Figure B.6: A) hydroxylamine and B) diglycolamine.

Both were effective in removing photoresist at 65°C for 30min. HDA like MEA is an amine and has a hydroxide group. HDA is explosive and hence is diluted by water to 50% by volume.

The addition of CO_2 caused an exothermic reaction thereby increasing the solution temperature of HDA to 37°C. HDA removed the photoresist film and with CO_2 addition, HDA was partially effective; half the resist remained after treatment. Although HDA is somewhat effective even with addition of CO_2, the HDA solution must contain water for safety reasons. For GXLs the inclusion of water causes problems due to the phase separation between water and CO_2 because CO_2 has very limited solubility in water. As a comparison at 40°C and 735psi the mole fraction of CO_2 in methanol is 0.310 whereas it is 0.015 for water[14, 15].

For the high pressure CO_2 studies, HDA was not pressurized with CO_2 because in CO_2 the water and HDA may phase separate causing an explosion hazard. EKC830 was used at 65°C for 30min at 1000psi but the film was not removed. When the temperature was increased to 85°C, photoresist removal was achieved. EKC830 contains diglycolamine (DGA) which apparently becomes chemically active at 85°C according to

the process conditions on the EKC website. In addition, the higher temperature means that the GXL contains less CO_2 and hence consists of more concentrated DGA which promotes film removal.

2-(2-Aminoethylamino) Ethanol and 2-Methoxyethylamine

Based on the chemistry of 2-2 aminoethoxy ethanol (diglycol amine or DGA) used in EKC830, other amines that are chemically and structurally similar such as 2-(2-aminoethylamino) ethanol (AEAE) and 2-methoxyethylamine (MXEA) were tested. Figure B.7 shows the molecule structures.

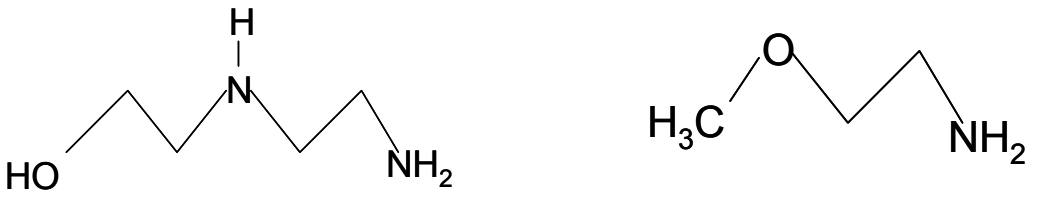

A B

Figure B.7: Molecular structure of A) 2-(2-aminoethylamino) ethanol and B) 2-methoxyethylamine

MXEA has similar properties (e.g., boiling points and flash points) to ethanol and methanol whereas AEAE is similar to DGA. Table B.1 compares these properties.

Table B.1: Boiling points and flash points of some of the amines and alcohols investigated.

Chemical	Boiling Point (^oC)	Flash Point (^oC)
2-methoxyethylamine (MXEA)	95	12
Methanol	65	12
Ethanol	78	12
2-2 aminoethoxy ethanol (DGA)	220	127
2-(2-aminoethylamino) ethanol (AEAE)	238	129

DGA and AEAE both removed the photoresist film at 65^{o}C and 30 minutes. MXEA was not as effective but appeared to dissolve the film as indicated by the color change of the fluid from clear to orange which reflected the color of the dissolved photoresist. After CO_2 addition, DGA, AEAE, and MXEA had exothermic reactions with peak

temperatures of 87°C, 100°C, and 80°C respectively. As expected, CO_2 additions significantly increased the viscosity of DGA and AEAE; however, the viscosity increased moderately for MXEA. Although DGA and AEAE were unable to remove the photoresist film after CO_2 exposure, MXEA was better able to remove the film. In addition, unlike in its pure form where the film seemed to dissolve, the film was removed in chunks with CO_2 added MXEA. Although MXEA is flammable and corrosive, these qualities are comparable to TMAH and other removal solution chemistries. Interestingly, according to the HMIS (Hazardous Materials Identification System) and NFPS (National Federation for Personal Safety) rating in the MSDS for MXEA, the reactivity number was listed as zero.

Ethanol was added to MXEA to dilute the solution and also to reduce the viscosity as was carried out previously with MEA. The mixture was 1:1 by volume, but the diluted solution was unable to remove the film at 65°C for 30min. Although MXEA cannot be diluted, it is the only solution besides HDA that can remove the photoresist film even after CO_2 addition at 65°C. HDA cannot be pressurized with CO_2 due to phase separation but MXEA may be pressurized with CO_2 as a GXL.

MXEA also containes an ether linkage and does not have a hydroxide group like the other alcohol amines. The hydroxyl group promotes the miscibility in water. This property is normally very important environmentally, because disposal of water soluble solvents is easier; however, for GXLs this property is not critical. Another ether that was investigated was propylene glycol methyl ether (PGME) but it did not contain the vital amine group that causes film removal. The amine attacks the carbonyl in the photoresist

which makes it soluble in an alkaline solution[1]. The molecular structure of PGME is shown in Figure B.8.

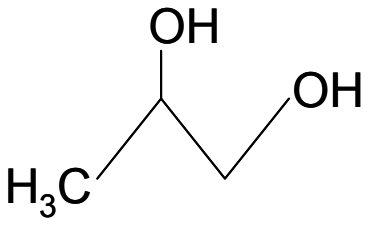

Figure B.8: propylene glycol methyl ether.

With or without CO_2 addition at 65°C and 30 minutes, the PGME could not remove photoresist films. Ethers are less reactive and hence probably are not able to remove the film without the presence of a reactive amine group.

High pressure studies using MXEA and CO_2 were performed. The process conditions were 65°C for 30mins at 500psi, 775psi, 1000psi, and 1800psi. All pressures were effective for photoresist removal, but only at pressures above 1000psi did the MXEA liquid seem to readily dissolve the CO_2 and expand as indicated by visual volume expansion. The viscosity of MXEA was measured before and after CO_2 addition to be 0.84cP and 123cP, respectively, for non-pressurized fluids. This is a large difference considering that the solution densities changed only slightly to 0.8544 and 1.0662, respectively.

These experiments indicate that CO_2 addition to primary amines inhibits photoresist removal and increases fluid viscosity. MXEA can remove photoresist films with CO_2 addition; Table B.2 summarizes the results.

Table B.2: All experiments were run at 65°C for 30min with a Shipley SPR3012 positive photoresist baked at 180°C for 15min.

Compound	Without CO_2	With CO_2
Monoethanolamine	Yes	No
Diethanolamine	No	No
Triethanolamine	No	No
Hydroxylamine	Yes	partial
2-(2-aminoethylamino) ethanol	Yes	No
Diglycolamine	Yes	No
2-methoxyethylamine	Yes	Yes
Propylene Glycol	No	No
Choline Hydroxide	No	No

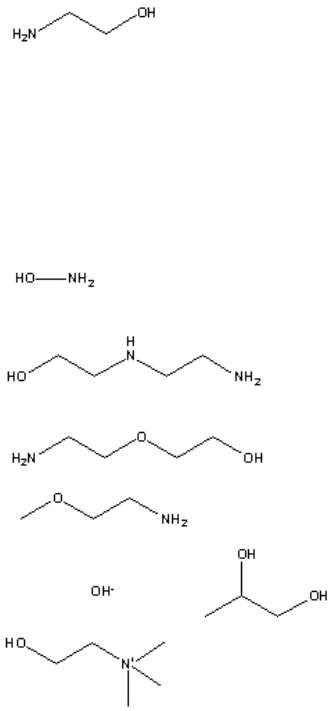

Conclusions

EKC amine based chemistries were used to remove positive photoresist films. Initially, monoethanol amine (MEA), choline hydroxide (COH), and propylene glycol PPG) were chosen to remove the films. MEA and COH serve as the removal agents while PPG is the solvent and dilution agent. Although MEA was able to remove the photoresist at 65°C for 30min, upon exposure to CO_2 the chemistry was ineffective. The inclusion of COH and PPG only diluted the fluid and made it less effective as well. EKC solvents such as EKC265 which contains hydroxylamine (HDA) and EKC830 which contains diglycolamine (DGA) effectively removed the photoresist at 65°C for 30min. Unlike MEA, HDA and DGA were somewhat effective in removing the photoresist but not completely at 65°C. Based on the chemistry of diglycolamine, 2-(2-

aminoethylamino) ethanol and 2-methoxyethylamine were selected as possible candidates that would be effective even after CO_2 addition.

At pressures from 500psi to 1800psi CO_2 expanded MXEA at 65^oC for 30min was able to remove the films. However with CO_2 incorporation, MXEA became fairly viscous but remained effective. When MXEA was diluted with ethanol, its effectiveness in film removal was lost. Although MXEA is a possible candidate for GXL formation, the viscosity must be decreased in order to ensure penetration into small feature sizes for current and future ICs.

References

1. Lee, W. M. *A Proven Sub-micron Photoresist Stripper Solution for Post Metal and Via Hole Processes*; Dupont-EKC Technology: 1996.

2. Song, I.; Spuller, M.; Levitin, G.; Hess, D. W., Photoresist and Etch Residue Removal using Gas-Expanded Liquids. *Journal of The Electrochemical Society* **2006,** 153, (4), G314-G318.

3. Long, M. L., Contamination Control and Concerns in VLSI Lithography. In *Handbook of Contamination Control in Microelectronics*, Tolliver, D. L., Ed. Noyes Publications: New York City, NY, 1988; p 354.

4. Myneni, S.; Hess, D. W., Post-Plasma-Etch-Residue Removal Using CO_2-Based Fluids. *Journal of The Electrochemical Society* **2003,** 150, (12), G744-G750.

5. Myneni, S.; Hess, D. W., Post Plasma Etch Residue Removal Using CO_2-Based Mixtures: Mechanistic Considerations. *Journal of The Electrochemical Society* **2005,** 152, (10), G757-G765.

6. Levitin, G.; Myneni, S.; Hess, D., Post Plasma Etch Residue Removal Using CO2-TMAHCO3 Mixtures: Comparison of Single-Phase and Two-Phase Mixtures. *Journal of the Electrochemical Society* **2004,** 151, (6), G380-G386.

7. Sakaino, K.; Adachi, S., Properties of silicon (111) and (100) surfaces etched in choline solution. *Journal of the Electrochemical Society* **2002,** 149, (9), G543-G549.

8. Levitin, G.; Myneni, S.; Hess, D. W., Reactions Between CO2 and Tetramethylammonium Hydroxide in Cleaning Solutions. *Electrochemical and Solid State Letters* **2003,** 6, (8), G101-G104.

9. Weiland, R. H.; Dingman, J. C.; Cronin, D. B.; Browning, G. J., Density and Viscosity of Some Partially Carbonated Aqueous Alkanolamine Solutions and Their Blends. *Journal of Chemical and Engineering Data* **1998,** 43, (3), 378-382.

10. Bavbek, O.; Alper, E., Reaction Mechanism and Kinetics of Aqueous Solutions of Primary and Secondary Alkanolamines and Carbon Dioxide. *Turk J Chem* **1999,** 22, 293-300.

11. Yeh, A. C.; Bai, H., Comparison of ammonia and monoethanolamine solvents to reduce CO2 greenhouse gas emissions. *Science of the Total Environment* **1999,** 228, (2,3), 121-133.

12. Veawab, A.; Aroonwilas, A.; Chakma, A.; Tontiwachwuthikul, P. *Solvent Formulation for CO2 Separation from Flue Gas Streams*; Faculty of Engineering University of Regina: Regina, SK Canada.

13. Winterbone, D. E., *Advanced Thermodynamics for Engineers*. John Wiley and Sons: New York City, NY, 1997; p 142.

14. Chang, C. J.; Chiu, K.-L.; Day, C.-Y., A new apparatus for the determination of P–x–y diagrams and Henry›s constants in high pressure alcohols with critical carbon dioxide. *Journal of Supercritical Fluids* **1998,** 12, 223-237.

15. Wiebe, R.; Gaddy, V. L., The solubility of carbon dioxide in water at various temperatures from 12° to 40° and at pressures to 500 atmospheres. Critical phenomena. *Journal of the American Chemical Society* **1940,** 62, 815-817.

APPENDIX C

ALTERNATIVE AMINE CHEMISTRIES AND DETERMINATION OF FILM REMOVAL UNIFORMITY

Introduction

Alternative Amine Chemistries

According to previous literature and the data described in Appendix B, our experiments indicated that the order of the amine group had an effect on the reactivity with CO_2; tertiary amines were less reactive with CO_2 than primary amines but at the expense of reduced photoresist removal capability. Reactivity was gauged by the increase in amine solution temperature upon CO_2 exposure. Among the many amines tested, the primary amine 2-methoxyethylamine was the only one effective in removing a Shipley SPR3012 photoresist that was baked at 180^{o}C for 15min. The photoresist was removed after immersion in a liquid bath at 65^{o}C for 40min with and without the addition of CO_2.

Our studies determined that 2-methoxyethyl amine (MXEA) is an effective photoresist removal agent that is moderately compatible with CO_2; however, the increased viscosity limits its viability as a removal agent for future ICs. Beilstein Commander® was used to identify other possible amine chemistries based on 2-methoxyethyl amine. . Appropriate amines must be compatible with CO_2, maintain low viscosity, and be able to remove the photoresist film. Beilstein Commander searches for chemicals based on specific parameters. The parameters chosen were an ether group, amine group, and a hydrocarbon chain with less than four carbon atoms. The ether group

appears to be important to reduce the amine reactivity with CO_2. The amine group is necessary because it serves as the removal agent. A carbon chain with four carbons is essential because the longer chain hydrocarbons are more viscous. Many chemistries matched these parameters but only four chemistries were investigated at EKC as shown in Figure C.1. The other chemistries were not chosen because they were not commercially available from major chemical vendors such as Sigma Aldrich and VWR.

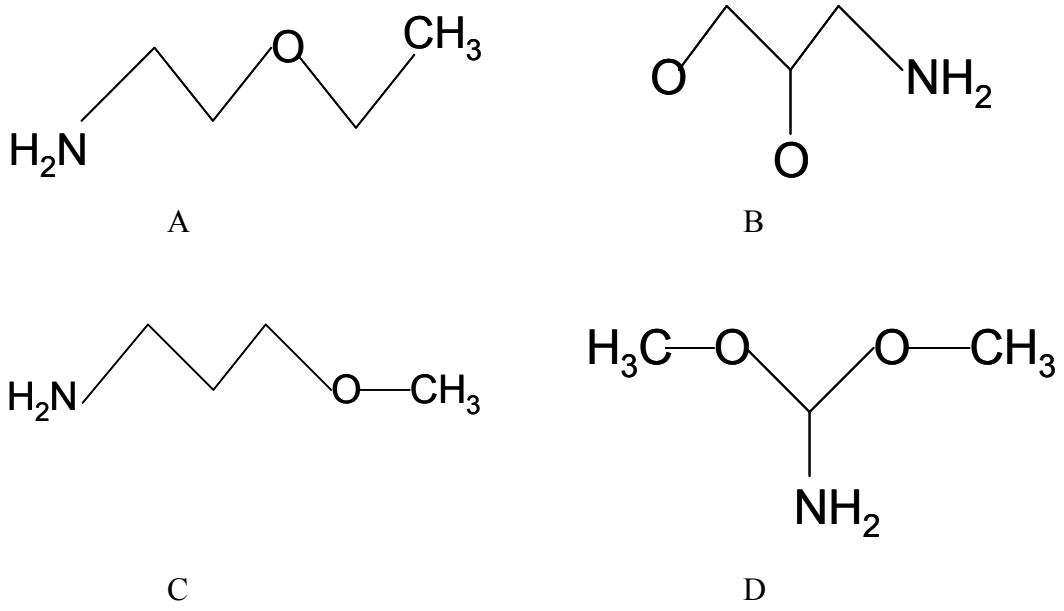

Figure C.1: A) 2-ethoxyethyl amine, B) 3-amino-propane-1,2-diol, C) 3-methoxy-propylamine, and D) dimethylformamide-diemthyl-acetal.

2-ethyoxyethyl amine was chosen because it had a longer hydrocarbon chain following the ether group than does MXEA. 3-aminopropane 1,2 diol was chosen because it has two terminal oxygen atoms. 3-methoxypropylamine was chosen because it had a longer hydrocarbon chain than 2-ethyoxyethyl amine, between the nitrogen and oxygen atoms. Dimethylformamide-dimethylacetal was chosen because it had two ether linkages. Each of the chemicals offers differences that may improve the removal effectiveness of the chemical even with the addition of CO_2 as described above.

However, only one of these chemistries was tested due to safety concerns or physical property limitations with the other three. N,N dimethylformamide dimethylacetal fumes can form an explosive mixture with air. 3-amino-propanol 1,2 diol is highly viscous. 3-methoxypropylamine is highly flammable, corrosive, and sensitive to air. Since the hazard level of two of these chemicals is extremely high, and the viscosity of the third is problematic from the standpoint of residue removal from small, high aspect ratio openings, actual implementation into an IC process is unlikely. As a result, these three chemical were not investigated as candidates for GXLs. The remaining chemical, 2-ethoxyethylamine, was tested for photoresist removal efficiency and CO_2 compatibility.

Determination of Film Removal Uniformity

Prior studies by Spuller indicated that CO_2 mole fractions in ethanol up to 0.75 were able to remove a PHOST (polyhydroxystyrene) photoresist film, albeit the sample sizes were only $1cm^2$ [1]. The PHOST film had been baked for 5min at 120°C and exposed to 700psi CO_2 expanded ethanol for 10min at room temperature. Analogous conditions were to be replicated using the 8" wafer high pressure system. Isopropyl alcohol (IPA) was chosen as the solvent to test the removal uniformity across an 8" wafer. IPA, like other low molecular weight alcohols, can incorporate CO_2 effectively as shown in Figure C.2.

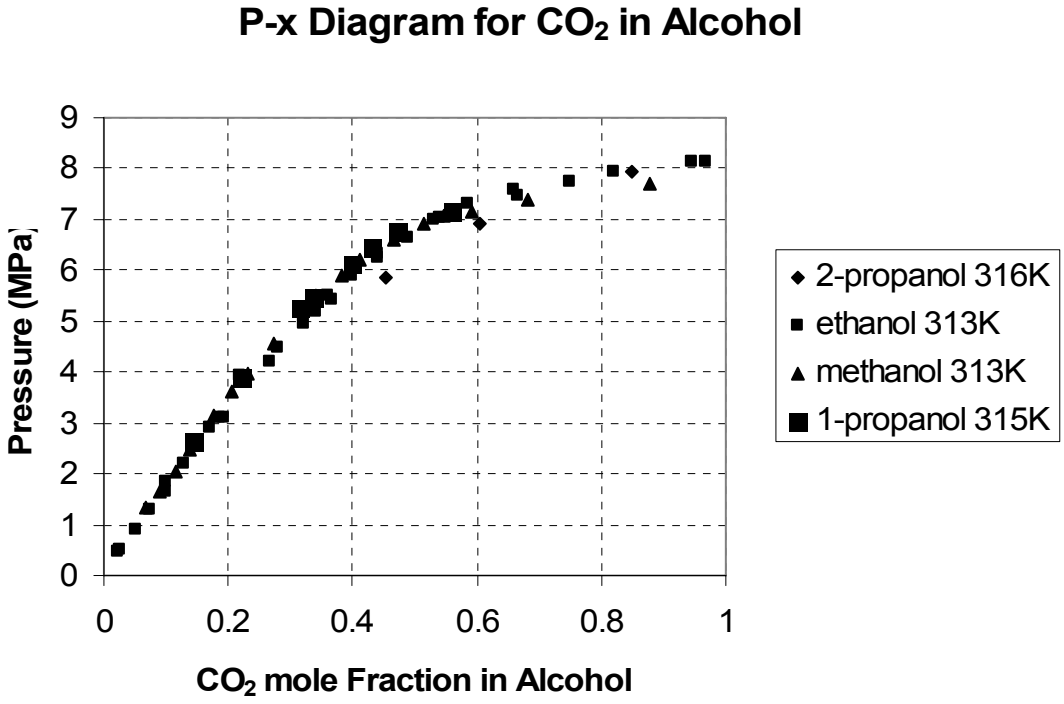

Figure C.2: CO_2 mole fraction in various alcohols[2-5].

Experimental Method

A positive photoresist (Shipley SPR3012) coated silicon wafer was used as the test wafer. The film thickness was 1.8μm according to factory specifications. The wafer was baked for 15min at 180°C to toughen the film. The wafer was cut into small 1cm^2 pieces and immersed in EXEA at 65°C for 30min. The samples were rinsed with isopropyl alcohol using a squirt bottle. CO_2 was bubbled into EXEA reagent grade from Sigma Aldrich and the experiment was repeated. Contact angle measurements were performed using FTA200 to confirm complete film removal.

To test the 8" wafer cleaning system, a silicon wafer with a novolac based I-line 365nm wavelength photoresist served as the experimental sample. The system in Figure B.2 was modified slightly in that the small high pressure Parr reactor 4566 functioned as

a holding/mixing chamber to allow equilibration of the gas and liquid. In addition, heating tape was wrapped around the large 8" wafer reactor to control the temperature in the wafer chamber. Beaker studies using IPA were carried out as preliminary tests.

The mini Parr reactor was filled with 150mL of ethanol and the CO_2 was pressurized to 700psi. Upon opening the valve to the large 5gal chamber Parr reactor 4555, the pressure immediately dropped from 700psi to ~450psi due to the large increase in volume. The 8" wafer system has a volume of 1L. Even with both Isco pumps running it was difficult to immediately pressurize the system back to 700psi; 6 min were required. Two minutes was necessary to depressurize the system to unload the sample.

After exposure to the cleaning solution, the sample was dried using a nitrogen gas stream. A J.A. Woollam VASE L2W16D.830 ellipsometer was used to determine Cauchy parameters, refractive index, and remaining photoresist thickness. The refractive index and thickness were used as starting points for analyses of thickness as determined by the Gaertner ellipsometer that was able to scan the entire wafer and so establish a thickness distribution.

Results and Discussion

Alternative Amine Chemistries

2-ethoxyethylamine was able to remove the film with and without CO_2. From contact angle measurements, a blank wafer had a contact angle of 14.8^o while the cleaned wafer after 2-ethoxyethylamine exposure had a contact angle of 27.3^o. Although the contact angles are different, even when EKC830 which is specially designed for photoresist removal was used, the contact angle was 21.5^o. The uncleaned wafer had a contact angle of 37.3^o. Although the contact angles varied, this may be due to incomplete

rinsing of the fluids after exposure. XPS analysis would have been more conclusive, but this capability was unavailable at the EKC facility.

As expected, the 2-ethoxyethylamine (EXEA) reacted with CO_2 to form a viscous solution. The initial hypothesis was that the EXEA should react less than its 2-methoxyethylamine (MXEA) sibling because EXEA is a slightly larger molecule with a molecular weight of 89.1g/mol versus 75.1g/mol for MXEA. However, this was not the case; both solutions reached a temperature of 80^{o}C upon exposure to CO_2 for 2 min. EXEA is a larger molecule but apparently was not large enough to generate an appreciable difference in reactivity. EXEA was equally effective in removing a photoresist film as was MXEA. Unfortunately, like MXEA, the viscosity of EXEA increased significantly from 0.78 to 126.3cP after CO_2 exposure. A low viscosity liquid is necessary in order to reach the bottom of the small vias and trenches for residue removal. The amine and CO_2 studies indicate that these molecules do not offer compatible chemistries. Clearly, other gases or removal chemistries need to be investigated such as amines with ethane gas or CO_2 with salts.

Determination of Film Removal Uniformity

Before testing the more difficult to remove baked photoresist samples, an unbaked sample was tested at room temperature and 725psi of CO_2 using IPA as the removal solvent for 10min. A thin layer of liquid was observed on the wafer surface indicating that the wafer was exposed to the GXL during the entire processing time. After the N_2 drying step, the 8" wafer was re-exposed to the ethanol GXL at 700psi for 10min at room temperature.

In Figures C.3 and C.4, the photoresist film refractive index distributions after the first and second GXL exposures, respectively, are displayed.

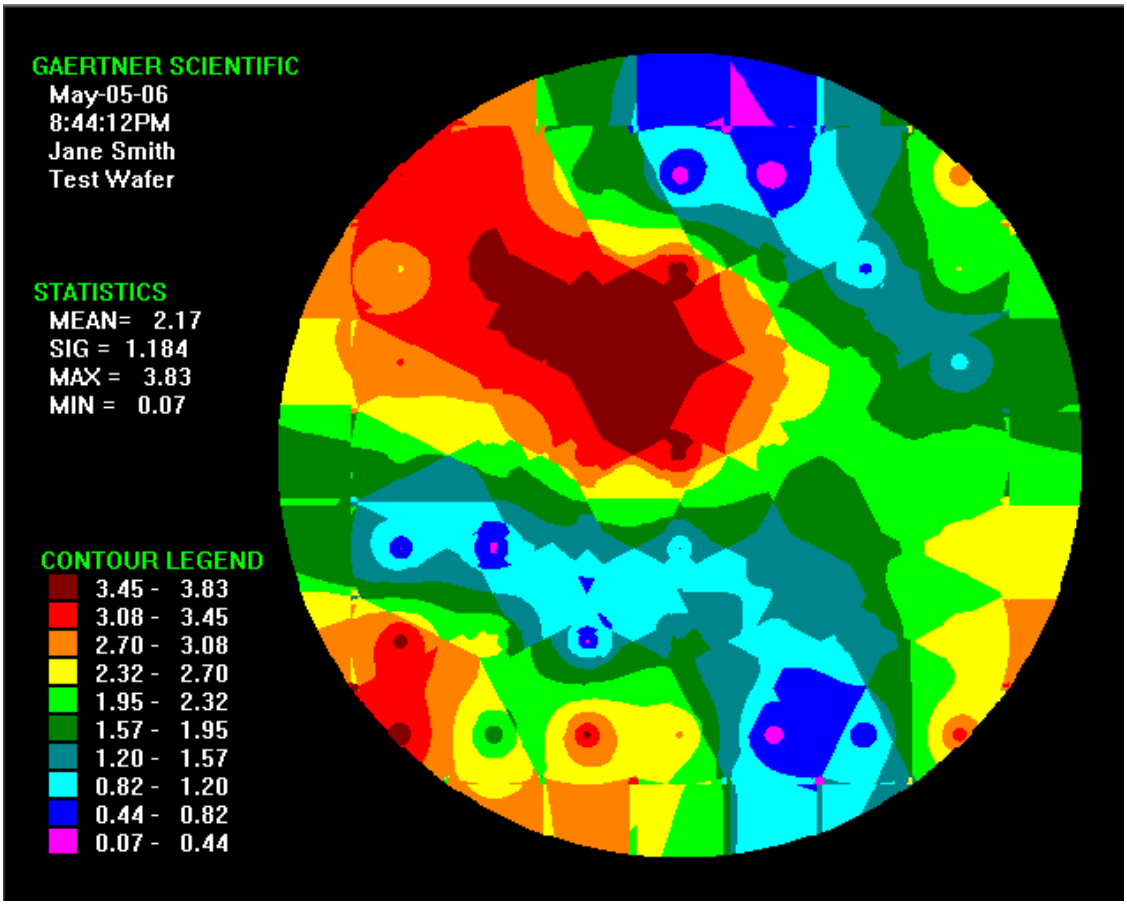

Figure C.3: Refractive index topography of 8" wafer after first GXL exposure at 700psi for 10min at room temperature.

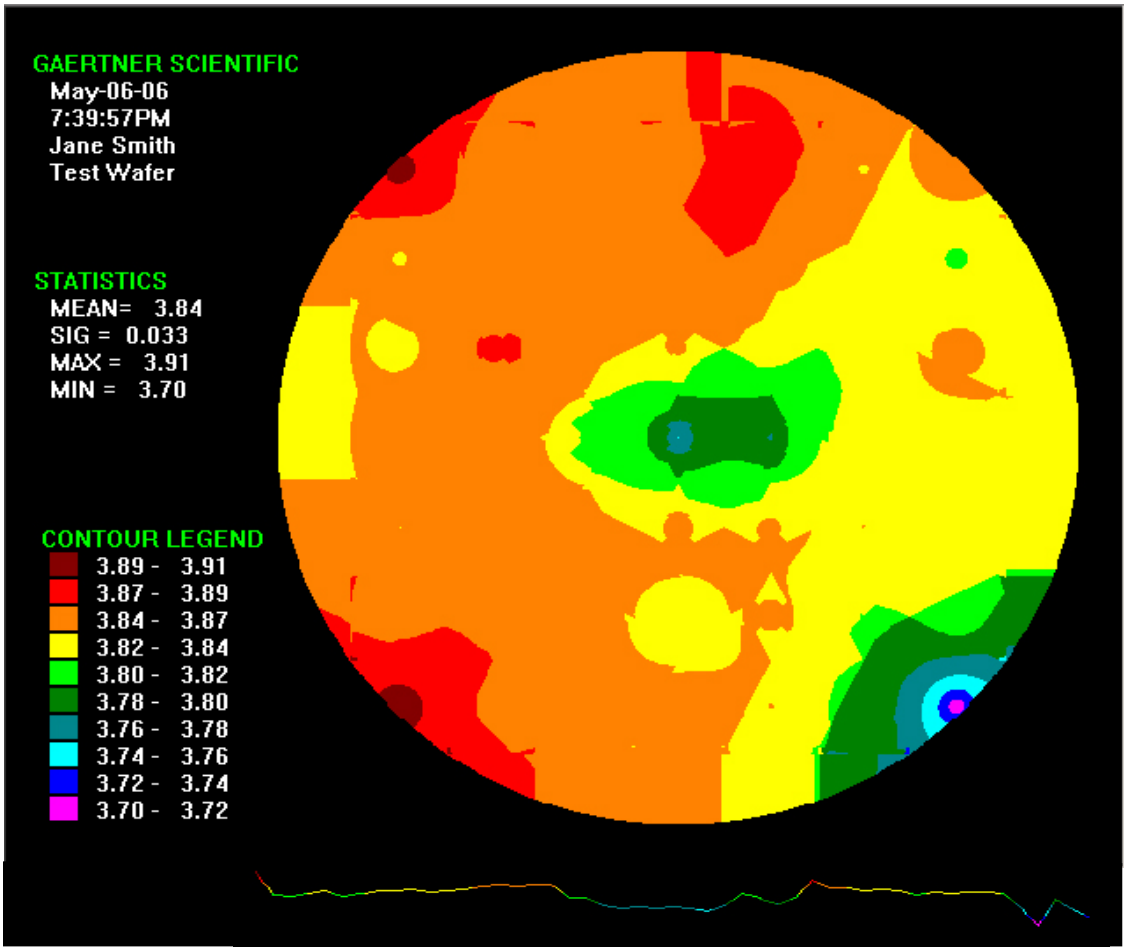

Figure C.4: A Refractive index topography of 8" wafers after second GXL exposure at 700psi for 10min at room temperature.

Clearly after the second GXL exposure, the surface was more uniform as indicated by the similar shade of color representing the refractive index. The refractive index of silicon is 3.85 and values close to this number indicate that photoresist removal has occurred.

Figure C.5 shows the variance in photoresist thicknesses after the second GXL exposure.

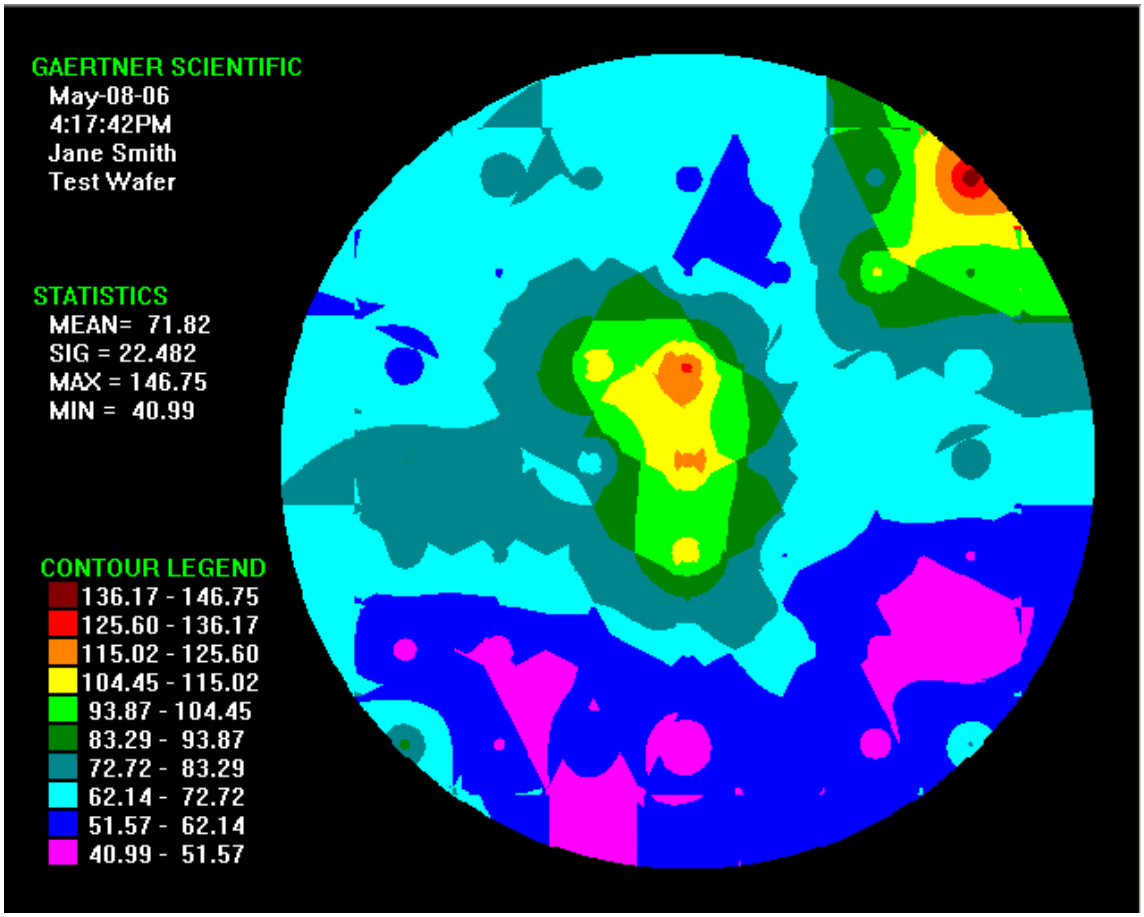

Figure C.5: Film thickness topography after second GXL exposure.

The relatively uniform film removal indicates that scaling of GSL processes is possible; however, two exposures were necessary to completely remove the film. To reduce the number of exposures, a higher temperature was employed using IPA. The temperature was 43°C and the pressure was 1090psi which gave a mole fraction of 0.75 CO_2 in the IPA to imitate the mole fraction for the ethanol study done by Spuller[1, 5]. At these conditions, the IPA the film was removed in one step. Figure C.6 shows the film thickness topography.

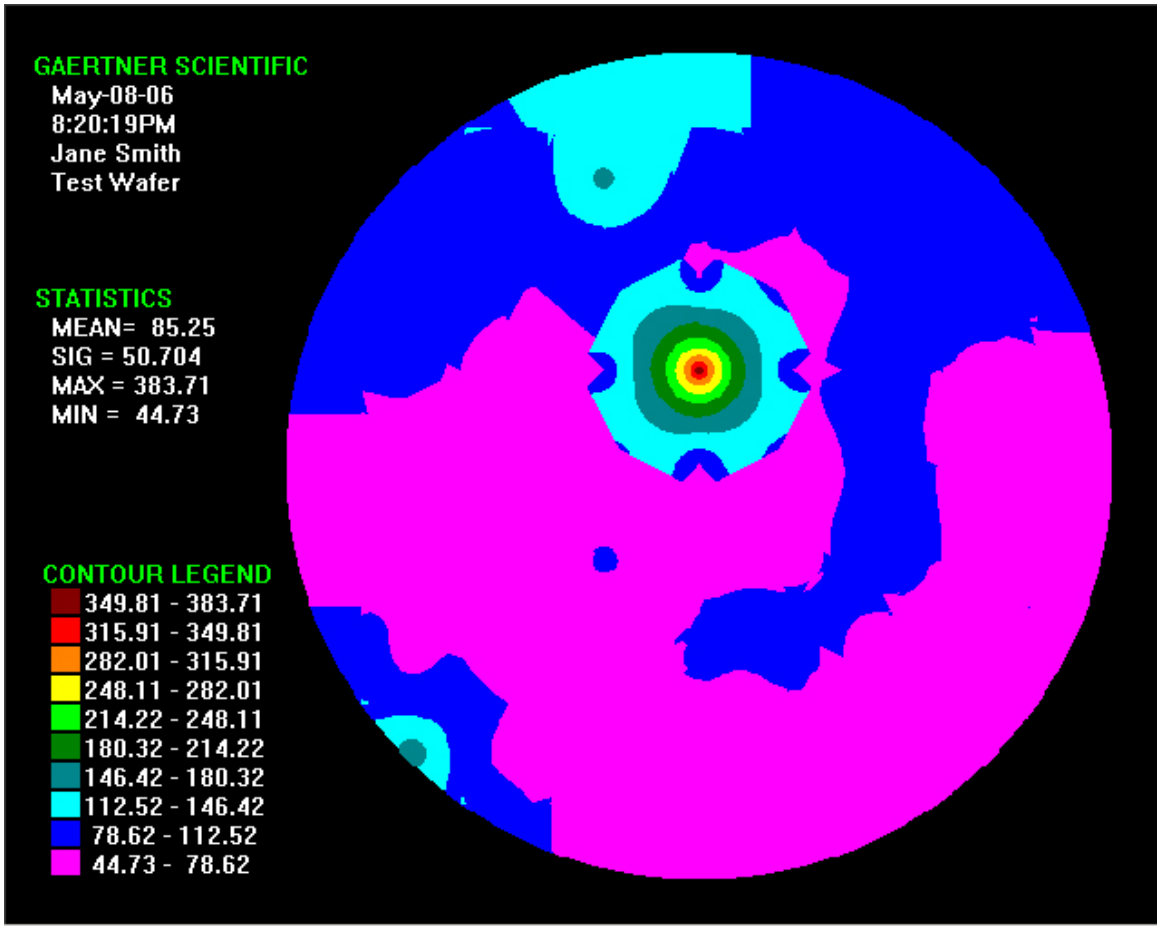

Figure C.6: Topography of wafer after exposure to CO_2 expanded ethanol at 1090psi and 43°C.

Contact angle measurements were performed on the 8" wafers and the average contact angle was approximately 25° which is very close to the contact angle of 27.3° obtained from the EKC830 exposure.

Due to the heating tape limitation and initial loading of 150mL of IPA, higher temperature and pressure studies were not feasible. However, the experiments performed at the relatively low temperature of 43°C and pressure of 1090psi demonstrated that GXLs can be used to remove photoresist films.

Conclusions

Amines and CO_2 are essentially incompatible cleaning solution components due to the formation of carbamates, reactivity between CO_2 and amine, and high viscosity of the fluid mixture[6]. Thus, to design effective GSL cleaning approaches, alternative chemistries need to be investigated. In order to invoke the use of amine chemistries, a non-reactive gas such as ethane could be used. If on the other hand, CO_2 must be employed, then other removal chemistries such as the use of a salt, ammonium fluoride, dissolved in an alcohol should be effective. Indeed, Advanced Technology Materials Inc. has filed a patent that uses a high pressure ammonium fluoride solution[7] The patent applies both to particle removal and post etch residue removal, although the solvent used is methanol with supercritical CO_2 rather than a GXL . The fluid composition is 5-20wt% methanol and 0.01-2wt% fluorine at 50^{o}C and pressures ranging from 1000psi to 7500psi.

Preliminary experiments with the 8" wafer system demonstrate that scaling of GSL cleaning approaches is possible although some conditions (e.g., temperature) may need to be enhanced to aid in photoresist film removal. In addition, studies using our reactor system suggest that a larger holding/mixing chamber would have been more effective in transferring the GXL to the main chamber.

References

1. Spuller, M. Resist and Residue Removal Using Gas Expanded Liquids. PhD, Georgia Institute of Technology, Atlanta, 2003.

2. Galicia-Luna, L. A.; Ortega-Rodriguez, A., New Apparatus for the Fast Determination of High-Pressure Vapor-Liquid Equilibria of Mixtures and of Accurate Critical Pressures. *J. Chem. Eng. Data* **2000,** 45, 265-271.

3. Chang, C. J.; Chiu, K.-L.; Day, C.-Y., A new apparatus for the determination of P–x–y diagrams and Henry's constants in high pressure alcohols with critical carbon dioxide. *Journal of Supercritical Fluids* **1998,** 12, 223-237.

4. Vandana, V.; Teja, A. S., Vapor-Liquid Equilibria in the Carbon Dioxide + 1-Propanol System. *J. Chem. Eng. Data* **1995,** 40, 459-461.

5. Radosz, M., Vapor-Liquid Equilibrium for 2-Propanol and Carbon Dioxide. *J. Chem. Eng. Data* **1986,** 31, 41-45.

6. Weiland, R. H.; Dingman, J. C.; Cronin, D. B.; Browning, G. J., Density and Viscosity of Some Partially Carbonated Aqueous Alkanolamine Solutions and Their Blends. *Journal of Chemical and Engineering Data* **1998,** 43, (3), 378-382.

7. Korzenski, M. B.; Ghenciu, E. G.; Xu, C.; Baum, T. H. Removal of particle contamination on patterned silicon/silicon dioxide using supercritical carbon dioxide/chemical formulations. US Patent Number 6,943,139, 2002.

VITA

INGU SONG

Ingu Song was born on November 17, 1980 to Chulkun Song and Jaehyun Song in Seoul, South Korea. He graduated from L.V. Berkner High School in Richardson, TX in 1999. Then moved to freezing cold Ithaca, NY to attend Cornell University and graduated with a BS in chemical and biomolecular engineering in 2003. Upon graduation he sought refuge in warm Atlanta, GA to attend graduate school at the Georgia Institute of Technology. He finished his PhD in chemical and biomolecular engineering in September of 2007 and returned to his hometown of Dallas, TX to work as a process engineer at Texas Instruments.